Polymer Composite Spinal Disc Implants

Brody Allen Frost

Thesis submitted to the faculty of the Virginia Polytechnic Institute and State University in partial fulfillment of the requirements for the degree of

Master of Science
In
Materials Science and Engineering

Earl J. Foster
Aaron S. Goldstein
Mark Van Dyke

August 9, 2017
Blacksburg, Virginia

KEYWORDS: Spinal anatomy, spinal degeneration, lower back pain, intervertebral discs, polyurethane composites, cellulose nanocrystals.

Polymer Composite Spinal Disc Implants

Brody Allen Frost

ACADEMIC ABSTRACT

The goal of this research study was to create an artificial annulus fibrosus similar to that of the natural intervertebral disc, as well as find preliminary results for vertebral endplate connection and nucleus pulposus internal pressure, for the correction of disc degeneration in the spine. The three-part composite samples needed to demonstrate good shock absorption and load distribution while maintaining strength and flexibility, and removing the need for metal in the body, something of which no current total disc replacement or spinal fusion surgery can offer. For this study, the spinal disc was separated into its three different components, the annulus fibrosus, the nucleus pulposus, and the vertebral endplates, each playing a vital role in the function of the disc. Two low-cost materials were selected, a Covestro polyurethane and cellulose nanocrystals, for the purpose of creating a polymer composite spinal disc implant. A methodology was established for creating the cast composite material for use as an annulus fibrosus, while also investigating its mechanical properties. The same composite material was used to acquire preliminary results for vertebral endplate connection to the synthesized annulus, however no additional material was used to determine or mimic the mechanical properties of these endplates, due to time constraints. Also because of time constraints, the nucleus used in this study was only comprised of water with no other additives for preliminary testing since the natural nucleus is comprised of about 80-90% water. These properties were then compared to the mechanical properties of the natural disc, so that they could be finely tuned to emulate the natural disc. It is shown in this study that the composite material, when swelled in water, was able to mimic the annulus fibrosus in tensile strength and modulus, however showed higher compressive strength and modulus than ideal. The samples also did not undergo any permanent deformation within the realm of force actually introduced to the natural disc. The vertebral endplates showed decent adhesion to the synthesized annulus, however there were slight defects that became failure concentrators during compression testing. The nucleus showed promising results maintaining good internal pressure to the system causing better compressive load distribution, with barreling of the samples.

Polymer Composite Spinal Disc Implants

Brody Allen Frost

GENERAL AUDIENCE ABSTRACT

Spinal disc degeneration is a very prevalent problem in today's society, effecting anywhere from 12% to 35% of a given population. It usually occurs in the lumbar section of the spine, and when severe enough, can cause bulging and herniation of the intervertebral disc itself. This can cause immense lower back pain in individual's stricken with this disease, and in the US, medical costs associated with lower back pain to exceed $100 billion. Current solutions to this problem include multiple different treatment options of which, spinal fusion surgery and total disc replacement (TDR) are among the most common. Although these treatments cause pain relief for the majority of patients, there are multiple challenges that come with these options. For example, spinal fusion surgery severely limits the mobility of its patients by fusing two vertebrae together, disallowing any individual movement, and TDR can cause hypermobility in among the vertebrae and offer little to no shock absorption of loads. Therefore, a better treatment option is needed to relieve the pain of the patients, as well as maintain equal motion, shock absorption, and load cushioning to that of the normal intervertebral disc and remaining biocompatible. The goal of this research study was to create a three-component system, like that of the natural intervertebral disc, for the use of spinal disc replacement and to replace current options. The fabricated system was comprised of the three components found in the natural intervertebral disc; the annulus fibrosus, the nucleus pulposus, and the vertebral endplates. Because the system will need to go in-body, the materials used were all characterized as biocompatible materials; the polyurethane currently being used in medical devices and implants, and the cellulose nanocrystals (CNCs) coming from natural cellulose in sources such as wood and plants. The results determined that the mechanical properties of the system can be fine-tuned in order to mimic the natural strength and cushioning capabilities of the natural disc, based on CNC content added to the polyurethane, and when all three components of the system are added together, the compressive stress-strain is most similar to the natural disc in compression. However, the system did show failure in the connection between the annulus fibrosus and vertebral endplates, causing herniation of the nucleus similar to the initial problem attempting to be solved. For this, more ideal fabrication methods should be researched in the future including 3D printing techniques, injection molding, and roll milling. As well as alternate fabrication techniques, cell grow and viability should be determined to show that cells don't die once the system in implanted.

Acknowledgements

I would like to thank my advisor, Dr. Johan Foster, for taking me in as his graduate student and helping me with his advice, knowledge, and support on this project, as well as with his help revising this document. I would like to thank Dr. Mark Van Dyke and Dr. Aaron Goldstein for their cooperation as my committee members, and for their help revising this document. I would like to thank Dr. Thomas Staley for allowing me access to the testing facilities in Randolph, and for his past help with my senior design project, in which this study was based. I would like to thank Mac McCord for all of his help with the Instron compression testing. I would like to thank my senior design group of Morgan Schneider, Ben Messina, and Will Gardner for their help with the preliminary stages of this study based off of our senior design project. I would like to thank the members of FAMG, under Dr. Foster, for all of the laboratory help that they contributed to this study. I would also like to thank the James F. Powell Fellowship, for which this study was funded. I would like to thank the entire Materials Science and Engineering department staff, especially Kim Grandstaff, for all of their administrative support. Finally, I would like to thank my friends and family for all of their confidence, guidance, and support.

Table of Contents

List of Figures

List of Tables

1. Introduction

1.1 Human Spinal Anatomy

The spine, or vertebral column, is a bony structure that houses the spinal cord and extends the length of the back, connecting the head to the pelvis [1]. It can be separated into five distinct sections, the cervical spine, the thoracic spine, the lumbar spine, the sacrum, and the coccyx, all of which are comprised of independent bony vertebrae and intervertebral discs [2], **Figure 1**.

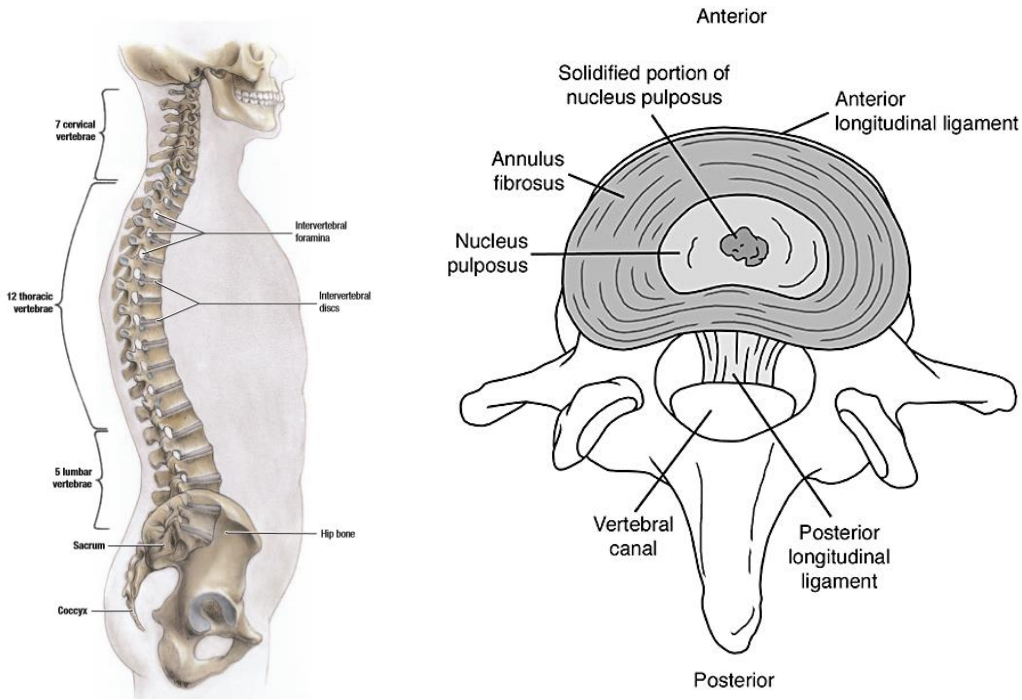

Figure 1. Overview of the vertebral column (left). Anatomy of the vertebrae and intervertebral discs (right) [2, 3]. (Used under fair use, 2017).

The most important function of the spine is to protect the spinal cord, which is the nerve supply for the entire body originating in the brain [1]. Along with this major function, it includes others such as supporting the mass of the body/head and withstanding external forces, allowing for mobility and flexibility to absorb energy and protect against impact, and attaching to the muscles and ligaments of the trunk for postural control and spinal stability [4]. To better describe the differences between the spinal column sections, each one has been further discussed.

1.1.1 Cervical Spine

The cervical section of the spine consists of seven vertebrae (C1 – C7) and six intervertebral discs, and extends from the base of the skull to the top of the trunk, where the thoracic vertebrae and rib cage start [2], **Figure 2**. The cervical spine's major functions include supporting and cushioning loads to the head/neck, protecting the spinal cord extending from the brain, and movement of the head and neck [5].

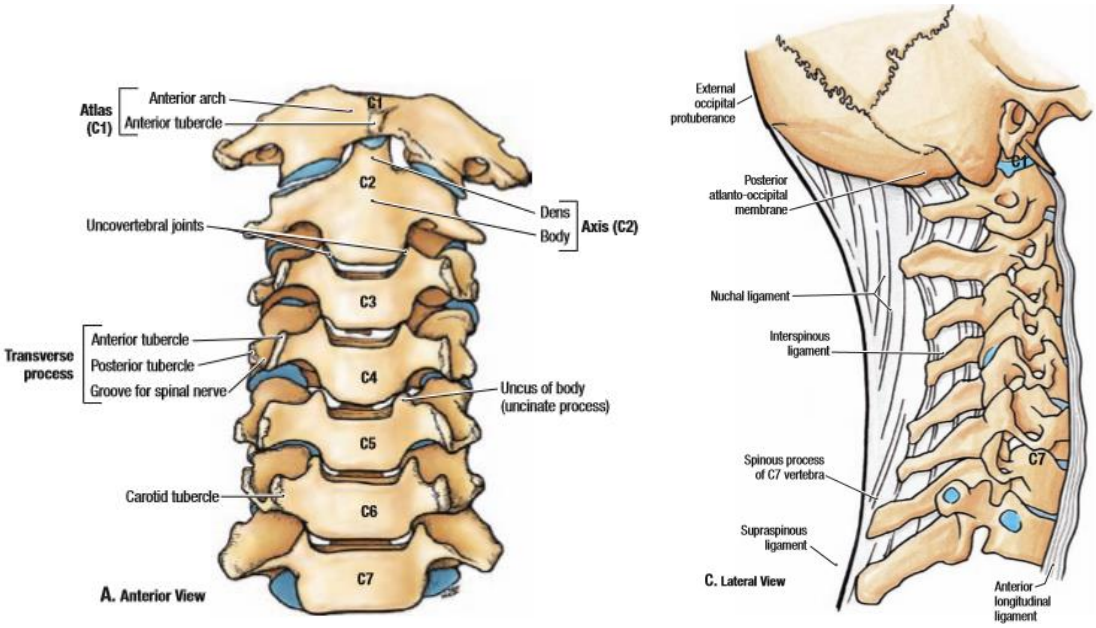

Figure 2. Anterior (left) and lateral (right) view of the cervical spine to show vertebrae shape and curvature [2]. (Used under fair use, 2017).

Of these seven vertebrae, the atlas (C1) and the axis (C2) are among the most important for rotation and movement of the head [6]. The atlas is the only cervical vertebra that does not contain a vertebral body, but instead has a more ring-like structure for cradling the skull at the occipital bone, creating the atlanto-occipital joint. This joint in particular makes up for about 50% of the heads flexion and extension range of motion [5 - 7]. The axis contains a large bony protrusion (the odontoid process) that extends from the body, superiorly, into a facet on the ring-shaped atlas, forming the atlanto-axial joint [5, 6]. This connection allows the head and atlas to rotate from side to side as one unit, and accounts for about 50% of the neck's rotation, as well as having the function of transferring the weight of the head through the rest of the cervical spine

[5 - 7]. The rest of the vertebrae (C3 – C7), have significantly reduced mobility, however are mainly used as support for the weight bearing of the head and other loads put onto the neck.

The cervical spine is so important because the nerves that stem from the spinal cord through the cervical spine, if damaged, can cause dramatic negative impacts on an individual's daily life, even potentially leaving them paralyzed from the neck down [8]. These nerves include; C1, C2, and C3 nerves which are responsible for control of the head and neck, as well as sensations for the head and sides of the face; C4 nerve that controls the shoulders and the diaphragm (breathing), as well as sensations for the neck and top of the shoulders; C5 nerve that controls the upper body muscles such as deltoids and biceps, as well as sensations in the shoulders and outer part of the arm down to about the elbow; C6 nerve that controls the wrist extensors and some innervation to the biceps, as well as sensations in the top of the shoulders that run down the side of the arm to the thumb side of the hand; C7 nerves that controls the triceps, as well as sensations from the shoulder down the back of the arm and into the middle finger; C8 nerve that controls the hands, as well as sensations in the lower part of the shoulder that extend down the arm into the pinky side of the hand [8]. Therefore, the cushioning and support of loads by the intervertebral discs are crucial to the longevity of these nerves, since they run through the same joint separation [9]. However, because of the extensive movement that occurs in the cervical spine, the intervertebral discs go through drastic changes in stresses and strains causing them to be much more susceptible to injury, which can cause damage to or impingements on these nerves [9].

1.1.2 Thoracic Spine

The thoracic section of the spine consists of twelve vertebrae (T1 – T12) and twelve intervertebral discs, and extends from the bottom of the cervical spine to the beginning of the lumbar spine [2], **Figure 3**. The thoracic spine's major functions include heavy load bearing and protection of the spinal cord, supporting posture and stability throughout the trunk, and connection of the rib cage that houses and protects vital organs, such as the heart and lungs [10].

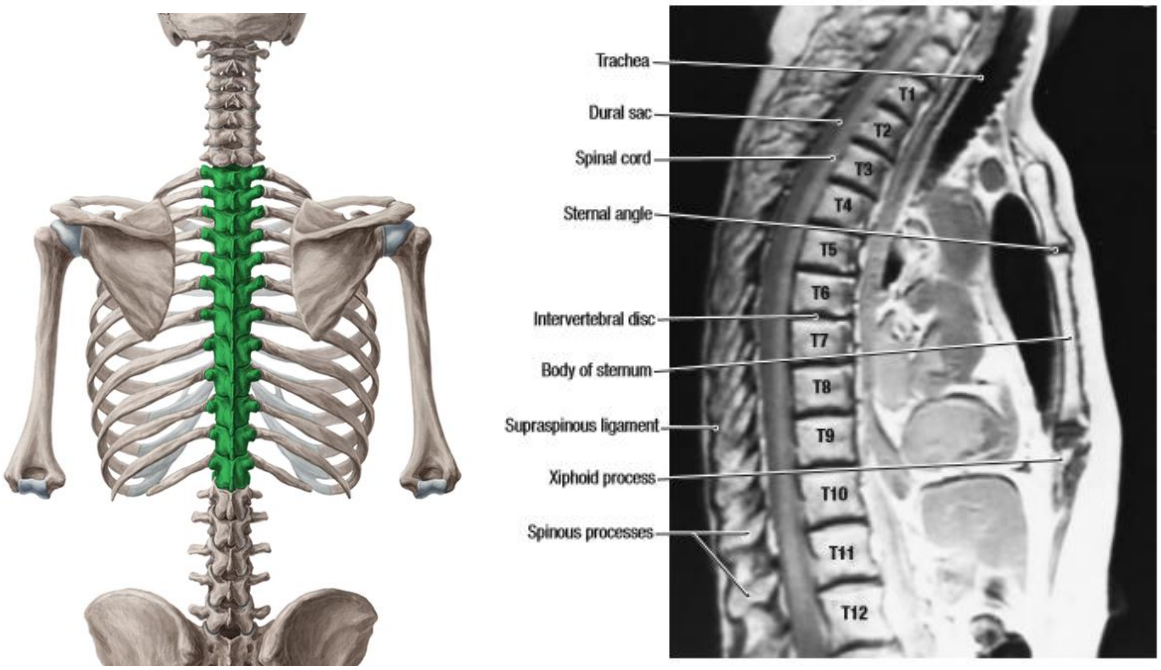

Figure 3. Thoracic spine's relativity to the other sections of the spine (cervical above and lumbar below). Each thoracic vertebra is shown with its respective rib attached, forming the surrounding ribcage (left) [11]. Midsection MRI image showing curvature of a normal, healthy thoracic spine from the right side of the patient (right) [2]. (Used under fair use, 2017).

The thoracic spine is special because with the rib cage-sternum complex intact, its load bearing capacity becomes three times greater than without. Also, the significant decrease in mobility due to the solid structure of the ribcage allows for much greater stability and support of the entire trunk, usually leading to less cases of disc degeneration [10, 12]. The vertebrae that make up the thoracic spine, although none are especially different like that of the atlas and axis previously discussed, do have some slight differences from each other as the vertebral column descends. The vertebral bodies size (thickness, width, and depth) drastically increase descending from T1 to T12, as each vertebra is expected to bear an increasing amount of weight transferred by the vertebrae above [13]. All other features stay relatively the same throughout, except for the T11 and T12 vertebrae in which no ribs are connected, resulting in much smaller transverse processes. Along with this change towards the end of the thoracic spine, the T12 vertebra has distinct thoracic characteristics superiorly and lumbar characteristics inferiorly for articulation with the L1 vertebra, allowing rotational movements with T11 while disallowing movements with L1 [13].

The thoracic spine contains nerves that are much less specialized per vertebrae like that of the cervical and lumbar spine, however they are no less important. The nerves that stem from the spinal cord in this section power the muscles that lie around (major back, chest, and abdominal muscles) and between (intercostal muscles) the ribs [14]. The sympathetic nervous system, which stems from the entire thoracic spine and top two lumbar vertebrae and help power the intercostal muscles, is necessary for vital involuntary functions such as increasing heart rate, increasing blood pressure, controlling breathing rate, regulating body temperature, air passage dilation, decreasing gastric secretions, bladder function (bladder muscle relaxation, and storage of urine), and sexual function [14]. The thoracic spine and sacrum are the only sections of the spinal cord that these involuntary nervous systems stem from. The other nerves, which produce voluntary movement, include; T1 nerve which help the C8 nerve with the hands and fingers, and sensations they include; T2 – T5 nerves that control the upper chest and upper back muscles; T6 – T8 nerves that control the lower chest, upper abdominal, and middle back muscles; T9 – T12 nerves that control the middle and lower abdominal, and the lower back muscles [14]. As mentioned previously, with these nerves passing through the same proximity as the intervertebral discs, cushioning of loads and proper weight dispersion is crucial for disc health and nerve protection, although the structural support of the ribcage makes damage to these discs much less prevalent [12].

1.1.3 Lumbar Spine

The lumbar section of the spine consists of five vertebrae (L1 – L5) and five intervertebral discs, and extends from the bottom of the thoracic spine to the beginning of the sacrum, which attaches the spine to the pelvis [2], **Figure 4**. The lumbar spine's major functions include heavy load bearing and protection of the spinal cord during locomotion and bending/torsion of the trunk, and providing maximum stability while maintain crucial mobility of the trunk about the hips/pelvis [15].

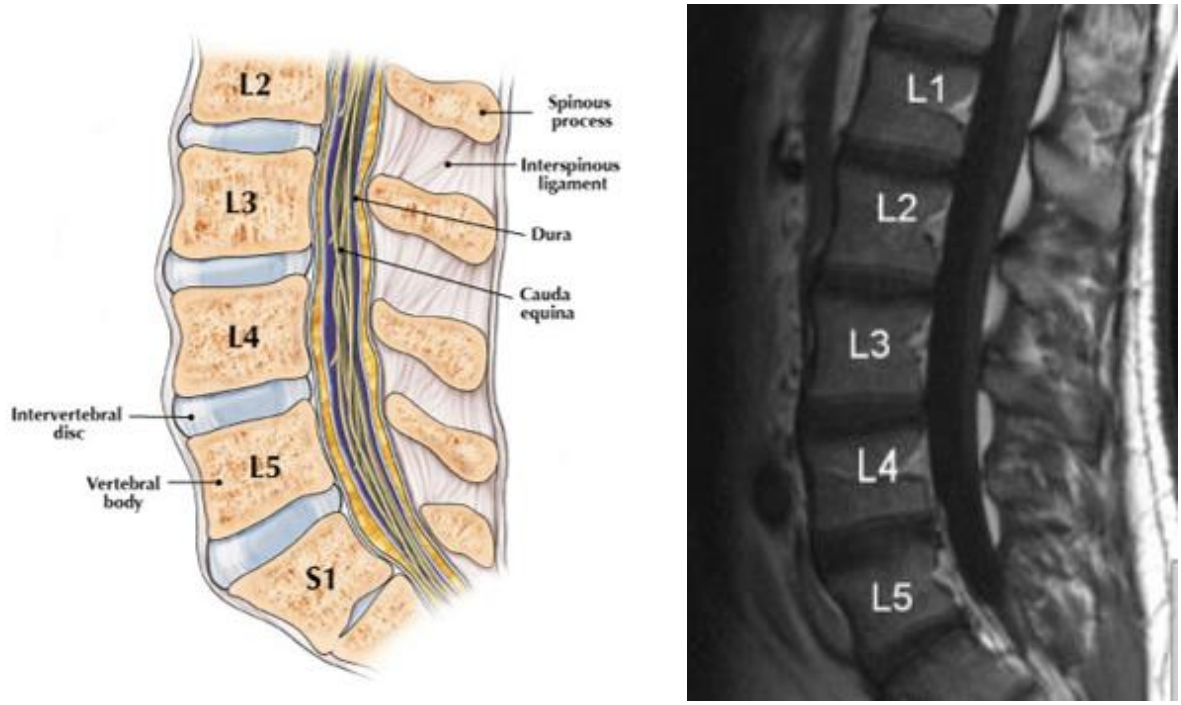

Figure 4. Lateral view of the midsection of the lumbar spine (left), as well as midsection MRI image (right), showing normal curvature and brief anatomy of the intervertebral discs and vertebrae [16, 2]. (Used under fair use, 2017).

This particular section of the spine needs to be the most resilient due to the vital functions it provides. Not only does it need to support all of the transferred weight from the previous spinal sections (virtually the entire human body), but it also needs to be able to retain its mobility under these strenuous conditions. The lumbar spine, from bending over to standing straight, can go through more than a 50º range for the average person (± 28.0º from 0º bend) [17]. As well as bending motion, rotation becomes a big factor, with each normal lumbar segment having the ability to undergo up to 7º - 7.5º of rotation [18]. When weight is added to these conditions, such as bending over to pick up a backpack or a weight from the floor, an immense amount of stress and strain is induced into the lumbar spine [19]. Because of this, the vertebrae and intervertebral discs in the lumbar spine are the greatest in thickness, width, and depth [20]. The L1 vertebra starts out with a thickness, width, and depth greater than any of the cervical or thoracic vertebrae, and the trend only continues as the lumbar spine continues to descend to the L5 vertebra [20]. Although the vertebrae increase in size as the lumbar spine descends, none of the vertebrae themselves are specialized in any way like the aforementioned atlas and axis of the cervical spine. The L5 vertebra is not much different

than the others other than size, but since it is the most inferior vertebra in the spine, it takes more load bearing responsibility than any other vertebra in the spine making it a necessity to be the biggest and strongest [21, 22].

The lumbar spine contains nerves that are much more similar to those of the cervical spine, in that each one that comes out of the different levels have very specialized functions, which if damage can hinder an individual's daily life and potentially leave them paralyzed from the waist down [23, 24]. These nerves control mainly the front of the lower extremities, and include: L1 nerve that controls partial lower back, partial lower abdominal, and partial hip flexor muscles; L2 nerve that controls muscles that extend or flex the hip joint (hip flexors, outer gluteus/gluteus medial), and groin regions; L3 nerve that controls major quadriceps muscles in order to extend the leg and straighten the knee; L4 nerve that controls the ankle muscles that cause dorsi-flexion of the foot (drawing the toes upwards), great toe, and outer quadriceps muscle; L5 nerve that control outer muscles of the lower extremity (iliotibial tract, tibialis anterior), and major foot muscles [25]. The L1, L2, L3, and L4 nerves share sensations for the anterior and inner surfaces of the lower extremity; L4 and L5 nerves share sensations for the foot; L4 creates sensations in the medial side of great toe; L5 helps create sensations in posterior and outer surfaces of the lower extremity [25]. With all of the load bearing, torsion, and bending, these nerves tend to have the most significant chance to be impinged or damaged, compared to any other spinal section [24, 26].

1.1.4 Sacrum

The sacrum consists of five fused vertebrae (S1 – S5) that connect to the pelvis at the sacro-iliac joint, and acts as the only skeletal connection between the trunk and the lower body [2]. While in adolescence, the sacrum remains unfused, however as an individual grows into adulthood, the sacrum begins to fuse together. The fusion of the sacrum tends to begin with the lateral elements fusing around puberty, and the vertebral bodies fusing at about 17 or 18 years of age, becoming fully fused by 23 years of age [2], **Figure 5**. The sacrum has few active roles in the body, however one of those roles are incredibly vital, being the bridge between the hips with the rest of the spine [27], **Figure 6**.

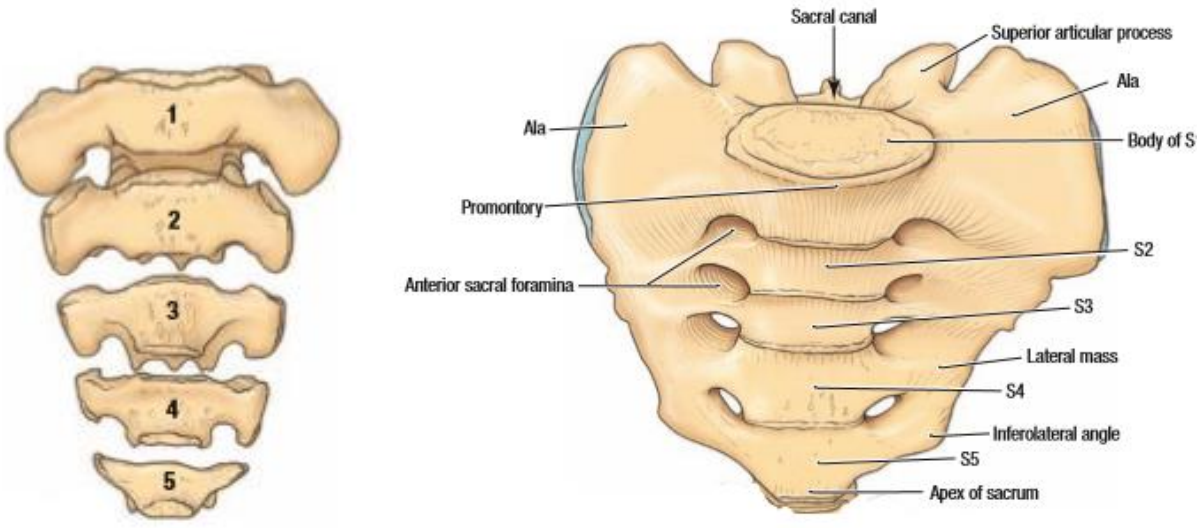

Figure 5. Anterior view of the sacrum of an adolescence (left) compared to the sacrum of an adult, after the fusion of the vertebrae (right) [2]. (Used under fair use, 2017).

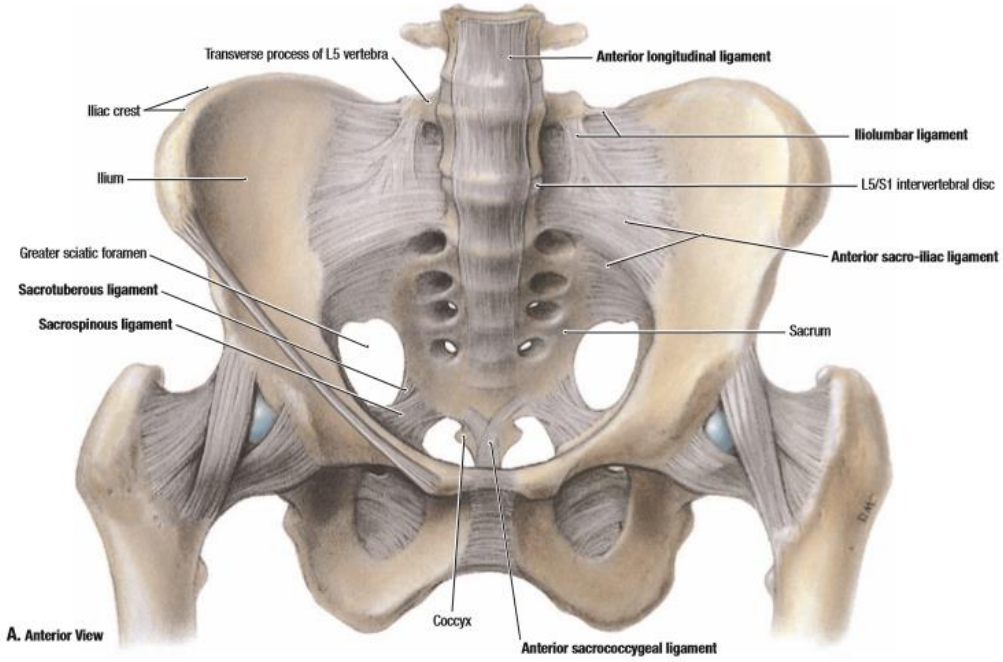

Figure 6. Anterior view of the fixed connection between the fused sacrum and the pelvis, as well as the L5 vertebra being intertwined amongst ligaments of the pelvis [2]. (Used under fair use, 2017).

Although the sacrum has no intervertebral discs, it does have very important nerves that stem from the spinal cord, going through the entire the lower extremity. The most important and commonly injured of these nerves travels through the L5/S1 space which is more commonly known as the sciatic nerve. When this nerve is damaged or impinged it leads to pain and numbness down the legs hindering much of an

individual's way of life [28]. Among the sciatic nerve, the sacrum contains other nerves including: S1 nerve that controls the ankle muscles that cause plantar-flexion of the foot (pointing the toes downwards); S2 nerve that helps control toe muscles; S2– S5 nerves that control the external sphincter muscles of the anal canal and the urethra, and the bladder. Although the sacrum spinal nerves aren't involved in many voluntary motor functions, the S2 – S4 does house the parasympathetic nervous system, which controls involuntary functions including, slowing heart rate, constriction of air passages, increasing gastric secretions, bladder function (bladder muscle contraction, and release of urine), bowel function, and sexual function (erectile function and lubrication) [29]. Because the nerves running through the sacrum have no risk of being impinged by bulging or herniated discs, other than the L5 /S1 nerve which is more associated with the lumbar spine, the sacrum will not be discussed further.

1.1.5 Coccyx

The coccyx consists of three to five fused vertebrae (four is most common) that are connected to the bottom of the sacrum, and is usually referred to as the tail bone [2], **Figure 7**. The coccyx's major functions include acting as an attachment site for pelvic tendons, ligaments, and muscles, mainly those of which make up the pelvic floor, and supporting and stabilizing the body while in a sitting position [30].

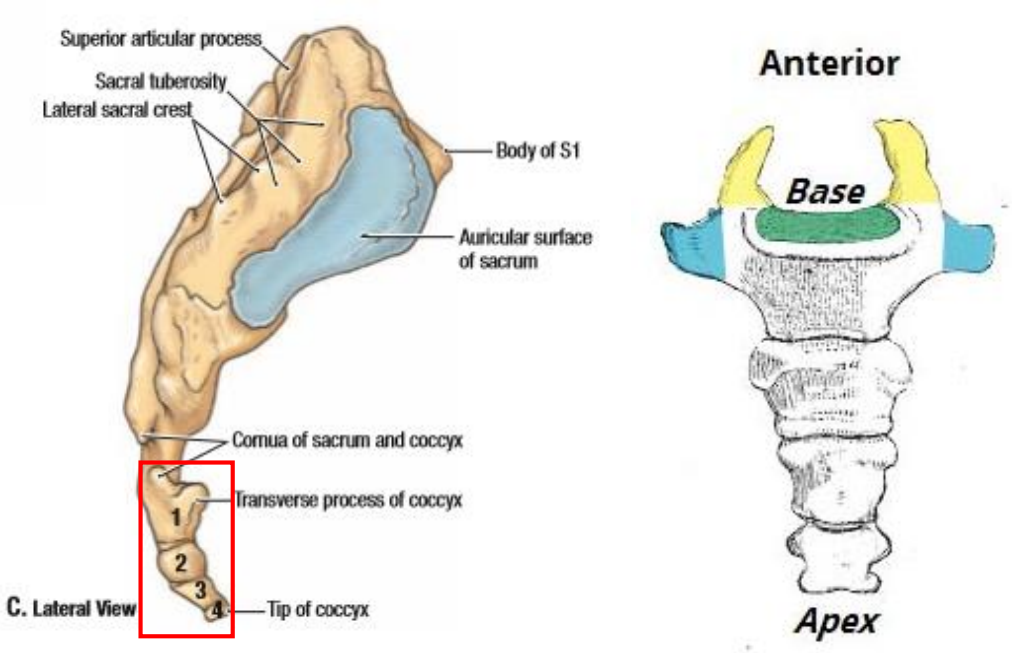

Figure 7. Lateral view of the coccyx in relation to the sacrum (left), and an anterior view of the four fused coccyx vertebrae (right) [2]. (Used under fair use, 2017).

The coccyx has no intervertebral discs nor do any nerves pass through it, therefore it is insignificant with regards to disc degeneration and disc damage.

1.1.6 Intervertebral Discs

Every vertebra in the cervical (excluding the C1 and C2 vertebrae), thoracic, and lumbar spines are separated by intervertebral discs, each named for the two vertebrae they sit between (e.g. C6-C7, T7-T8, and L4-L5, also sometimes denoted as L4/L5). These discs make up about 20 – 30% of the spine, and have incredibly important functions including load cushioning, reducing stress caused by impact (shock absorber), weight dispersion, allowing for movement of individual vertebrae, and allowing for the passage of nutrients and fluid to the spine and spinal cord [31]. Although each disc grants almost identical functions to the spine, based on their locations in the spine, their structure and mechanical properties change to adapt to the different loads, stresses, and strains produced on the individual sections of the spine [32]. For example, as the expected weight-bearing role of each disc increases, descending from the base of the skull along the length of the spine, the cross-sectional area of the discs also increases **Figure 8.** The pressure exerted on the discs however, does not increase to the same extent due to the fact that the cross-sectional area increases in the caudal direction [32].

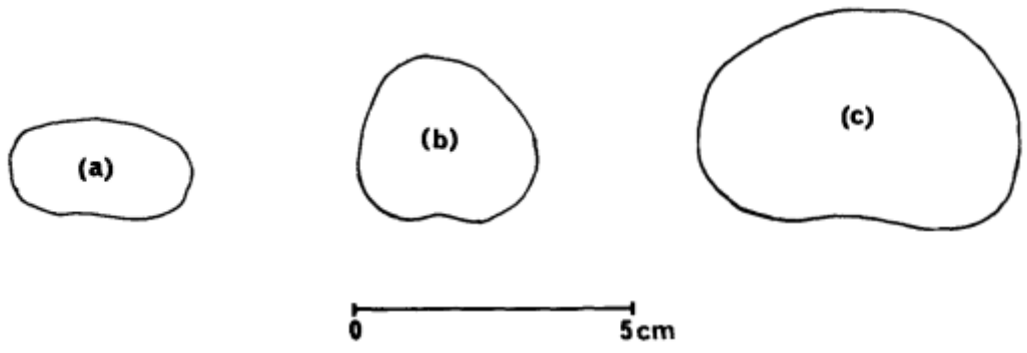

Figure 8. Cross-sectional shapes of (a) C7-T1, (b) T7-T8, and (c) L4-L5 intervertebral discs [32]. (Used under fair use, 2017).

Along with the changes in the cross-sectional areas of the discs, the thickness of each disc changes throughout the spine as well. The cervical and lumbar spines have been shown to have much thicker discs than that of the thoracic spine, most likely being adapted to the range of motion expected from these sections, for both flexion-extension and torsion [32], **Figure 9**.

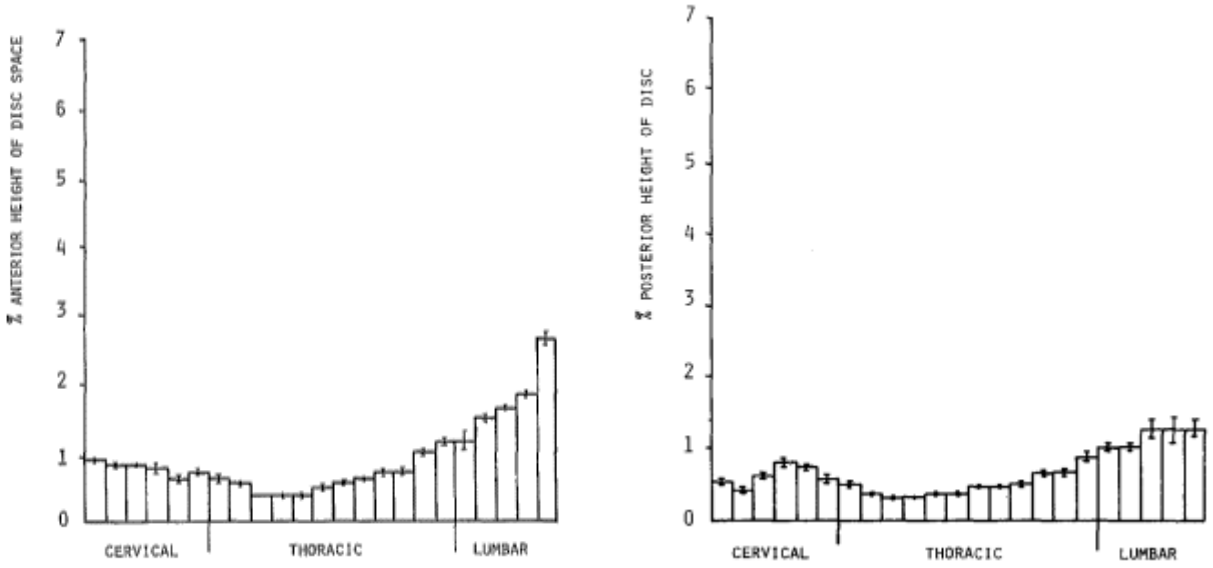

Figure 9. Mean anterior disc height, expressed as a percentage of the total length of the spine, measured from lateral radiographs for C2-C3 to L5-S1 (left). Mean posterior disc height, expressed as a percentage of the total length of the spine, measured from lateral radiographs for C2-C3 to L5-S1 (right) [32]. (Used under fair use, 2017).

As the discs increase in thickness, the length of reinforcing fibers of the annulus fibrosus increase as well. This change allows for a decrease in fiber strain caused by a given movement for thicker discs compared to thinner discs [32]. Although there is a general trend between the structural and mechanical properties of the intervertebral discs and the spinal sections they belong to, each individual disc of the same section have their differences as well.

1.1.6.1 Cervical Discs

The cervical spine consists of six intervertebral discs (C2/C3 – C7/T1), with the absence of a disc between the atlas (C1) and the axis (C2) [2]. These discs are smaller in cross-sectional area than any of the other discs in the spine, due to the load bearing role of the cervical spine being much less than that in any

other section, therefore decreasing the need for load distribution [32]. The average cross-sectional areas of the cervical discs are as follows; C2/C3 having an area of 190 mm^2; C3/C4 having an area of 280 mm^2; C4/C5 having an area of 240 mm^2; C5/C6 having an area of 300 mm^2; C6/C7 having an area of 460 mm^2; C7/T1 having an area of 440 mm^2 [32]. However, with the extent of flexion/extension and rotation throughout the cervical spine, the discs have the greatest disc height to vertebral body height ratio than those in the other sections of the spine [32]. The average thicknesses of the cervical discs are as follows; C2/C3 having a thickness of 3.51 mm; C3/C4 having a thickness of 3.74 mm; C4/C5 having a thickness of 4.07 mm; C5/C6 having a thickness of 4.45 mm; C6/C7 having a thickness of 4.11 mm; C7/T1 having a thickness of 4.5 mm [33, 34]. In adults, the maximum flexion and extension of the cervical spine occurs around the C5/C6 disc, therefore its thickness is representative of such and will be, on average, thicker than the others. The cervical discs also show a maximum thickness in the anterior section and a minimum height in the posterior section, giving the natural convex curvature as previously mentioned [33], **Figure 10**.

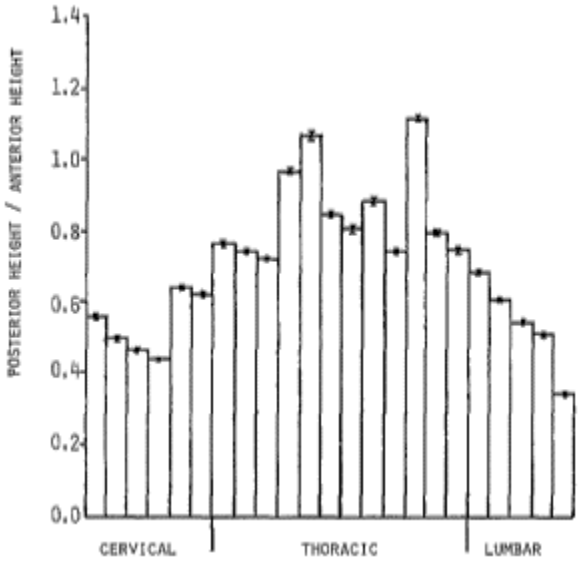

Figure 10. Posterior height divided by anterior height of discs C2-C3 to L5-S1. The nearer the value of this ratio to 1.0, the less wedge-shaped is the disc [32]. (Used under fair use, 2017).

Because of the mobility of the cervical spine, its discs have a significantly higher chance of becoming damaged from bending and torsion, making it the second most common spinal section for disc injury [35].

1.1.6.2 Thoracic Discs

The thoracic spine consists of twelve intervertebral discs (T1/T2 – T12/L1) [2]. These discs are greater in cross-sectional area than the cervical discs, however are still less than that of the lumbar discs. This is due to the amount of extra load transferred to the thoracic spine from the vertebrae above, therefore increasing the need for greater load distribution [32]. The average cross-sectional areas of the thoracic discs are as follows; T1/T2 having an area of 510 mm^2; T2/T3 having an area of 490 mm^2; T3/T4 having an area of 485 mm^2; T4/T5 having an area of 450 mm^2; T5/T6 having an area of 605 mm^2; T6/T7 having an area of 750 mm^2; T7/T8 having an area of 710 mm^2; T8/T9 having an area of 900 mm^2; T9/T10 having an area of 840 mm^2; T10/T11 having an area of 1080 mm^2; T11/T12 having an area of 1170 mm^2; T12/L1 having an area of 1190 mm^2 [32]. Although the thoracic discs are greater in cross-sectional area than the cervical discs, they are still thinner in comparison. This is because the thoracic spine does not go through as much flexion/extension and rotation as the other sections of the spine, mainly due to the attachment of the rib cage [32]. The average thicknesses of the thoracic discs are as follows; T1/T2 having a thickness of 4.4 mm; T2/T3 having a thickness of 3.5 mm; T3/T4 having a thickness of 3.3 mm; T4/T5 having a thickness of 3.2 mm; T5/T6 having a thickness of 3.5 mm; T6/T7 having a thickness of 4.1 mm; T7/T8 having a thickness of 3.9 mm; T8/T9 having a thickness of 5.3 mm; T9/T10 having a thickness of 4.8 mm; T10/T11 having a thickness of 6.5 mm; T11/T12 having a thickness of 5.4 mm; T12/L1 having a thickness of [34, 36, 37]. Although the majority of the thoracic discs also show a greater height in the anterior section as opposed to the posterior section (exception of T4/T5, T5/T6, and T10/T11), like that of the cervical discs, the difference is not to the same extent as the other sections of the spine [32], **Figure 11**.

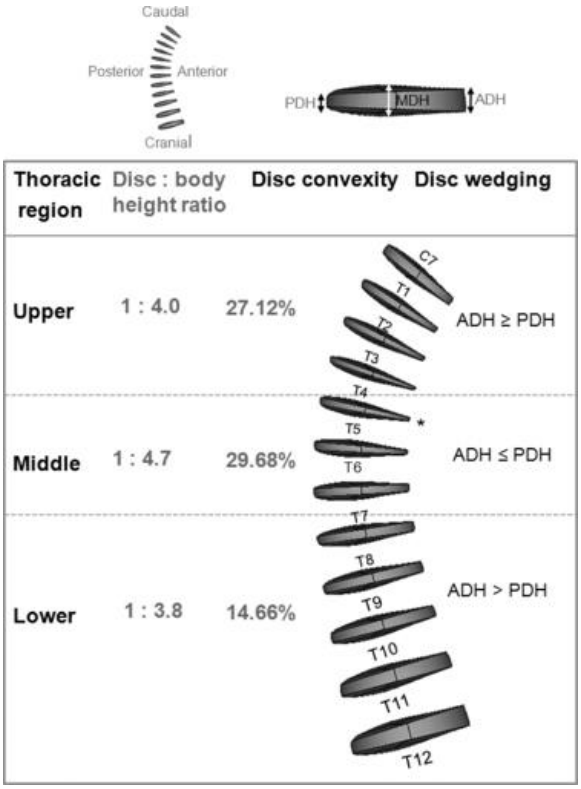

Figure 11. Geometric model of the human thoracic discs from C7/T1 to T11/T12, constructed with parameters derived from morphometric analyses. The thinnest disc was found in the disc level T4/T5, and disc shape was determined by the relationships between the anterior, middle and posterior disc heights (ADH, MDH, PDH) [34]. (Used under fair use, 2017).

Because of the lack of mobility throughout the thoracic spine, its discs tend to have very little torsional stress, giving them a very low chance to become injured from degradation. However, if a high impact is sustained in the thoracic spine, there is a possibility of disc damage, although it is much more common for one of the vertebra to fracture before damage to the disc occurs [38].

1.1.6.3 Lumbar Discs

The lumbar spine consists of five intervertebral discs (L1/L2 – L5/S1) [2]. These discs have the greatest cross-sectional area out of all of the spinal sections, with L2/L3 – L5/S1 being virtually equal. This is because the lumbar discs need to withstand the greatest amount of load without building up too much pressure and failing [32]. The average cross-sectional areas of the lumbar discs are as follows; L1/L2 having an area of 1400 mm^2; L2/L3 having an area of 1640 mm^2; L3/L4 having an area of 1690 mm^2; L4/L5 having an area of 1660 mm^2; L5/S1 having an area of 1680 mm^2 [32]. Like the cervical spine, the lumbar spine

goes through an incredible amount of flexion/extension and torsion causing a great deal of stress and strain on the discs. Due to these factors, they have to be extremely thick, relative to the other discs, so as well as having the greatest amount of surface area, the lumbar discs also have the greatest thickness [32]. The average thicknesses of the lumbar discs are as follows; L1/L2 having a thickness of 7.65 mm; L2/L3 having a thickness of 8.9 mm; L3/L4 having a thickness of 9.25 mm; L4/L5 having a thickness of 9.9 mm; L5/S1 having a thickness of 9.35 mm [37, 39]. The lumbar discs also have a high ratio of anterior disc thickness to posterior disc thickness, the greatest being the L5/S1 disc, causing the lumbar spine's natural convex curvature similar to the cervical spine (refer to **Figure 10**) [37, 39]. Because of the mobility of the lumbar spine and the tremendous loads it must endure, sometimes being in the thousands of newtons, its discs have a significantly higher chance of becoming damaged from bending and torsion, making it the most common spinal section for disc injury [40].

1.1.7 Intervertebral Disc Composition

Each intervertebral disc is a complex structure comprised of three main components, a thick outer ring of fibrous cartilage called the annulus fibrosus, a more gelatinous core called the nucleus pulposus, and cartilage vertebral endplates. These components give certain necessary properties to the intervertebral discs' structural integrity and properties as a whole [41], **Figure 12**.

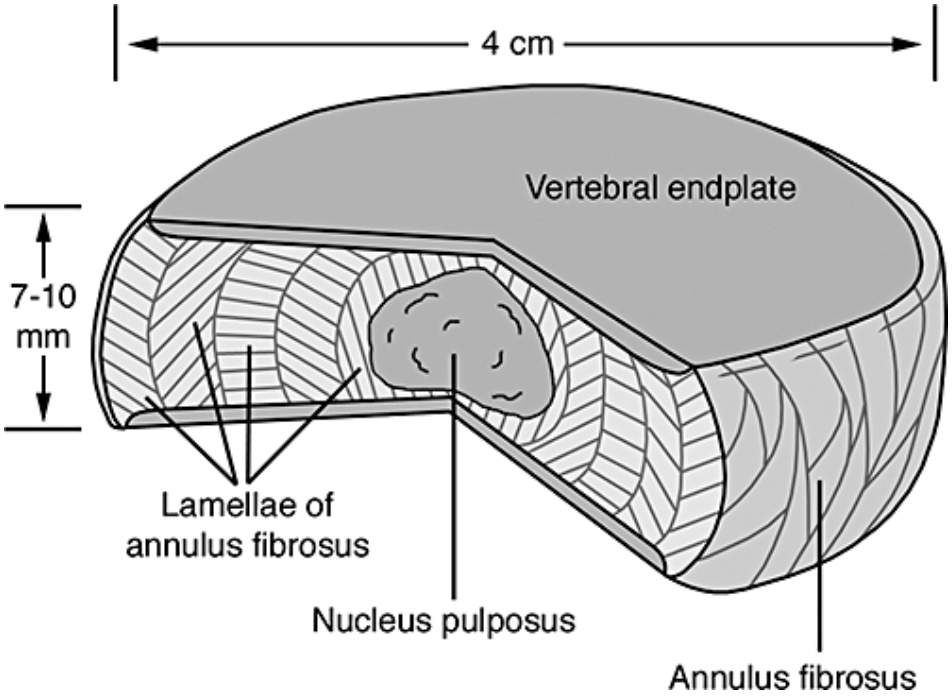

Figure 12. A cut out portion of a normal disc depicting the nucleus pulposus, vertebral endplates, and annulus fibrosus. The chosen intervertebral disc is 4 cm wide and 7-10 mm thick [41]. (Used under fair use, 2017).

Along with the components mentioned above, the discs have a constant blood supply and flow of nutrients throughout to ensure the spinal cord and cells within the discs are healthy. This helps with the biochemical elements vital to keep the discs alive and functioning properly [42]. To better understand the functions and properties of each component, they will be further broken down for more concise detail.

1.1.7.1 Annulus Fibrosus

The annulus fibrosus consists of concentric rings, or lamellae, surrounding the nucleus pulposus, and is referred to as having two main sections, the inner and outer annulus fibrosus. Both of these sections are composed of mostly water (70-78% inner and 55-65% outer wet weight), fibrocartilage (type I and type II collagen, 25-40% inner and 60-70% outer dry weight), proteoglycans (11-20% inner and 5-8% outer dry weight), and other factors involved in extracellular-matrix, however with increasing radial distance from the nucleus, the concentration of some of these components change, mainly collagen and proteoglycans [3, 43, 52]. These cells and tissues help create the more rigid structure of the annulus fibrosus necessary to carry out its vital roles in the intervertebral discs. The structure of multiple lamella and alternating collagen

fiber angles help give the annulus fibrosus its major functions including, housing the nucleus pulposus, keeping it under pressure and from impinging on the spine, and enabling the disc to withstand complex loads with its inhomogeneous, anisotropic, and nonlinear mechanical behaviors [44].

1.1.7.1.1 Cells and Tissues

There are three main cells and tissues found in the annulus fibrosis; fibrocartilage (collagen fibrils), proteoglycans, and other factors involved in the extracellular-matrix (ECM). Each play a vital role in the performance and health of the annulus fibrosus, and without such could not support the demands of the spine [44].

Collagens are important by playing structural roles and contributing to the mechanical properties, organization, and shape of the annulus fibrosus tissues, and come in many different isoforms, more than 28 of which have already been identified. It is one of the most abundant ECM proteins in the body, and can take multiple structures of either fibril forming or short-helix [45]. The annulus fibrosus contains only fibril forming collagen, collagen type I and type II, which forms the fibrocartilage of the lamellae, **Table 1**. The collagen types I and II replace one another in a smooth gradient, transitioning from 100% type I in the furthest outer lamella, to 100% type II in the furthest inner lamella. Not only does the type of collagen change as radial distance increases, but the concentration of collagen as well, increasing from inner annulus to outer annulus [52]. This creates a smooth transition zone between the nucleus pulposus and the outer annulus fibrosus [46].

Table 1. Types of collagen found in lamellae of the annulus fibrosus [45, 74].

Collagen type	Structure	Genes	Alpha chains	% of total collagen content	Distribution
Collagen I	Large diameter, 67-nm banded fibrils	COL1A1 COL1A2	α1(I) α2(I)	0 → 100	Increases from inner to outer regions
Collagen II	67-nm banded fibrils	COL2A1	α1(II)	100 → 0	Decrease from inner to outer regions

All collagen consists of a triple helix structure comprised of three polypeptide chains [47]. These polypeptide chains, called alpha (α) chains, further diversify the collagen family by creating several molecular isoforms for the same collagen, as well as hybrid isoforms comprised of two different collagen types. The size of these α chains can vary from 662 to 3152 amino acids for humans, and can either be identical to form homotrimers or different to form heterotrimers [45]. Collagen type I is considered a heterotrimer consisting of α1(I) and α2(I), while collagen type II is considered a homotrimer consisting of only α1(II), both of which are found in the annulus fibrosus.

After the transcription and translation of the procollagen α chains, four distinct stages occur for the assembly of collagen fibrils. The first stage is importation into the rough endoplasmic reticulum, where the α chains are modified to form the triple-helical procollagen. The second stage is the modification of the procollagen in the Golgi apparatus and its packaging into secretory vesicles. The third stage is the formation of the collagen molecule in the extracellular space by cleavage of the procollagen. The final stage is the crosslinking between the collagen molecules to stabilize the supramolecular collagen structure [47], **Figure 13**. These collagen fibrils are vital to the structure, strength, and flexibility of the fibrocartilage in the annulus fibrosus lamellae.

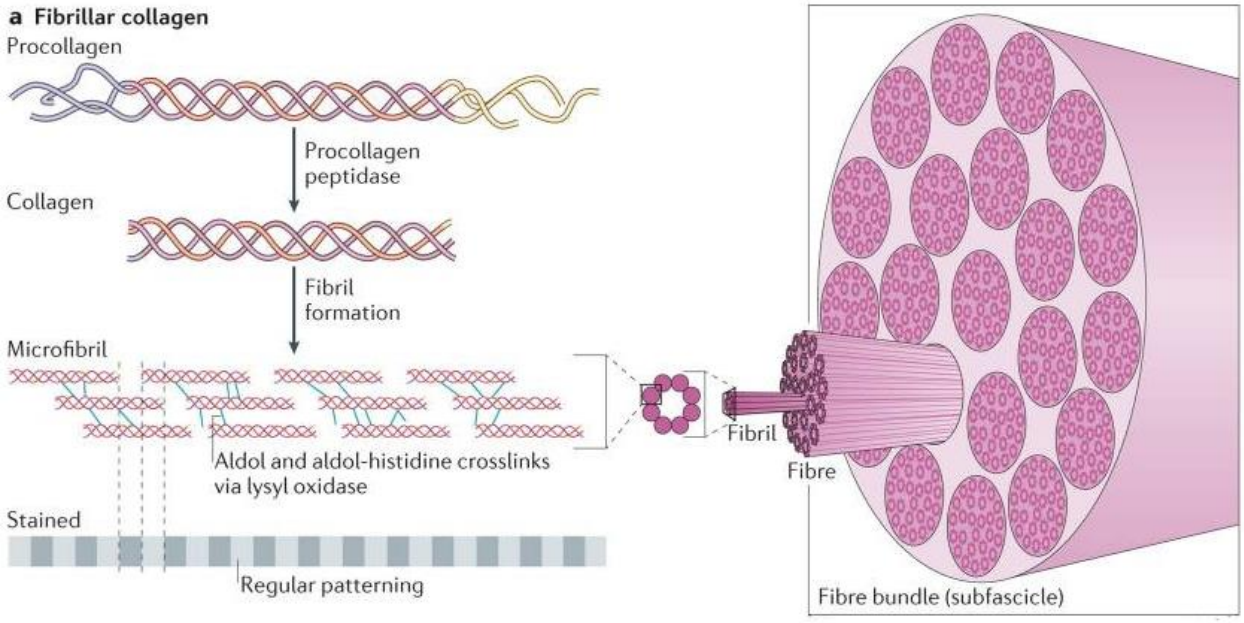

Figure 13. Construction of fibrillary collagen as described above [47]. (Used under fair use, 2017).

Proteoglycans are glycosylated proteins which have covalently attached highly anionic glycosminoglycans (GAGs). Major GAGs include heparin sulphate, chondroitin sulphate, dermatan sulphate, hyaluronan, and keratin sulphate [47]. They are less abundant proteins found in the annulus fibrosus ECM, and instead of being predominantly fibrillar in structure, like collagen, they form the basis of higher order ECM structures around cells. The main family of proteoglycans that have been implicated in fibrillary collagen assembly is the small leucine-rich repeat proteoglycans (SLRPs) due to their collagen-binding properties. These SLRPs consist of two regions, a variable N-terminal domain containing sulphated tyrosine and a conserved carboxy terminus that contains the leucine-rich repeats, and affect collagen fibril growth rate, size, morphology, and content [47].

Their major biological function is to bind water to provide hydration and swelling pressure of the tissue giving it compressive resistance, which are derived from the physiochemical characteristics of the GAG component of the molecule [48]. Inverse of the collagen, the proteoglycan concentration has an increasing gradient from outer annulus to inner annulus, or transition zone [52].

1.1.7.1.2 Structure

The annulus fibrosus has a unique structure consisting of anywhere from 15 to 25 distinct layers (lamellae), depending on the circumferential location, the spine level, and the individual's age, with the thickness of these individual lamellae varying both circumferentially and radially as age increases [49]. Each adjacent lamella is held together by discrete collagenous bridging structures, which are orientated radially to wrap around individual collagen fibers and prevent severe delamination [50]. Based on the location of the disc, the amount of collagen fibril bundles in each lamella can vary from 20 to 62 bundles over the total height of the disc, with an average interbundle spacing of 0.22 mm and bundle thickness of roughly 10 microns [49], **Figure 14**. These bundles sit at different angles ranging anywhere from 55º to 20º, alternating direction every other layer, and have a planar zig-zag (crimped) structure, allowing them to

be stretched and extend more as the crimps straighten out. This allows for the rotational and flexion/extension mobility of the spine [50, 51].

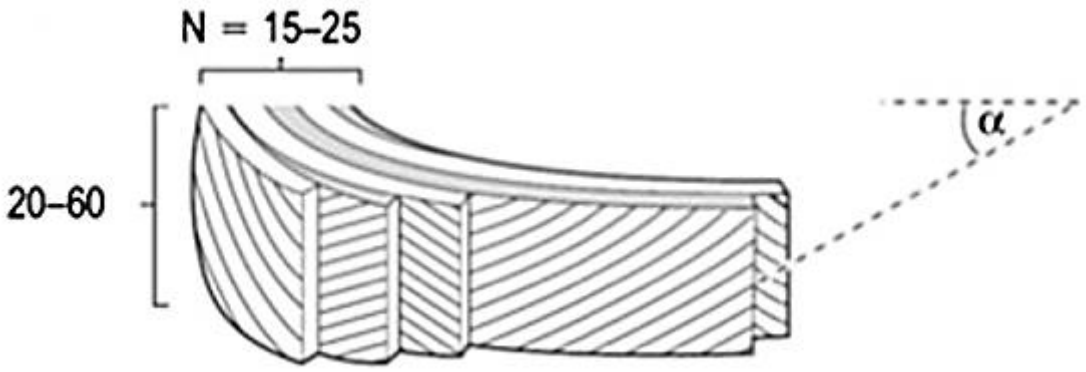

Figure 14. Diagram showing the detailed structure of the annulus fibrosus, with its 15 – 25 lamellae comprised of 20 – 62 collagen fiber bundles [50]. (Used under fair use, 2017).

The annulus fibrosus' unique structure helps give it its mechanical functions of containing the radial bulge of the nucleus, enabling a uniform distribution and transfer of compressive loads between vertebral bodies, and to distend and rotate, allowing and facilitating joint mobility [52].

1.1.7.1.3 Mechanical Properties

Like the collagen and proteoglycan concentration, the mechanical properties of the annulus fibrosus differ with an increase in radial distance, usually becoming stronger and stiffer towards the outer annulus. These mechanical properties are highly anisotropic and nonlinear in uniaxial tension, compression, and shear, and have a high tensile modulus in the circumferential direction [53]. In particular, the tensile properties of the lamella show drastic differences depending on what samples are tested and with what alignment they are tested. When testing parallel to the alignment of the collagen fiber bundles as opposed to perpendicular, the strength and modulus increases due to the strength and reinforcement given by the fibers, and the same correlation can be found when testing the outer lamellae as opposed to the inner lamellae [53, 54], **Table 2**.

Table 2. Tensile properties of the annulus fibrosus [55, 56].

Sample	Sample Specification	Yield Stress, MPa	Ultimate Stress, MPa	Elastic Modulus, MPa	Yield Strain, %	Ultimate Strain, %	Stiffness, N/m
Bulk Annulus	**Outer, A**	--	3.9 ± 1.8	16.4 ± 7.0	20 – 30*	65 ± 16	5.7 ± 3.4
	Outer, P	--	8.6 ± 4.3	61.8 ± 23.2	20 – 30*	34 ± 11	5.7 ± 3.4
	Inner	--	0.9	--	20 – 30*	33	1.2 ± 1.1
Single Lamella	**Parallel**	--	--	80 - 120	--	--	--
	Perpendicular	--	--	0.22	--	--	--

A/P, interior/posterior section of the annulus
Parallel/Perpendicular, alignment of testing in relation to the fiber orientation
* Only one value was ascertained for entirety of the annulus fibrosus

Although the elastic modulus of the lamella differs by a factor of roughly 500, with respect to fiber orientation, when tested together in relation to how the disc might actually perform, the modulus instead hovers around 18 – 45 MPa [56]. As the stress induced on the annulus fibrosus increases, the rigidity of the system increases. This mechanical behavior leads to the stiffening of the intervertebral disc tissue for larger strains, due to the uncrimping of the collagen fibers. Not only does the stiffness relate to amount of strain on the annulus fibrosus, but also the load rate of the induced stress [57].

The annulus fibrosus is the only section of the disc that undergoes tensile stress and strain, and it is usually due to these stresses that the collagen fibrils breakdown and deteriorate, making its unique tensile properties a focus when studying disc degeneration. However, while tensile properties are important for the understanding of how much stress and strain the annulus fibrosus can withstand, the injuries sustained are rarely due to a single impact, but more often the cyclic loading of the spine that causes deterioration of the collagen fibrils [55]. Therefore, because the disc goes through thousands of cycles on a daily basis, cyclic loading tests are crucial for the understanding of the annulus fibrosus' mechanical integrity. Cyclic loading tests were performed on the anterior and posterior sections of the annulus fibrosus, with different loads (% ultimate tensile strength, UTS) until either failure occurred or 10000 cycles had been reached. When the stress applied was less than 45% of the UTS, fatigue failure did not occur, meaning that the sample reached 10000 cycles [55].

Although not as important for the annulus fibrosus as it is for the nucleus pulposus, compressive stresses and strains do occur on the lamellae, **Table 3**. However, they have very little effect on the degradation of the annulus fibrosus, therefore are not tested to the extent of the tensile properties. Most often only the swell pressure (P_{sw}), modulus (H_A), and permeability (k) are measured [58].

Table 3. Compressive properties of the annulus fibrosus [58].

Section of Annulus Fibrosus	Swell Pressure, (P_{sw}), MPa	Modulus, (H_A), MPa	Permeability, (k), ($x10^{-15}$ m^4/N-s)
Anterior	0.11 ± 0.05	0.36 ± 0.15	0.26 ± 0.12
Posterior	0.14 ± 0.06	0.40 ± 0.18	0.23 ± 0.09
Outer	0.11 ± 0.07	0.44 ± 0.21	0.25 ± 0.11
Middle	0.14 ± 0.04	0.42 ± 0.10	0.22 ± 0.06
Inner	0.12 ± 0.04	0.27 ± 0.11	0.27 ± 0.13

1.1.7.2 Nucleus Pulposus

The nucleus pulposus resides in the middle of the disc surrounded by the annulus fibrosus, which keeps it from leaking into the spinal canal. It consists of randomly organized collagen fibers (15-20% dry weight) and radially arranged elastin fibers, housed in a proteoglycan hydrogel (50% dry weight), with chondrocyte-like cells interspersed at a low density of approximately 5000/mm^3 [3, 59]. The nucleus is an incompressible structure that it is made up of about 80-90% water, which helps it carry out its vital roles in the intervertebral disc of compressive load dispersion, compressive shock absorption, and keeping the inside of the disc swollen for necessary internal pressure [60].

1.1.7.2.1 Cells and Tissues

There are four main components found in the nucleus pulposus; collagen fibrils and elastin fibers (roughly 150 micrometers in length), proteoglycans, and chondrocyte-like cells. Each play a vital role in the performance and health of the nucleus pulposus, giving it the necessary material and mechanical properties to serve its functions [61]. Although the two similar components between the nucleus and the annulus were previously discussed (collagen type II and proteoglycan), the other two components, elastin fibers and chondrocyte-like cells were not.

Unlike the annulus fibrosus, the collagen in the nucleus forms a loose network, which is joined by the network of elastin fibers. The elastin fibers are necessary for maintaining collagen organization and recovery of the disc size and shape after the disc deforms under various loads. It accomplishes this with its unique structure of microfibrils forming a meshwork around a central elastin core, **Figure 15**. These microfibrils are structural elements of the nucleus' ECM, and have been found distributed in connective and elastic tissues such as blood vessels, ligament, and lung [62].

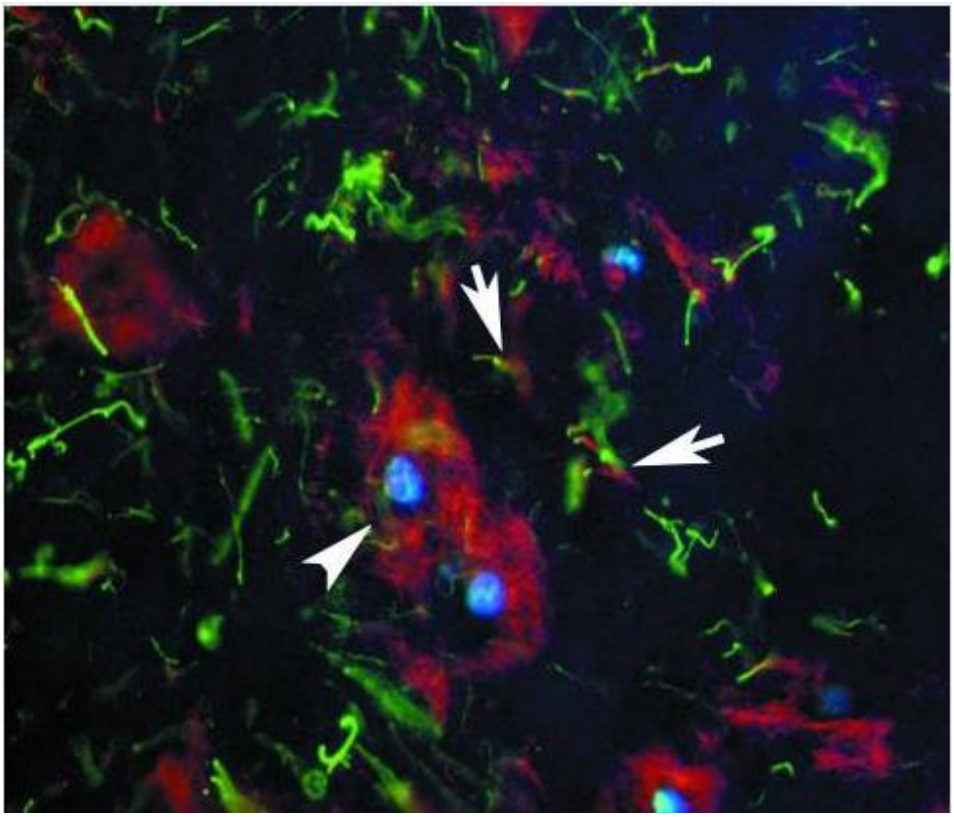

Figure 15. Fluorescence microscopic images of stained components in the nucleus pulposus. The microfibrils (red) show a tendency to hover/organize around the nucleus pulposus cells (blue), while the elastin fibers (green) have a tendency to stay dispersed through the entire ECM [62]. (Used under fair use, 2017).

The microfibrils play vital roles in the properties of the elastic fibers, such as conferring mechanical stability and limited elasticity to tissues, contributing to growth factor regulation, and playing a role in tissue development and homeostasis. Microfibrils are made up of a multicomponent system, consisting of a glycoprotein fibrillin core (three known types), microfibril associated proteins (MFAPs), and microfibril

associated glycoproteins (MAGPs). The MFAPs and MAGPs, as well as a few other peripheral molecules, contribute to link microfibrils to elastin, to other ECM components, and to cells [63].

In the nucleus pulposus, the chondrocyte-like cells act as metabolically active cells that synthesize and turnover a large volume of ECM components, mainly collagen and proteoglycans [64]. They produce and maintain the ECM with the presence of Golgi cisternae and well-developed endoplasmic reticulum, and are able to withstand very high compressive loads and help with the movement of water and ions within the matrix [65]. They also maintain tissue homeostasis, play a role in the physio-chemical properties of cartilage-specific macromolecules, and prevent degenerative diseases like degenerative disc disease and osteoarthritis. However, with age these cells start to become necrotic, increasing from about 2% at birth to 50% in most adults. This can lead to cartilage/collagen degradation, abnormal bone growth (osteophyte) formation on the vertebrae where bone on bone friction occurs, and stiffening of joints [61, 64].

1.1.7.2.2 Structure

The nucleus pulposus is a soft, gelatinous mass that is irregularly ovoid and is found under pressure in the center of the disc. Because it is mostly water (between 80-90%), it does not have a definite structure or form, but like a liquid, takes the shape of wherever it is confined [66]. From birth to adolescence, the nucleus pulposus is a semi-fluid mucoid mass formed by proliferation and degeneration of embryological notochord cells with a few scattered cartilage cells and collagen fibers. As age increases into adulthood, the notochord cells completely degenerate and become replaced by chondrocyte-like cells, which help give the nucleus its structure and mechanical properties. Also with age, the nucleus becomes less fluid-like and more cartilaginous as the collagen fibrils start to crosslink together forming fibers like that of the annulus [67].

1.1.7.2.3 Mechanical Properties

Being virtually an incompressible liquid, the nucleus pulposus does not endure any tensile stresses or strains, and the loads it can withstand in compression are largely due to the force that the annulus fibrosus can resist radially, as well as the swell pressure already exerted internally by the nucleus [56]. When tested

for compressive properties, the nucleus had to be confined so that accurate measurements could be taken, **Table 4**.

Table 4. Confined compressive properties of the nucleus pulposus [56].

Sample	Swell Pressure, (P_{sw}), MPa	Modulus, (H_A), MPa	Permeability, (k), ($x10^{-16}$ m^4/N-s)
Nucleus Pulposus	0.138	1.0	9.0

However, when observed with regards to everyday activities in situ, the lumbar compressive forces can fluctuate between 800 N and 3,000 N. This causes the nucleus to become pressurized up to 0.4 MPa while lying down, 1.5 MPa while standing or sitting, and up to 2.3 MPa while actively lifting [68]. Although the mechanical testing of the nucleus pulposus is not quite as extensive as that of the annulus fibrosus, it does not make it any less important to the structural and mechanical properties of the disc as a whole.

1.1.7.3 Vertebral Endplates

The vertebral endplates are situated on the top and bottom of each intervertebral disc, and are comprised of hyaline cartilage with proteoglycans for swelling properties [69]. Their main function is to connect the dense, harder cortical bone shell of the vertebrae to the annulus and nucleus via mechanical interlocking, and to keep the nucleus pressurized and from bulging into the soft, spongy/cancellous trabecular bone center of the vertebrae, **Figure 16**. The vertebral endplates are the strongest part of the intervertebral disc, and usually fail after the vertebral body has already fractured [50].

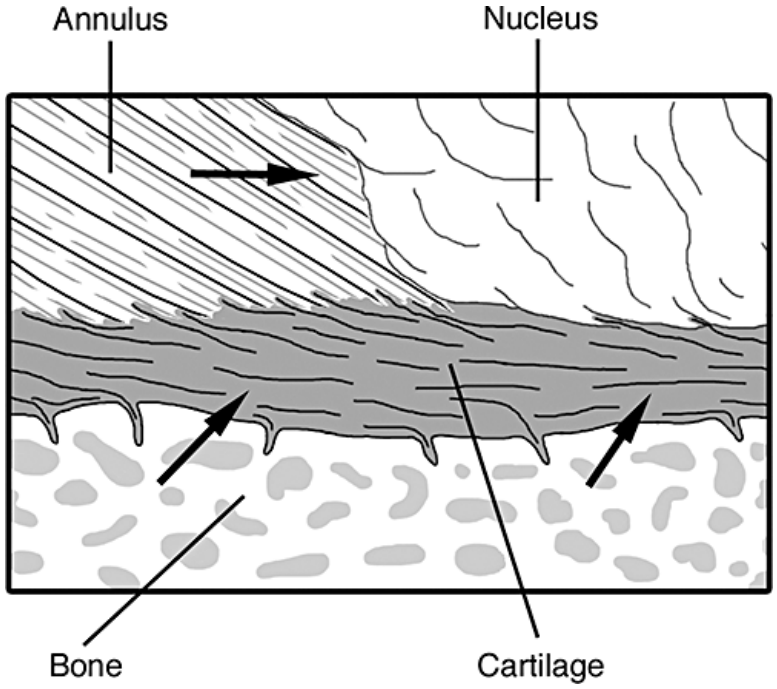

Figure 16. The connection of the hyaline cartilage vertebral endplate to the perforated cortical bone of the vertebral body and collagen fibers of the annulus and nucleus. The arrows in the figure refer to the direction of nutrients and blood flow through the different components of the disc, mainly coming from the bong through the vertebral endplates [3]. (Used under fair use, 2017).

The vertebral endplates also have the unique role of acting as the main transport for nutrients and blood flow in and out of the disc. This provides the nucleus and annulus with the cells and other required components that keep the disc alive, and from degenerating [68].

1.1.7.3.1 Cells and Tissues

The vertebral endplates are made up of three main components that give them their structural integrity and strong mechanical properties, hyaline cartilage, proteoglycans, and chondrocytes [69]. Although proteoglycans and chondrocytes were previously discussed, hyaline cartilage was not.

The hyaline cartilage of the vertebral endplates maintains very similar macromolecules in their ECM as that of the nucleus pulposus, however the ratios of proteoglycan to collagen content differs drastically. The typical ratio of proteoglycans (GAG level) to collagen in the endplates is roughly 2:1, which is why it has such stiff properties as compared to the nucleus which has a ratio of 27:1 [70]. Also, distinctively different from the annulus fibrosus' fibrocartilage which contain large collagen fiber bundles,

the endplates have fine collagen fibers similar to the nucleus, but they are closely packed together. The hyaline cartilage in the endplates are made up of multiple types of collagen such as Type I, II, IV, V, VI, IX, X, and XI, however Type X collagen is the most important [71], **Table 5**. Its main role is to act as a marker of hypertrophic chondrocytes and is involved with calcification. Collagen Type II is also found in abundance in the endplates, however with age, the inactivation of the collagen Type II gene leads to lower GAG levels making the endplates calcify becoming thicker and more irregular [69]. The other collagens, Type I, III, V, VI, IX, and XI are present in small amounts, and only contribute to a minor portion of the cartilage with the main functions of forming and stabilizing the collagen Type II fibril network [71].

Table 5. Types of collagen found in the hyaline cartilage of the vertebral endplates [45, 72, 73, 74].

Collagen type	Structure	Genes	Alpha chains	% of total collagen content
Collagen I	Large diameter, 67-nm banded fibrils	COL1A1 COL1A2	α1(I) α2(I)	<1
Collagen II	67-nm banded fibrils	COL2A1	α1(II)	90 – 95
Collagen III	Small diameter, 67-nm banded fibrils	COL3A1	α1(III)	<1
Collagen V	9-nm diameter banded	COL5A1 COL5A2 COL5A3	α1(V) α2(V) α3(V)	<1
Collagen VI	5-10 nm diameter beaded microfibrils, 100-nm periodicity	COL6A1 COL6A2 COL6A3	α1(VI) α2(VI) α3(VI)	<1
Collagen IX	Nonfibrillar, short-helix	COL9A1 COL9A2 COL9A3	α1(IX) α2(IX) α3(IX)	<1
Collagen X	Nonfibrillar, short-helix	COL10A1	α1(X)	1
Collagen XI	Fibril forming	COL11A1 COL11A2 COL2A1	α1(XI) α2(XI) α3(XI)	<1

All of the collagen structures and cellular make-up are the same for the hyaline cartilage as was previously discussed in the annulus fibrosus cells and tissues.

1.1.7.3.2 Structure

The vertebral endplates have two major structures, the collagen fibers of the cartilaginous section (roughly 0.1 to 0.2 mm thick) and the bony components of the vertebral section (roughly 0.2 to 0.8 mm thick). For the cartilaginous section, the collagen fibers, enveloped in a proteoglycan hydrogel, run horizontal and parallel close to the vertebral bodies, however the fibers then continue into the annulus fibrosus at an angle [3]. The integration between the collagen fibers in the nucleus and the endplates is more convoluted. For the vertebral section, the bony component of the endplate is a thick, porous layer of fused trabecular bone with osteocytes embedded within saucer-shaped lamellar packets, resembling the structure of the vertebral cortex [68].

The most important structural features of the endplate biomechanical functions are the thickness, porosity, and curvature. For example, thick, dense endplates with a high degree of curvature are stronger than thin, porous, and flat endplates [68]. They are typically less than 1.0 mm thick, and cover the entire surface area of the top and bottom of the intervertebral disc. The thickness across the width of the disc is not uniform, varying considerably, while tending to be the thinnest in the central region adjacent to the nucleus [69]. The density tends to increase towards the vertebral periphery where the subchondral bone growth starts, however porosity can increase up to 50 – 130% with aging and disc degeneration. Due to the variations throughout the structure of the vertebral endplate, its mechanical properties vary as well [75, 78].

1.1.7.3.3 Mechanical Properties

The mechanical properties of the vertebral endplates vary with the area on which the endplate was tested as well as the area of the spine from which the endplate was tested. The central area of the endplates tends to be the weakest, and increases in strength and stiffness radially towards the outer annulus. When tested in different sections of the spine, the endplates show a significant increase in strength and stiffness from superior to inferior sections of the spine. Not only do the properties change between spinal sections, but also within the same section, such as the stiffness and strength increasing as the lumbar spine descends (L1/L2 – L5/S1) [75]. Due to the unique structure of the endplates, they are able to withstand an incredible

amount of load, outlasting the vertebral body more often than not. The failure of the vertebral endplate tends to occur around 10.2 kN, however the failure of the vertebral body, usually due to fracture, occurs around 4.2 kN in individuals 60 years of age or older, and around 7.6 kN in individuals 40 years or younger [50, 76]. Not only do the endplates have great strength, but they also possess great stiffness properties (1965 ± 804 N/mm) that allow it to be semi-flexible during the loads put onto the spine. This helps the nucleus move and cushion loads more readily inside of the disc, while also protecting the endplates from tensile damage, of which they are most likely to fail [68, 77].

1.1.7.4 Blood Vessels and Nerve Supply

Because the intervertebral disc is one of the most avascular tissues in the human body, in a healthy adult, it tends to have very few blood vessels. However, during early stages of life, blood and lymph vessels can be found throughout the majority of the disc with the exception of the nucleus. With age, blood and lymph vessels found in the tissues of the disc start to decrease and migrate towards the outer parts of the disc, only extending into the annulus up to roughly 20 years of age, only extending into the vertebral endplates up to roughly 7 years of age, and never extending into the nucleus at any age, **Figure 17,** [3, 79].

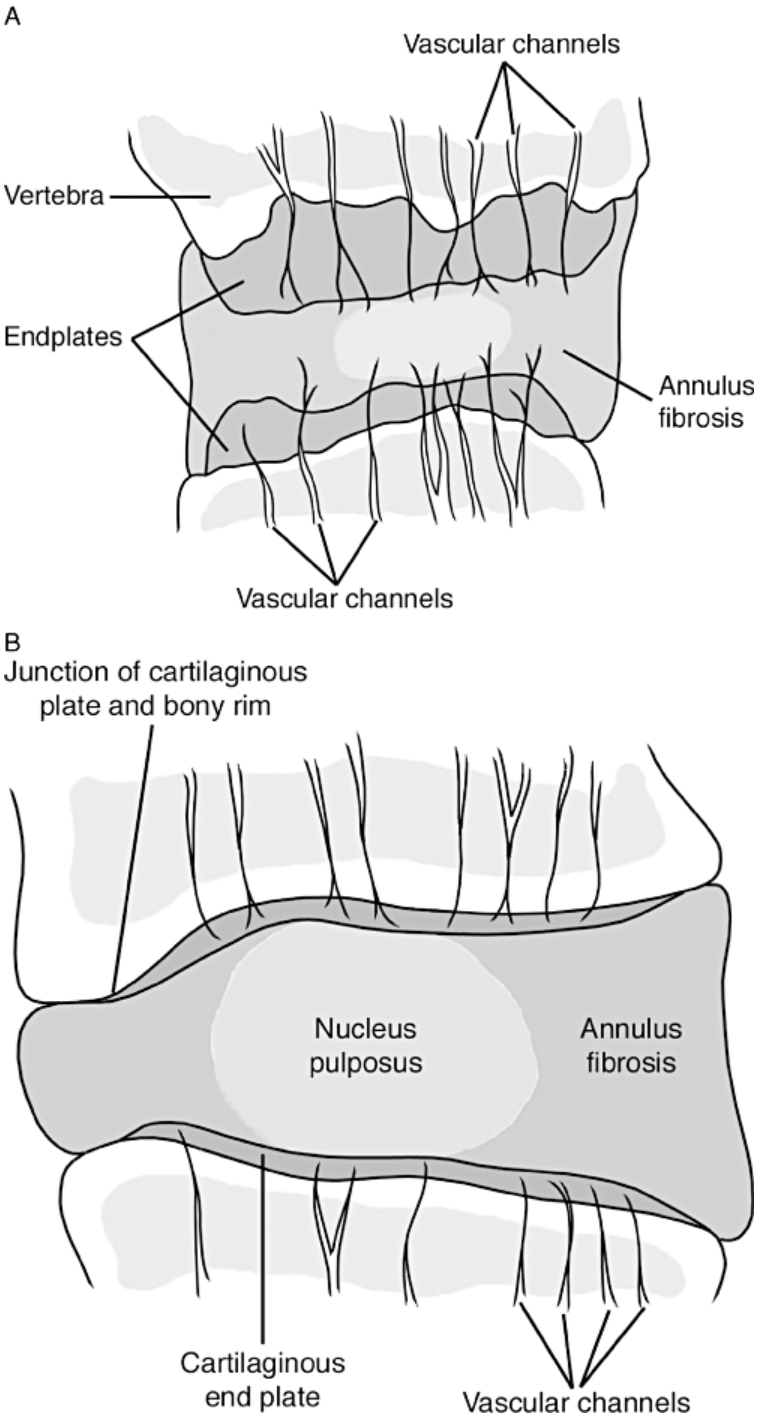

Figure 17. (A) represents the multiple longer and thicker vascular channels throughout the intervertebral disc a 10-month old girl, while (B) represents the vascular channels throughout the disc of a 50-year old adult, showing the retraction and thinning of the channels [3]. (Used under fair use, 2017).

In fetal and infantile ages, blood vessels perforate the endplates and extend into the inner and out annulus, however in adolescence and adults, blood vessels were only found in the outer annulus adjacent

to the insertion of ligaments. Given the size of the avascular structure, once these blood vessels retract from the disc in adulthood, the discs rely on long diffusion through the endplates and annulus for the nutritional supply of the disc cells [80]. The cellular capacity to survive under critical nutritional and metabolic conditions is therefore significantly reduced. This is said to contribute to the degeneration of the discs, giving a reason for the low structural and functional restoration properties of the disc tissues during aging, especially with regards to the poor nutritional situation of the cells in the nucleus [80].

The intervertebral discs are supplied by a variety of nerves, some of the most important residing in the cervical and lumbar spine. Recurrent sinuvertebral nerves innervate the posterior and some of the posterolateral aspects of the disc, and the posterior longitudinal ligament, branching off of the dorsal root ganglion extending from the spinal cord. The other posterolateral aspects receive branches from the adjacent ventral primary rami and from the grey rami communicantes [81]. Lateral aspects of the disc receive other branches from the rami communicantes, some of which cross the intervertebral disc and are embedded within the surrounding connective tissue of the disc, such as the origin of the psoas for the lumbar spine. Lastly, the anterior aspects along with the anterior longitudinal ligament are innervated by recurrent branches of rami communicantes, **Figure 18,** [81].

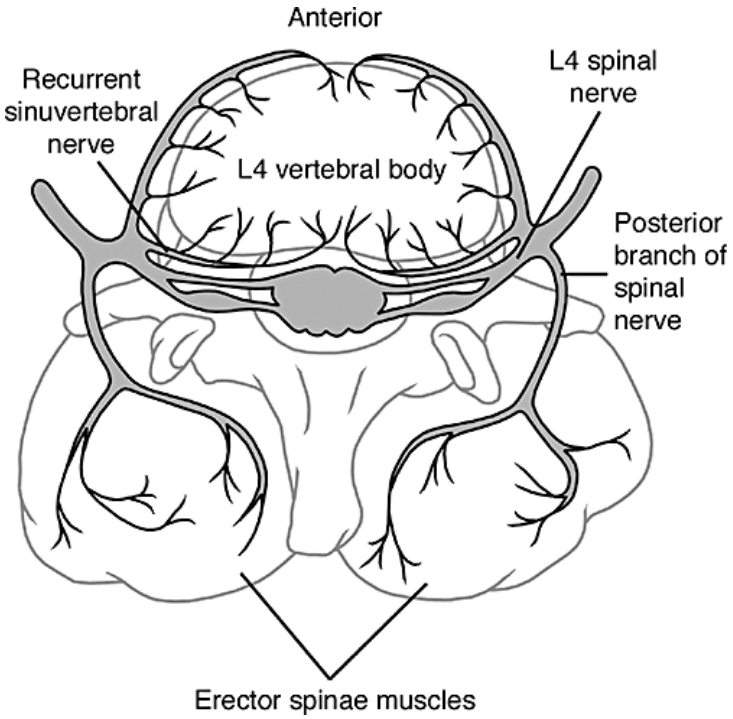

Figure 18. The innervation of a healthy intervertebral disc, showing the sinuvertebral nerves and rami communicantes extending into the vertebral foramen and the outer annulus of the disc [3]. (Used under fair use, 2017).

Opposite of blood vessels, in a healthy young adult the sensory nerve endings of the disc can be found on the superficial layers of the annulus and in the outer third of the annulus, only extending about 3 mm into the disc [82]. With age and degeneration, the nerves tend to creep into the inner parts of the disc by means of neoinnervation, arising from granulation tissue growing in the disc. This can cause innervation of the middle and inner annulus, and even potentially of the nucleus pulposus, which can bring significant problems with regard to lower back pain with the amount of pressure being induced onto the discs, and therefore pressure onto the nerves [82, 83].

1.2 Spinal Degeneration and Lower Back Pain

Back pain is a major health problem in Western industrialized societies, inflicting suffering and distress on a large number of patients and their families, especially those of old age, increasing with the increased aged population. The effects of this problem are vast, with prevalence rates ranging from 12% to 35%, and around 10% of sufferers becoming chronically disabled [84]. However, pain is not the only effect that lower back pain causes. With total costs, including direct medical costs, insurance, lost production, and

disability benefits, reaching into the billions of dollars, an enormous economic burden is placed on society [84]. In the United States alone, costs associated with lower back pain exceeds $100 billion per year, two-thirds resulting from lost wages and reduced productivity [85]. Among the other third are direct costs for medical treatments of back pain diagnoses, estimated at $34 billion out of the total $47 billion for all treatments for pain diagnoses in 2010. These costs include office-based visits, hospital outpatients, emergency services, hospital inpatients, and prescription drugs [86], **Table 6**.

Table 6. Out-of-pocket medical costs (in millions of US dollars) of lower back pain, mainly due to disc degeneration [86].

Conditions	Office-based	Hospital Outpatients	Emergency Services	Hospital Inpatients	Prescription Drugs	Total
Back Pain	$14,400	$3,000	$607	$13,500	$2,660	$34,167

Back pain is strongly associated with disc degeneration and injury, the majority of the time occurring in the lumbar spine due to the increased stresses, strains, and torsion compared to other sections, and the thoracic spine being the least affected [12].

Intervertebral discs are among the most avascular tissues in the human body, causing it to experience very little regenerative properties like that of articular cartilage. With the stresses and strains put onto the intervertebral discs on a day to day basis, along with aging, it is inevitable that they breakdown and become injured after years of wear and tear [87]. Multiple factors go into disc degeneration and injuries other than just age, such as genetic inheritance, impaired metabolite transport, altered levels of enzyme activity, cell senescence and death, changes in matrix macromolecules and water content, osteoarthritis, structural failure, and neurovascular ingrowth. Although genetic inheritance is the greatest risk factor, it does not cause discs to degenerate by itself, but instead increases their susceptibility to environmental factors like high and repetitive mechanical loading and smoking cigarettes [88].

1.2.1 Degenerative Disc Disease

Degenerative disc disease is defined by the degeneration of intervertebral discs due to aging and other environmental factors, with genetic inheritance playing a significant role in the rate of degradation. Approximately 50 – 70% of the variability in disc degeneration is caused by an individual's genetic inheritance [88]. The inherited genes associated with disc degeneration include those for collagen type IX, aggrecan, vitamin D receptor, MMP3, and cartilage intermediate layer protein. The strength of musculoskeletal tissue, like that of intervertebral discs, are affected by the products of these genes, such as the strength of the collagen fibrils throughout the annulus fibrosus. Although, an unfavorable genetic inheritance is present at birth, disc degeneration only becomes prevalent and common in the individual's 40's, and usually only in the lower lumbar spine [88]. Some individuals however, can become inflicted by this disease much earlier than the norm.

Disc degeneration can occur in individuals as young as 11 – 16 years of age, usually found in the lumbar section. This is due to the fact that discs tend to degenerate faster than any other musculoskeletal tissues [84]. Degenerative disc disease affects about 20% of people in their teens, showing mild signs of degeneration before their second decade of life. However, this disease increases drastically with age, causing around 10% of 50 year olds' discs and 60% of 70 year olds' discs to become severely degenerative hindering the daily activity of these individuals significantly [84].

Degenerative disc disease can affect the natural discs in many ways, causing them to undergo striking alterations in volume, shape, structure, and composition, that decrease the motion and alter the biomechanical properties of the nucleus pulposus and annulus fibrosus tissues, thus altering the mechanics of the spine [89]. Both the nucleus pulposus and annulus fibrosus experience changes individually, mainly in the altering of their material properties. Consequentially, because of the changes in the material properties of the substructures in the disc, such as collagen, proteoglycan, and water content, the major structural properties become hindered as well. The main structural effects tend to be the loss of swelling ability, and therefore volume of the nucleus, and tears or fissures forming in the annulus [90]. When these fissures are formed in the annulus, there is also frequently a cleft formation of some sort, particularly in the nucleus,

and the morphology becomes more and more disorganized, **Figure 18**. The vertebral endplates also go through some deformation and changes, such as porosity increasing anywhere from 50 to 130%, the natural curvature becoming less apparent and flattening out, and a significant decrease in the thickness by roughly 20 to 50% [68, 78]. These changes make the vertebral endplate much more likely to fracture under the stresses of the spine and tensile stresses induced by the nucleus.

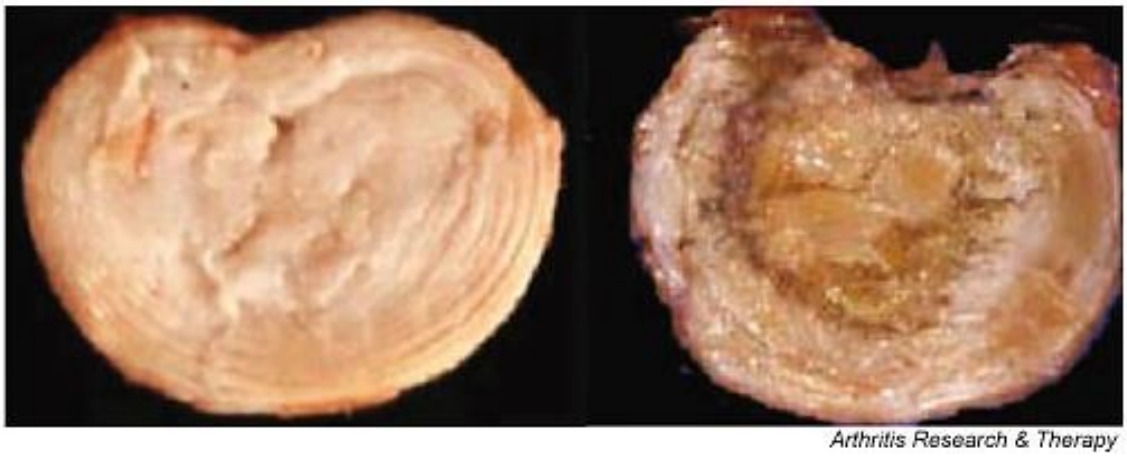

Figure 18. A healthy, normal intervertebral disc on the left, shows a distinct difference between the swollen, softer looking nucleus and the ringed annulus. However, during growth and skeletal maturation, the boundary between these components becomes less obvious, and with the nucleus generally becoming more fibrotic and less gel-like, like the highly degenerate disc on the right [84]. (Used under fair use, 2017).

Along with major structural changes, many cellular changes occur throughout the disc as well. With age and degeneration, comes an increased incidence in these cellular changes, including cell proliferation, cell death, mucous degeneration, decrease in proteoglycan content, collagen fibril cross-linking (mainly nucleus), granular changes, and concentric tears in the annulus [84]. To be more specific, nerve and blood vessels can be found in increasing numbers in the disc, during degeneration, causing cell proliferation in the nucleus, leading to cluster formation containing living, necrotic, and apoptotic cells. The cluster formations cause cell death to occur, because of the presence of cells with necrotic and apoptotic appearances. Unfortunately, these mechanisms tend to be very common with age, with more than 50% of cells in adult discs being necrotic [84].

As degeneration and symptoms get worse, the changes to the discs become more and more apparent. Therefore, a grading system has been put in place to determine the severity of the degeneration, ranking from Grade I to Grade V [91]. The ranks are based on disc structure, MRI signal intensity, distinction between the nucleus and annulus, and the height of the disc, **Table 7**.

Table 7. Distinction between different grades of disc degeneration based on MRI scans [91].

Grade	Structure	Distinction of Nucleus and Annulus	Signal Intensity	Height of Intervertebral Disc
I	Homogenous, bright white	Clear	Hyperintense, isointense to cerebrospinal fluid	Normal
II	Inhomogeneous with or without horizontal bands	Clear	Hyperintense, isointense to cerebrospinal fluid	Normal
III	Inhomogeneous, gray	Unclear	Intermediate	Normal to slightly decreased
IV	Inhomogeneous, gray to black	Lost	Intermediate to hypointense	Normal to moderately decreased
V	Inhomogeneous, black	Lost	Hypointense	Collapsed disc space

Although the grading scale has shifted from the previous system focusing on the posterior abnormalities of the discs, distinguishing among bulging, protrusion, and extrusion, (Grade I through Grade III respectively), the MRI images used for the current grading scale still show the symptoms of all three past grades, **Figure 19**. It can be seen that Grade II – III shows a slight bulging of the nucleus (more prominent in Grade III), Grade IV shows the beginning stages of protrusion of the disc, and Grade V shows a fully blown-out disc in which the entire nucleus has be extruded into the spinal canal [91].

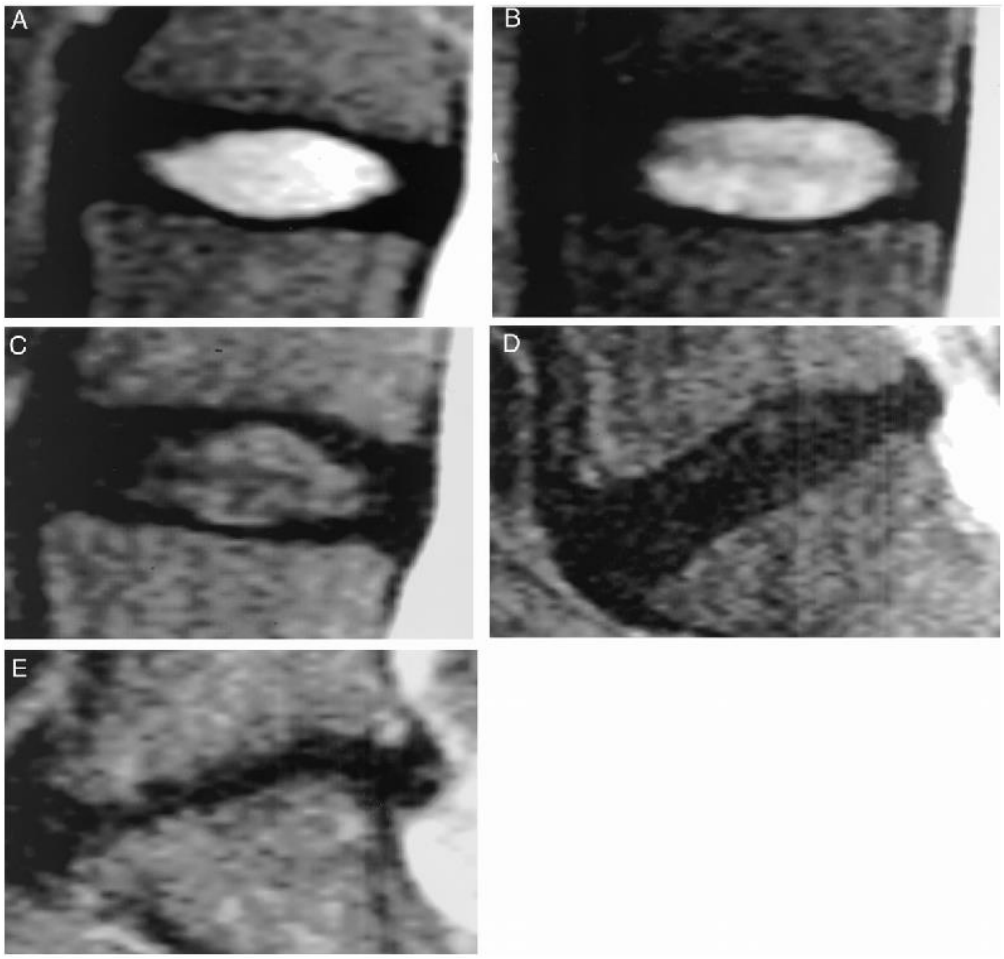

Figure 19. MRI scans showing the different grades of disc degeneration based on new grading system, A-E referring to Grades I-V: A is representative of Grade I degeneration, B is representative of Grade II degeneration, C is representative of Grade III degeneration, D is representative of Grade IV degeneration, and E is representative of Grade V degeneration [91]. (Used under fair use, 2017).

1.2.2 Osteoarthritis

Although not as common of a cause for disc degeneration as degenerative disc disease, osteoarthritis can have a significant impact on the structural changes of the intervertebral discs, causing major problems to arise later down the road. Osteoarthritis is a fairly common degenerative disorder of the articular cartilage associated with hypertrophic changes in bone, which tend to be involved in the facet joints and vertebrae of the spine, especially the lumbar spine [92]. Many risk factors can affect the probability as well as severity of osteoarthritis including genetic inheritance, female gender, past physical trauma, increased age, and obesity. Symptoms usually include joint pain that increases with movement, trouble or disability with activities of daily living, and lower back pain associated with narrowing disc

space. With the current U.S. population living longer and becoming more obese, osteoarthritis has become more common than it ever has before, affecting an estimated 27 million adults in the U.S. [92, 93].

Peripheral joints such as hips, knees, and hands, were most commonly thought of with regards to osteoarthritis, with prevalence in the spine often being ignored. However, the prevalence of disabilities and functional distress caused to the spine by osteoarthritis are actually quite high. In the lumbar spine, it is a very common condition, with a prevalence range of roughly 40 – 85% based on age, weight, and other factors specified. Also, the spinal degeneration process has been partly linked to osteoarthritis, with disc space narrowing from the formation of vertebral osteophytes, and facet joints structure changing due to the fact that it has similar pathological degenerative processes to appendicular joints [93]. Both the intervertebral discs and facet joints play vital roles in the motion of the spine, especially in the cervical and lumbar spines, therefore when they are heavily affected by osteoarthritis, the mobility of the spine can decrease significantly, and pain can ensue from even the slightest of movements.

Three main components are observed with regards to osteoarthritis in spine, referred to as the "three joint complex." These components include the structures of vertebral osteophytes, facet joint osteoarthritis, and disc space narrowing. With the amount of nerve supply running through all of these spinal structures, lower back pain can be generated by any of them [93]. With further progression of disc degeneration in the spine, the facet joints as well as vertebrae undergo more osteoarthritis, due to disc space narrowing, which in turn puts even more stresses onto the intervertebral discs. Facet joint osteoarthritis is a multifactorial process, that is highly affected by disc degeneration, leading to greater loads and motions endured by the joints, **Figure 20** [94].

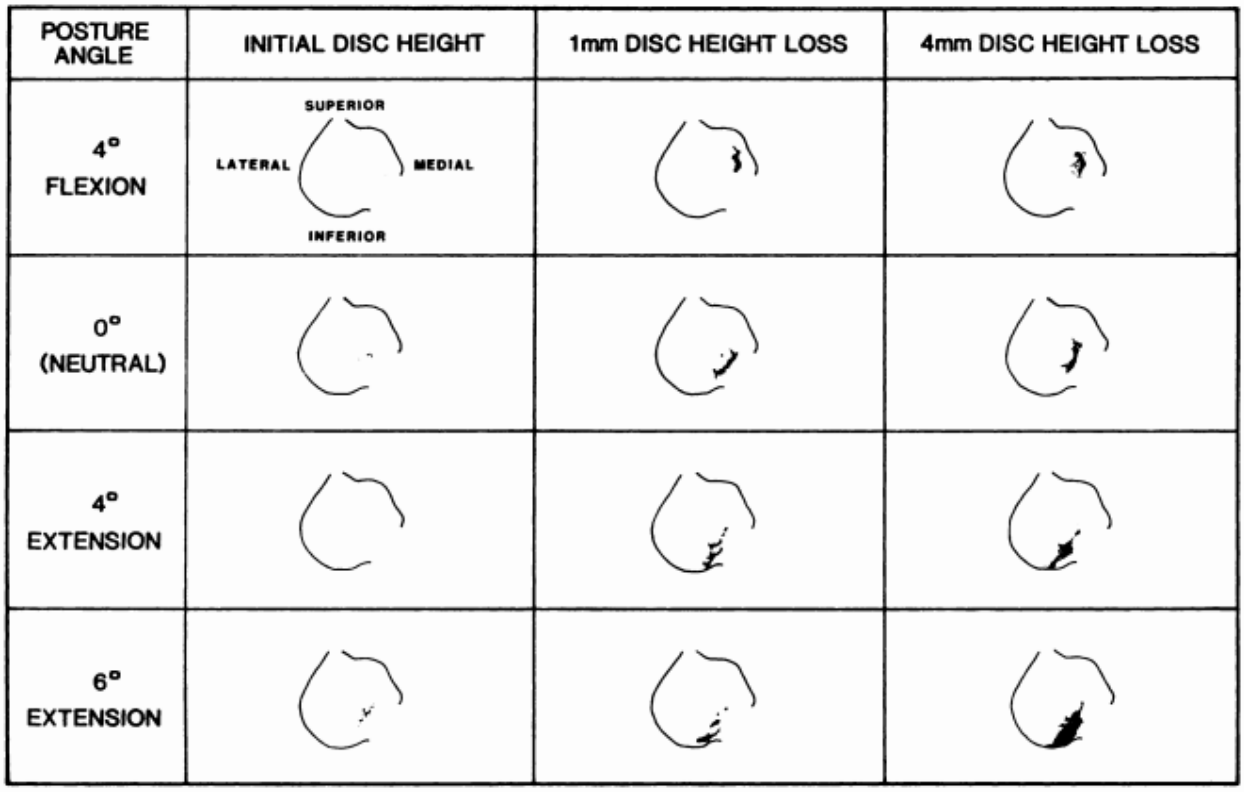

Figure 20. When tested in multiple flexion/extension scenarios at different levels of disc degeneration (loss of disc height), sets of imprints were obtained based on the degree of pressure on the facet joint. The density of the imprint increases with extension of the motion segment and with loss of disc height [94]. (Used under fair use, 2017).

This then leads to the breakdown of the layer of hyaline cartilage between the two subchondral bones, creating friction and grinding between them, and finally abnormal bone growth and pressure. However, facet joint osteoarthritis can still occur in the absence of disc degeneration, in which case causes more stress and motion on the intervertebral disc leading to quicker degeneration [95]. For the vertebral osteophytes, which refer to the abnormal bone growth on the vertebrae, disc space narrowing is highly associated with these bony outgrowth formations, which arise from the periosteum at the junction of the bone and cartilage, **Figure 21**.

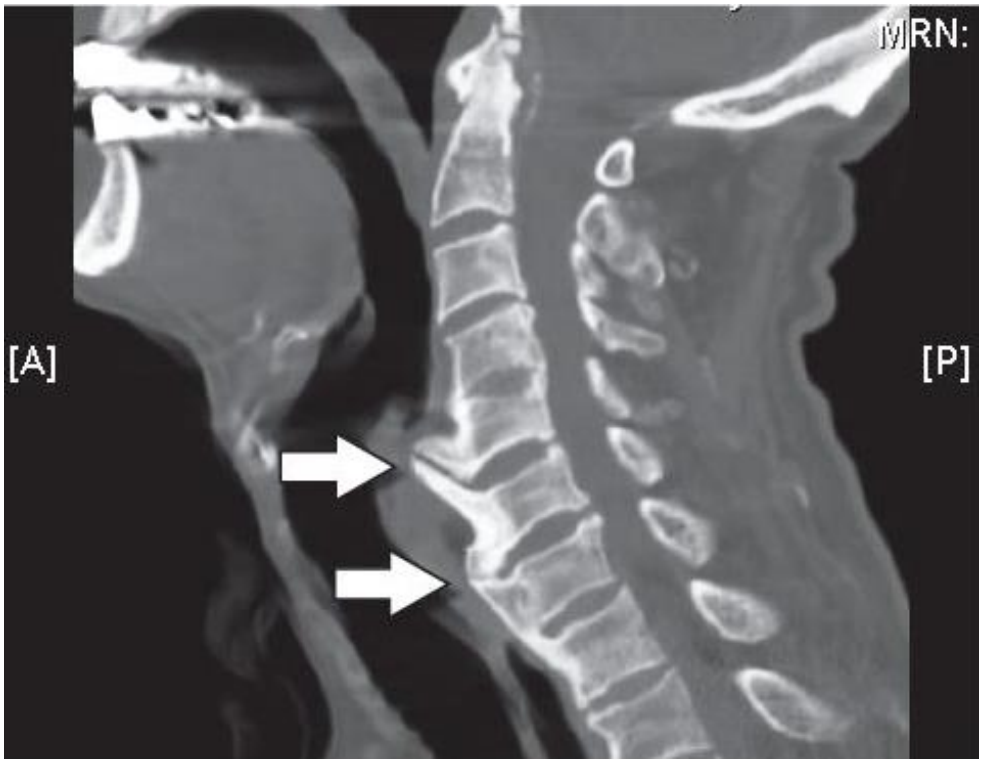

Figure 21. Sagittal CT image of the cervical spine showing large anterior osteophytes (indicted by the arrows) extending from C5 to C7, with affect to intervertebral disc space shown [97]. (Used under fair use, 2017).

Although it is highly correlated to disc degeneration, like that of the osteoarthritis in the facet joints, osteophyte formation in the vertebral column can occur without any signs of cartilage damage, implying that with the general aging process, they may form in an otherwise healthy joint [93]. In this case, the vertebral osteophytes can cause extra stresses on the discs, mainly in the annulus fibrosus, potentially weakening it for further degeneration, damage, and tears/fissures.

Osteoarthritis, along with the aforementioned degenerative disc disease and mechanical loading factors endured by the spine, can cause severe lower back pain because of the potential impingement and injury that can happen to the spinal cord in a couple ways such as bulging discs, disc prolapse and protrusion, and finally disc herniation/rupture and extrusion [96].

1.2.3 Bulging Disc

Bulging discs are considered the starting stage for problems with impingement to the spine and are generally associated with fatigue failure from mechanical loading and disc degeneration grades of Grade 0 (negligible degeneration), Grade I, and Grade II [98]. In the early stages of disc degeneration, when the annulus fibrosus starts to dry out and become more fibrous, the amount of mechanical strain it can take decreases. With high compressive loads that are put onto the discs that require the nucleus to push out causing pressure to the annulus, this can cause problems such as small tears part way through the lamellae. When some of these lamellae tear, usually in the posterior section of the disc, the pressure from the nucleus can make the discs bulge outwards due to the lack of support from the annulus, **Figure 22** 99].

Figure 22. MRI image showing a slight bulge of the annulus into the spinal canal without severe impingement [100]. (Used under fair use, 2017).

When the disc bulges into the spinal canal, it can put pressure onto the spinal cord and other spinal nerves, one of the most prominent being the sciatic nerve, causing pain and sometimes even numbness [24].

Although the pain from these bulging discs is bearable, if left untreated, they can lead to even more severe problems such as disc herniation.

1.2.4 Disc Herniation (Prolapse/Rupture)

Disc herniation, also referred to as disc prolapse, rupture, and extrusion, occurs in later stages of disc degeneration, Grades III – V, and is brought about by increased mechanical loading and fatigue of the annulus that has typically already started to bulge [98]. As the annulus becomes more and more fibrous with degeneration, there is an increase in tears through the lamellae due to the forces of the nucleus. When the tears penetrate all the way through the annulus, the nucleus starts to push out and leak into the spinal canal, **Figure 23** [99]. Unlike bulging discs, because the nucleus actually leaks into the spinal canal, it tends to have much more significant impacts on an individual's life due to the severe impingement on nerves of the spinal cord, causing pain, numbness, tingling, and weakness [101].

Figure 23. MRI image showing a full lumbar disc herniation with substantial spinal stenosis and nerve-root compression [100]. (Used under fair use, 2017).

The most common area for disc herniation is in the lumbar spine, particularly in the lower lumbar, with roughly 56% of herniations occurring in the L4/L5 disc and roughly 41% occurring in the L5/S1 disc [101]. Both of these disc herniations can play significant roles in the quality of an individual's life, since they both are involved with the sciatic nerve. The sciatic nerve, as mentioned in the above anatomy, runs all the way from the lower spine down through the back of the leg. When impinged, this can cause severe problems with motions such as standing up from a seated position, walking, bending over, and twisting of the upper body, and can cause pain, numbness, weakness and general discomfort throughout the entire low extremity. With disc herniation, surgery is almost always required to fix it, however with a bulging disc or other lower back pain, some other less invasive procedures exist [102].

1.3 Current Treatment Techniques

Depending on the severity of disc degeneration, and whether or not a disc is bulging or herniated, there are multiple treatment options, both invasive (surgical) and noninvasive (nonsurgical). The most common treatments include physical therapy, epidural injections, and medications for noninvasive, and radiofrequency ablation, spinal fusion surgery, synthetic total disc replacements, and annulus fibrosus repair for invasive. Along with these two options, other less-traditional treatments are being researched such as stem cells, growth factors, and gene therapy with the theoretical potential to prevent, slow, or even reverse disc degeneration [103].

1.3.1 Nonsurgical Treatments

1.3.1.1 Physical Therapy

With disc degeneration, comes lack of support and stability of the spine due to the decreasing biomechanical functions of the intervertebral disc. In order to regain this loss of function, the muscles surrounding the spine and supporting spinal loads must increase in strength and stability, therefore decreasing the need for intervertebral disc support for the spine. A great solution to this problem is physical/functional therapy, of which benefits include increased strength, flexibility, and range of motion [104]. Improving motion in a joint is one of the optimal ways to relieve pain. This can be accomplished by

stretching and flexibility exercises which improve mobility in the joints and muscles of the spine and extremities. The next is increasing strength with exercises that strengthen trunk muscles, providing greater support for the spinal joints, and arm and leg muscles, reducing the workload required by the spinal joints. Aerobic exercising has also been shown to relieve lower back pain by promoting a healthy body weight and improving overall strength and mobility [104]. Other therapies include manual therapy/deep tissue massaging, posture and movement education for daily life, and special treatments such as ice, electrical stimulation, or traction. Physical therapy does not reverse the age-related disc degenerative changes, however, healing should be promoted by stimulating cells, boosting metabolite transport, and preventing adhesions and re-injury, which in turn will relieve pain caused by degenerative disc disease [105].

1.3.1.2 Epidural Steroid Injections

Epidural steroid injections are one of the most common injections for relief of pain, by reducing inflammation caused by degenerative disc disease. The injections consist of cortisone, which has anti-inflammatory properties reducing and further preventing additional inflammation, combined with a local anesthetic, which offers immediate short-term pain relief. Both of these components help to turn off the inflammatory chemicals produced by the body's immune system that can lead to future flare-ups [106]. It is injected into the epidural space that surrounds the membrane covering the spine and nerve roots. Because it is administered so close to the area of pain, this treatment tends to have better effects and outcomes than that of oral and topical medications, however it can only be performed three times a year due to the negative side effects of the steroids in the body. The downside to this treatment is the fact that it is only short-term, with effects only lasting a couple of months. Also, it does not reverse the changes of degenerative disc disease already caused by aging, with over two-thirds of patients undergoing an additional invasive treatment within two years of the epidural injections [107].

1.3.1.3 Medications

For low to moderate lower back pain caused by degeneration of the discs and spine, oral and topical medications can be prescribed. These medications include over-the-counter acetaminophen (Tylenol) and non-steroidal anti-inflammatory drugs (NSAIDs), anti-depressants, skeletal muscle relaxants, neuropathic agents, opioids (narcotics), and prescription NSAIDs, each having individual and unique benefits depending on the severity and type of pain [108].

The acetaminophen and NSAIDs are usually taken for very low, dull chronic pain. Acetaminophen such as Tylenol is used to essentially block the brain's pain receptors, while NSAIDs such as ibuprofen, naproxen, or aspirin are used to reduce inflammation. The NSAIDs however, need to be taken on a daily basis because they work to build up an anti-inflammatory effect in the immune system [109]. This means that only taking them when pain is present does not work to limit inflammation as well as taking them regularly. Tricyclic anti-depressants are usually given for chronic lower back pain as well. These anti-depressants work similarly to acetaminophen, blocking pain messages on their way to the brain. They also help to increase the body's production of endorphins, a natural painkiller, and help individuals sleep better, allowing the body to regenerate and recover [108, 109]. Skeletal muscle relaxants, such as tizanidine and cyclobenzaprine, are needed for individuals who have acute back pain due to muscle spasms. When their muscles spasm, they put additional stresses onto the discs and spinal nerves causing intense pain through the spine. Neuropathic agents, such as Neurontin and Lyrica, are used when the nerves of the spine are impinged due to a bulging or herniated discs. These medications allow for the specific targeting of nerves to block signals sent to the brain in order to prevent pain. Opioids (narcotics), such as Vicodin and Percocet, are used in extreme cases of spinal pain given their addictive qualities. They work by attaching to receptors in the brain, similar to acetaminophen, however with much higher strength and effect, tending to cause side effects such as slow breathing, general calmness/drowsiness, and an anti-depressant effect. Prescription NSAIDs work exactly the same as over-the-counter NSAIDs, however they tend to work better given their increased strength and potency [108, 109].

1.3.2 Surgical Treatments

1.3.2.1 Radiofrequency Ablation

Radiofrequency ablation is the technique of using heat put through the tip of a needle, either by continuous or pulsed radiofrequency, to denervate an injured disc causing pain to an individual. Nerves of which can be denervated to help with low back pain consist of the facet nerves, sympathetic nerves, communicating rami, and nerve branches in the disc itself. After anesthesia is administered to the procedure site, a needle or electrode is inserted into the disc or near the small nerve branch, under X-ray, fluoroscopy, CT, or MR guidance [110, 111]. When in the right position, the tip of the needle or electrode is heated up to the point in which it causes damage, or heat lesions, to the nerves, destroying them to the point that back pain is relieved. Pain can be relieved usually for 6 to 12 months, and in some cases can last for a few years. It is one of the less invasive operations, and therefore is considered an outpatient surgery, in which the patient is put under local anesthesia and can go home that day without being hospitalized [110, 111]. This procedure is usually recommended for patients who have already undergone procedures such as epidural steroid injections, facet joint injections, sympathetic nerve blocks, or other nerve blocks with pain relief lasting shorter than desired. The average cost of this procedure ranges anywhere from $2,000 to $5,000 based on practitioner, amount of nerves destroyed, and location of spine. If, however degenerative disc disease becomes too severe, this method will not be suitable for long term, and other surgeries or total disc replacements will have to be considered.

1.3.2.2 Spinal Fusion Surgery

Spinal fusion surgery has been widely accepted as a useful treatment option for correcting severe disc degeneration disease, however its efficacy and success remain controversial. Multiple approaches for this procedure can be taken such as posterolateral fusion, anterior lumbar interbody fusion, posterior lumbar interbody fusion, and lateral lumbar interbody fusion, each being a minimally invasive technique to lumbar spinal fusion [103]. For this treatment, the damaged disc is completely removed from the spine and replaced with a titanium cage filled with a calcium phosphate, or hydroxyapatite [112], that sits in between the two vertebrae. Titanium plates are then attached to the vertebrae above and below the titanium cage, using

titanium pedicle screws as fasteners, to offer additional support to the spine after surgery, **Figure 24**. This allows for stability of the spine and correct anatomic alignment of the spinal segments by sharing the loads acting on the spine, until the point in which solid biological fusion occurs into a single bone [113]. This is important because if the adjacent segment motion is altered, it can lead to further degeneration of additional discs and motion segments [103]. Once this occurs, the patient can opt to have the plates and screws removed via another surgery.

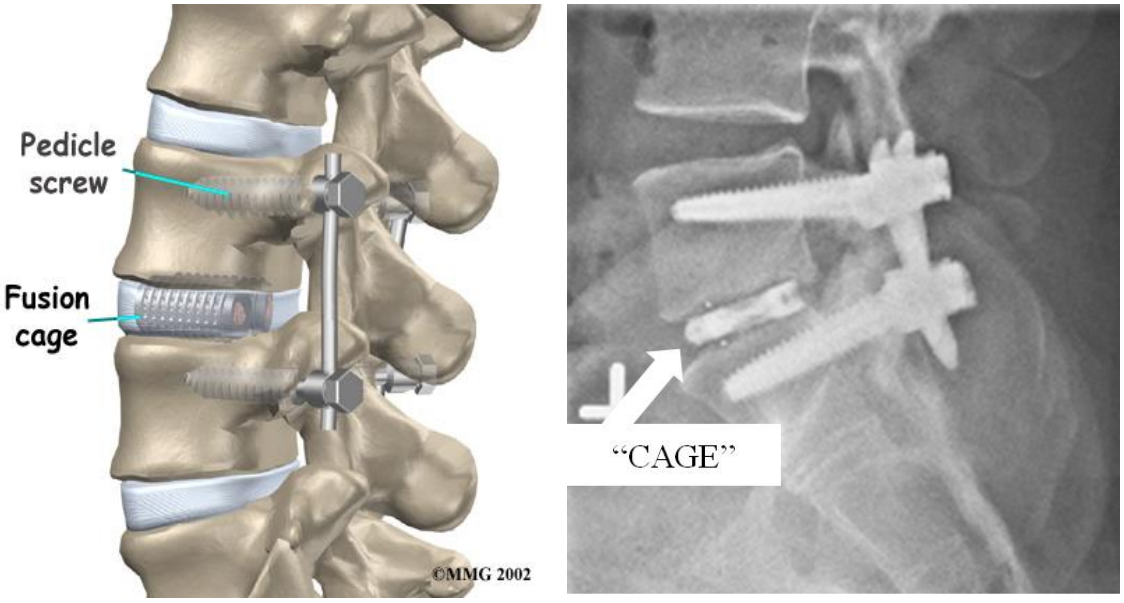

Figure 24. Example image of spinal fusion surgery using titanium cages loaded with hydroxyapatites and pedicle screws and rods to keep stability and anatomic alignment in spinal segment [117]. (Used under fair use, 2017).

Although spinal fusion surgery tends to alleviate discogenic pain associated with degenerative changes, due to eliminating motion between certain vertebrae, some other problems can arise that could potentially be more detrimental in the long run. When two vertebrae are fused together, there becomes no load absorbing center, which severely limits shock absorption and increases loads and stresses on surrounding tissues and discs, as well as limiting mobility [103, 113]. This gives way to additional intervertebral disc degeneration in the adjacent levels, which will then potentially need to be fused as well. However, since the lumbar is the main contributor to the mobility of the spine, preserving that mobility is vital to everyday activity. For this reason, most doctors refuse to fuse more than three levels of the spine

together so to not hinder the movements of everyday life and cause more problems than leaving the damaged disc in the spine [114]. It is estimated that over 137,000 cervical and 162,000 lumbar spinal fusion surgeries are performed every year in the United States alone, totaling over 325,000 fusions, each costing over $34,000 for the average hospital bill, excluding professional fees and equipment fees [115, 116]. In the last few years however, interest in total disc replacement instead of spinal fusion surgery has grown due to their ability to retain motion of the lumbar motion segments [115].

1.3.2.3 Total Disc Replacement

Total disc replacements (TDR) offer the mobility that is required for the lumbar section that spinal fusion surgery does not, however, they are still not as mainstream as fusion surgery [115]. In order for a TDR to be considered effective, the implant must fulfill four main requirements: (1) A solid, nondestructive interface with the adjacent vertebral bodies; (2) provide mobility to mimic the range of motion of the natural disc; (3) resist wear and tear in the body to reduce debris contamination in the body; (4) have the ability to absorb shock and distribute loads evenly and effectively [118]. With all of these requirements, the lumbar section TDR must perform at a higher level of efficiency than that of the cervical spine due to the extra loads it must bear. Compared to the cervical spine, the lumbar spine supports more weight and encounters moments of much greater magnitude, therefore needs a TDR that performs at a higher level. Lumbar TDR can be classified according to their configuration, materials, bearing type, and regulatory status, **Table 8**. The configurations of the TDR devices are designed to maximize range of motion within the realm of natural disc mobility and permit the most freedom. Each configuration of TDR is dependent upon the type of modules involved in the working disc, therefore current designs are built around a bearing for maximum mobility [118]. The bearing systems used include one-piece (1P), Metal-on-Metal (MoM), or Metal-on-Polymer (MoP), with MoM and MoP bearings using a ball and socket design to allow for motion in all directions. Only two lumbar disc prostheses have currently been approved for use by the FDA, the Charite from DePuy Spine and the Prodisc-L from Synthes, although many more are becoming prevalent through trial testing such as Maverick, Kineflex, Freedom, and Mobidisc [118].

Table 8. Summary of current TDR classification, materials, bearing type, and regulatory status [118].

Device	Classification	Biomaterials	Bearing Design	References	Examples of Manufacturer
CHARITE	MoP	CoCr-UHMWPE	Mobile	[10,15–18]	DePuy Spine
Prodisc-L	MoP	CoCr-UHMWPE	Fixed	[15,19]	DePuy Synthes
Activ-L	MoP	CoCr-UHMWPE	Mobile	[20]	Aesculap
Mobidisc	MoP	CoCr-UHMWPE	Mobile	[10,21]	LDR Medical
Baguera	MoP	DLC coated Ti-UHMWPE	Fixed	[15]	Spineart
NuBac	PoP	PEEK-PEEK	Fixed	[22]	Pioneer
Maverick	MoM	CoCr-CoCr	Fixed	[15]	Medtronic
Kineflex	MoM	CoCr-CoCr	Mobile	[10,15]	SpinalMotion
Flexicore	MoM	CoCr-CoCr	Constrained		Stryker
XL-TDR	MoM	CoCr-CoCr	Fixed	[10,23]	NuVasive
CAdisc-L	One piece (1P)	PU-PC graduated modulus	1P	[10,15,24]	Rainier Technology
Freedom	1P	Ti plates; silicone PU-PC core	1P	[10,15]	Axiomed
eDisc	1P	Ti plates; elastomer core	1P	[10,15]	Theken
Physio-L	1P	Ti plates; elastomer core	1P	[10,15,25,26]	NexGen Spine
M6-L	1P	Ti plates; PU-PC core with UHMWPE fiber encapsulation	1P	[15]	Spinal Kinetics
LP-ESP (elastic spine pad)	1P	Ti endplates; PUPC coated silicone gel with microvoids	1P	[3]	FH Orthopedics

Although there are a lot of different TDR options, each has their disadvantages, with only the two previously mentioned even being FDA approved. Ball and socket bearing systems give way to the possibility of hypermobility within the motion segment, greater amounts of debris from wear, and stress concentration within bearing itself which causes higher stresses to act on the vertebrae. It has also been shown that these systems show no elastic shock absorption properties, even between MoM and UHMWPE cores (MoP) [119]. The one-piece bearing systems were designed to potentially counteract the above flaws by adequately mimicking the natural disc behavior; reducing the number of surfaces on which wear can occur, reducing the hypermobility of the joint, and distributing load and absorbing shock [118, 119]. The flaws with the one-piece systems however, are that the elastomer core used suffers greater chance of material tears either within the material or between adhesion between the different materials, they experience short fatigue life, and are still fairly young designs needing further evaluation of wear and

corrosion resistance [118]. Creep deformations and hysteresis properties of the elastomeric material may be limiting factors as well [119]. Each TDR system experiences failure through two mechanisms of degradation of the implant, wear and corrosion. These degradations are to be expected with articulating bearings in harsh environments, however act more heavily on some materials as opposed to others, **Table 9**.

Table 9. Common problems of different implant materials and their effects leading to failure [118].

Bearing Type	Material	Problems	Effects
Ball and socket	CoCr	Reactive wear ions Fibrous particules	Metal sensitivity reactions, Inflammation, Osteolysis
		Metallosis	
		No shock absorption	Compressive stresses on vertebral bodies
	UHMWPE	Wear debris large wear volume	Bone resorption, Osteolysis
		Plastic deformation	
		Increased ROM	Facet and ligament loading
		No shock absorption	Compressive stresses on vertebral bodies
	PEEK	Prosthesis migration	Biomechanical incompatibility, stress on remaining annulus, total ejection of device
		Endplate reaction	Severe biological rejection
1P	PUPC	More studies necessary	

When using MoM devices, the degradation due to wear is minimal when compared to MoP devices and PEEK-on-PEEK devices (PoP), however it does not make it any less dangerous to the body. Although the volume of wear particles might be smaller, the CoCr wear particles are chemically reactive within the body causing corrosion, tribocorrosion, and toxic and biological responses, such as metallosis, biological reactions, osteolysis, and inflammation. When MoP devices wear, the particles produced tend to be fine,

needle and fiber-shaped particles which are less chemically reactive than the metal particles although bigger in size. The PoP devices shows properties of resisting expulsion of nucleus particles, and superior fatigue resistance and wear resistance, however severe biological reactions occur causing device rejection and migration of device into surrounding muscle tissue [118]. Each of these systems have their benefits and disadvantages when compared to each other, however when compared to spinal fusion surgery, shows great advantages in the range of mobility. If a disc has undergone some degeneration, but is not yet to the point of spinal fusion or total disc replacement, other actions can be taken such as annulus fibrosus repair.

1.3.2.4 Repair of Annulus Fibrosus

The annulus fibrosus is involved in almost any pathological condition of the degenerating spine, therefore when its function becomes impaired, plays a fundamental role in two specific clinical situations. It acts as the main source of discogenic low back pain, and as the origin of disc herniation due to its insufficiency caused by degenerative disc disease. As previously discussed, when small fissures occur in the annulus, a repair process takes place in which granulation tissue is formed along with neovascularization and concomitant ingrowth of nerve fibers. This causes chronic discogenic pain throughout the disc due to the pressure being sustained by the nerves. Annulus fibrosus repair is the procedure to fix those tears before the disc herniates, and is usually performed in relatively young patients with very minor degenerative changes. Efficient annulus repair could significantly limit the need for future surgeries in certain cases in which there is potential of disc herniation, however no herniation has currently occurred. When the ruptures are treated, the focus is on improving cell-biomaterial interaction, using an initial implant to provide immediate closure of the tear and maintain mechanical properties of the disc, while the cellular component starts the regenerative process within the disc [120]. The most straight-forward solution is suturing the annulus tear shut helping give the disc a stronger tendency to heal itself, however, its sole purpose is the containment of the nucleus pulposus and does not compensate for the loss of the annulus nor reverse the biomechanical changes [121]. One way to adjust for the lack of compensation is the addition of some sort of growth factor in order to enhance the regenerative process of the annulus tissue. One such growth factor

is Transforming Growth Factor (TGF), which is used in combination with a bioactive microfibrosus poly(L-lactide) scaffold. This electrospun scaffold allows for the closure of the defect site while releasing the TGF induces an anabolic stimulus on the annulus cells, mimicking the ECM environment of the tissue. The scaffolds and TGF release have already proven to encourage rapid growth showing significantly greater amounts of glycosaminoglycans (GAGs) and total collagen in the annulus tissue than without [122]. Annulus fibrosus repair gives great advantages to those who have yet to have a full disc herniation and who are only experiencing minimal degeneration, giving them the opportunity to forgo the potential chance for future surgery. This solution however, is not a cure since there is a good chance for the healed site to once again give way during the individual's lifetime.

1.3.3 Conclusions, Challenges, and Future Directions

Although great strides have been made in the field of degenerative disc disease, there is still a lot more progress to be made, given the challenges faced with every treatment option currently available. In early stages of degenerative disc disease, noninvasive treatments or treatments such as radiofrequency ablation and annulus fibrosus repair can be of great help, however they only help the symptoms instead of the actual cause. Noninvasive treatments face the challenges of only dealing with some of the symptoms of the pain rather than dealing with the actual degeneration of the discs, therefore allowing the discs to continue to degrade to the future point of needing invasive treatments. Radiofrequency, although good for reducing pain, has the challenge of only lasting short term, a few months to a year in most cases. Also, it is an expensive procedure to have done every six months [110]. Annulus repair seems to be a better option for young adults with degeneration to the point just before herniation to significantly reduce need for future surgery, but faces challenges of, again, only fixing the symptoms of the main problem as well as not being to mend any biological changes/losses within the annulus [120]. When disc degeneration gets even worse, greater procedures need to take place such as spinal fusion surgery and TDR. Spinal fusion surgery is, as of today, the most common life-long solution to severe disc degeneration, however is struck with multiple challenges such as significantly limiting mobility and adding additional stresses to the adjacent motion

segments potentially causing greater degeneration in other intervertebral discs [113]. TDR has been shown to help retain the mobility that spinal fusion cannot, but can sometimes lead to hypermobility of the joint, can wear and corrode causing a biological reaction in the body, and more often than not, does not distribute load nor absorb shock, but rather transfers it directly into the adjacent vertebrae [118]. With all of these options facing difficult challenges, a couple of future outlooks have been identified. Almost all of the future solutions include some form of gene therapy, regeneration, or scaffold with cell releasing properties. Gene therapy and regeneration with growth factors and other cells such as TGF-β1 and ADAMTS5 have been researched in rats for early stage trials showing greater GAGs and total collagen for the TGF-β1, and successful suppressing of degradation of nucleus pulposus tissue for ADAMTS5. Along with these, in rabbit models, a similar approach was used to target caspase 3 in order to disrupt the execution of apoptosis [103]. Another system was researched, using a scaffold of collagen and hyaluronan, or entrapped chitosan gel, in which disc cells and growth factors were implanted. This will be used in an attempt to produce a tissue with a similar molecular composition to native nucleus pulposus tissue [123]. In most current efforts, FDA-cleared Phase III adult stem cells were used in a test study to treat chronic lower back pain associated with DDD. The use of mesenchymal precursor cells directly injected into the lumbar disc will hopefully show some ability to regenerate lost tissue of the disc [124]. Another future direction is to look more into the regeneration and repair of the annulus tissues as opposed to the nucleus tissues. Efforts for novel therapies have mainly been directed towards nucleus tissues regeneration and replacement, however a main challenge is the development of strategies and techniques that deal with the degenerated annulus, preferably in a combined approach with the nucleus [125]. This will hopefully help propel the future of annulus repair ceasing the need for herniation surgeries such as fusion surgery or TDR, and fix the main problem before it occurs instead of just treating the symptoms.

2. Scope and Objectives

The main goal of this study was to create an artificial annulus fibrosus similar to that of the natural intervertebral disc, as well as find preliminary results for vertebral endplate connection and nucleus pulposus internal pressure, in order to correct disc degeneration in the spine. The three-part composite samples needed to demonstrate good shock absorption and load distribution while maintaining strength and flexibility, and removing the need for metal in the body, something of which no current total disc replacement or spinal fusion surgery can offer. The composite samples will also need to last for life, or at least equivalent to most TDR of 50 years, being able to withstand cyclic loading under the stresses and strains observed during everyday activities, without undergoing fatigue failure. The annulus will need to be mimicked in tension and compression to show that the disc will not fail due to an exceedingly high moment from bending or torsion. The nucleus will need to show an increase in internal pressure causing the samples to barrel like a natural disc, instead of failing due to buckling. The vertebral endplates will need to show great connection, so that the nucleus will not leak out and cause failure due to herniation of the disc. The endplates will also need to incorporate a method for bone growth in order to mechanically interlock to the adjacent vertebrae. The entire composite sample as a whole will need to allow its properties to be fine-tuned based on the level of lumbar intervertebral disc replaced, in order to make sure it mimics the natural disc properties as similarly as possible. When being compared to the natural disc the composite samples will need to show similar properties in most aspects, with the exception being the incorporation of living cells. When being compared to spinal fusion surgery and total disc replacement, the composite samples created will need to show significant benefits for forward progression in the field of disc degeneration disease treatments.

3. Materials and Methods

3.1 Material Selection

For the polymer matrix, two Covestro polyurethanes were tested, Texin RxT70A and Texin RxT85A (PU 70 and PU 85 respectively). Both polyurethanes are biocompatible and currently used in medical devices, do not biodegrade in the body, and have outstanding abrasion and permanent deformation resistance, impact strength, flexibility, soft qualities to allow for cushioning of loads, and excellent hydrolytic stability [128]. PU 70 has a shore hardness of 70A, a tensile strength of 25.5 MPa, ultimate elongation of 70%, and a flexural modulus of 14.5 MPa, while PU 85 has a shore hardness of 85A, a tensile strength of 36.6 MPa, ultimate elongation of 610%, and a flexural modulus of 26.9 MPa [128]. With these factors taken into account, and with some preliminary testing **(SI Figure S1 and S2)**, it was decided that the PU 85 was the best option for the polymer matrix. However, this material by itself was not strong enough to support the weight bearing of the spine, so cellulose nanocrystals were used as a stiffer reinforcement. CNCs are biocompatible, rod-like nanoparticles that could be used to fine tune the mechanical properties of our composite given their strong, stiff, and resilient qualities. The chemical dimethylformamide, DMF, was used as the solvent for both the polymer and the CNCs to create a solution of each to later be used for cast samples.

3.2 Cast Sample Method

Two solutions were made, a 40 mg/mL solution of CNCs in DMF and an 80 mg/mL solution of PU 85 in DMF. The CNC solution was made by weighing out 8 g of dry CNCs and mixing them in 200 mL of DMF via shaking and sonication until completely dispersed. The PU 85 solution was made by weighing out roughly 32 g of PU 85 resin and mixing it with 400 mL of DMF. The solution was then put on a hot plate at 140^{o}C, and stirred at 1000 rpm until all the PU 85 resin had dissolved. Once the two solutions had been made, they were added together to make 10 g samples in composition ratios of 100 wt% PU 85 (PU 100/0), 90 wt% PU 85 to 10 wt% CNCs (PU 90/10), 80 wt% PU 85 to 20 wt% CNCs (PU

80/20), and 70 wt% PU 85 to 30 wt% CNCs (PU 70/30). When the solutions had been added together into the specified compositions, they were placed in an oil bath at 140ºC while stirring at 750 rpm until enough DMF was evaporated out to make a gelatinous substance. The gelatinous substance was then transfer into a Teflon dish, put onto a hot plate at 80ºC, and left over night for the rest of the DMF to evaporate out. After drying out overnight, the samples were removed from the hot plate, and put into a vacuum oven at 80ºC and -27 in.Hg for 4 hours or until all DMF was removed. The same procedure was replicated for PU 70.

3.3 Fabrication of Samples for Testing

3.3.1 Samples for Tension Testing

Once all of the DMF was removed, each sample was then hot pressed at roughly 138ºC at 3 MPa of pressure for 5 minutes, using 0.9 – 1.0 mm aluminum spacers to ensure uniformity of thickness throughout the film. The films were cut into approximately 2.0 cm wide ribbons using a razor blade. Three of each composition of ribbons were placed into a beaker filled with deionized water (DI water), in order to swell the CNCs, while three of each composition remained dry **(Figure 25)**. After tension tests, it was determined that PU 85 would be the only polymer matrix used with compositions PU 100/0, PU 90/10, and PU 80/20, and that all samples will be swelled in DI water before testing.

Figure 25. Samples made for DMTA tension testing (dry on the left, wet on the right).

3.3.2 Ringed Samples for Compression Testing

The same procedure as the samples for tension testing was used to create ribbons for the ringed samples, however the ribbons were roughly 0.3 mm thick and 9.0 mm wide. Each composition had a cumulative of 500 mm and 650 mm of ribbons measured out in length to be coiled together (about 10-12 ribbons of varying length per sample), and used an inner diameter of roughly 15 mm and 12 mm, respectively **(Table S3 for dimensions)**. The 650 mm samples used a greater ratio of annulus fibrosus to nucleus pulposus diameter to determine the effects that adding additional rings had on the mechanical properties, while the 500 mm samples used the same dimension ratio as a natural intervertebral disc. After each samples lengths were measured, the inner diameter was measured on one strip of ribbon, and DMF was used to melt the ribbon in position to form a ring with that specified diameter. All the remaining ribbons were wrapped around the inner ring, with the most outer ring being glued together using DMF just as the inner ring was, final samples shown below **(Figure 26)**. This ensured that the middle rings would not unravel, however were still able to delaminate so that they would act as individual rings when tested. The DMF glued rings were then dried in the vacuum oven using the same procedure as mentioned before to

remove all of the DMF. Every ringed sample was then swelled in DI water for at least 48 hours before testing to ensure swelling throughout entire sample.

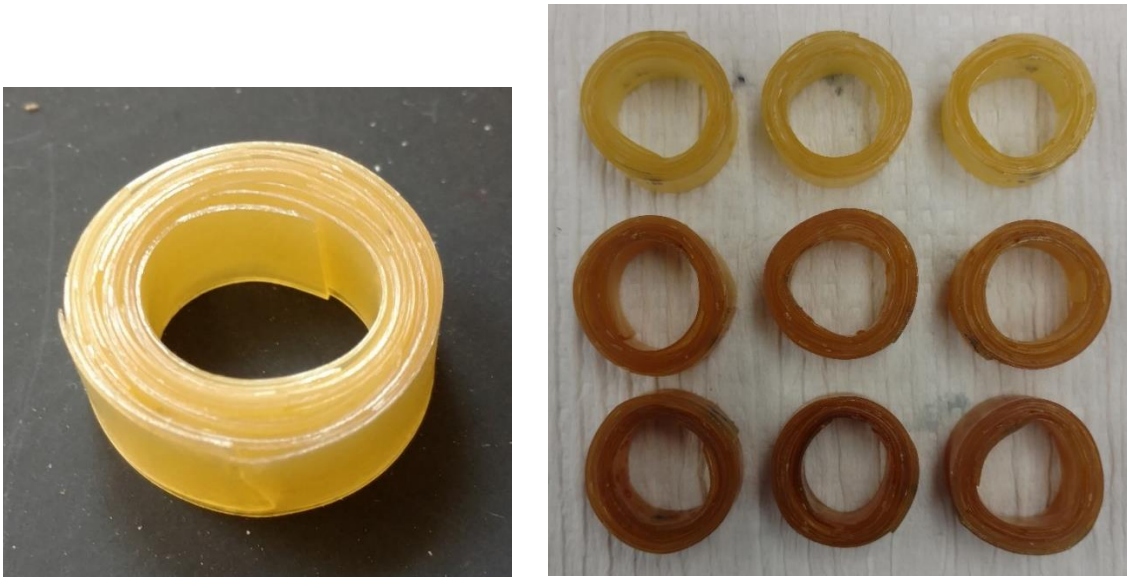

Figure 26. Ringed samples created from ribbons. In order from top to bottom, PU 100/0, PU 90/10, PU 80/20. The left image shows the 650 mm samples and the right shows the 500 mm samples.

3.3.3 Ringed Samples with Attached Nucleus and Endplates

Additional ringed samples were created using the same procedure as specified above. Using the same composition as each of the ringed samples, the composite material was pressed into roughly 0.3 mm thick films to be used as endplates. Four circles were cut out of each composition for each ringed sample made, matching the circumference of the ringed samples. Once the endplates had been made, two were attached to each end, using DMF, to seal off the ringed samples and create a 0.6 mm thick endplate on each side matching that of a natural lumbar disc **(Table S4 for dimensions)**. A syringe was then used to fill the middle of each specimen with water to preliminarily simulate the inside pressure of the nucleus, puncturing only one side of the sample. The small hole that was created by the syringe was then closed off using the PU 85 solution in DMF **(Figure 27)**.

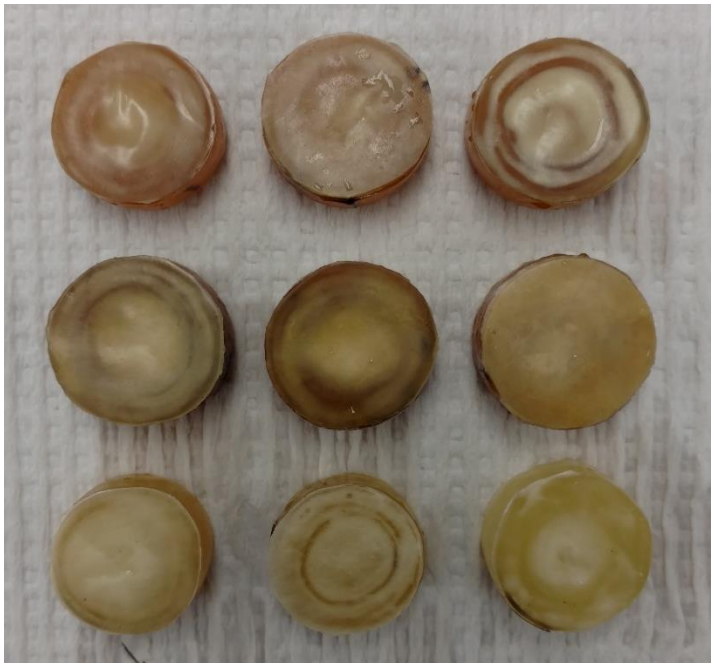

Figure 27. Ringed samples after endplates were attached and middle swelled with water.

3.4 Mechanical Testing

Both tension and compression tests were run on the samples for characterization of mechanical properties such as strength and elastic moduli. Tension tests and initial compression tests were done with the dynamic mechanical thermal analysis machine (DMTA). Stress vs. strain curves were recorded, using isometric force tests, in which the force increased by 3 N per minute until a maximum of 18 N was reached. This was repeated three times for each composition, as well as swelled and dry for tension testing. The DMTA did not have enough force to sufficiently test the compressive strength of the ringed samples, therefore an Instron tension-compression machine was used to determine the compressive properties of these samples. The Instron used a 1 kN load cell, compressing the samples at a continuous 5 mm displacement per minute. This was repeated three times for each composition used for the ringed and nucleus samples (PU 100/0, PU 90/10, PU 80/20) swelled only.

3.5 Isolation of Phosphorylated Cellulose Nanocrystals (p-CNCs)

Isolation of p-CNCs used an adapted procedure from a referenced paper, “Isolation of thermally stable cellulose nanocrystals by phosphoric acid hydrolysis” [129]. Based on the data from the study referenced, to get the optimal results only a 10.7 M solution of phosphoric acid was used, the oil bath was pre-heated to 100^{o} C, and the mixture was stirred in the oil bath for 90 minutes. When centrifuging, the settings were set to 10,000 rpm for 10 minutes, as opposed to the 3600 rpm for 15 minutes. The dialysis and lyophilizing process remained the same.

3.6 Conductometric Titration of p-CNCs

The conductometric titration process used for the p-CNCs was an adapted procedure from a referenced paper, “Isolation of thermally stable cellulose nanocrystals by phosphoric acid hydrolysis” [129]. Only a neat medium containing hydrochloric acid and water, and the same medium containing p-CNCs were titrated, since sulfated CNCs (s-CNCs) and uncharged CNCs (H-CNCs) were not needed for the hydroxyapatite/bone growth application, therefore charge density of s-CNCs and H-CNCs was not needed.

3.7 Transmission Electron Microscopy (TEM)

A TEM: JEOL 2100 microscope was used with an accelerating voltage 200 kV and a current of 108 µA for TEM micrographs. Samples were prepared by dropping 20 µL of an aqueous p-CNC dispersion (p-CNC content of 0.1 mg/mL) onto a carbon supported copper grid [129]. After one minute of letting the aqueous dispersion set, a stain was applied to it for 15 seconds (NANOVAN), then the sample quickly dunked into a beaker of DI water. The sample was put into a TEM box, and subsequently dried in a desiccator overnight.

3.8 Statistical Analysis

A two-way ANOVA was conducted to determine the main effect and the interaction effect between the two independent variables on the dependent variable using an alpha level of 0.05. The two independent variables, factors, used were the total lengths of the samples and the concentration of CNCs per sample, acting on the dependent variable of the samples' mechanical properties.

4. Results and Discussion

4.1 Fabrication

The processing and fabrication method for the samples resulted in only slight effects to the repeatability of the samples' dimensions, **(Table S3 and S4)**. Although the standard deviations between each samples are almost negligible, the slight difference in widths between each ribbon used for the ringed samples was just enough to cause some variations in the compression tests. This was due to the fact that the greater width ribbons came into contact with the Instron compression plates before others, however the effects caused could only be seen within the first 5 - 20 N causing a negligible effect to the results observed and determined. When the endplates were attached to the ringed samples, it created much more uniformly level surfaces that came in contact with the Instron compression plates. Therefore, compression tests were not affected by surface height differences, however they were affected by the connection strength between the endplates and the ringed samples. When sealed with DMF, the connection was made to be as complete as possible, however slight defects could be detected making the connection not ideal or as secure as needed. These defects are where the samples tended to fail during compression tests, leading to the leaking of the water put into the system to synthesize the nucleus and resulting in depressurization of the center of the system.

4.2 DMTA Tension Testing

DMTA tension testing was performed on each of the polyurethane/CNC composites. When tested dry, PU 90/10, PU 80/20, and PU 70/30 composites had a much higher tensile modulus and tensile strength than what was required to match the natural annulus fibrosus. When tested after being swelled for at least 48 hours, the tensile modulus and tensile strength significantly decreased to better resemble that of the natural annulus fibrosus **(Figure 28 and 29, Table 10)**. Although the samples were not tested in increased temperature, simulating body temperature, all materials used are thermally stable up to well beyond body temperature. These results indicate that when submerged in a fluid such as water, like that of the actual

spine, the composite material will act more like the natural disc, sitting between the values of 18 – 45 MPa for the linear tensile modulus. Ultimate stress and strain could not be determined since each sample tested reached either the maximum displacement or force allowed by the DMTA.

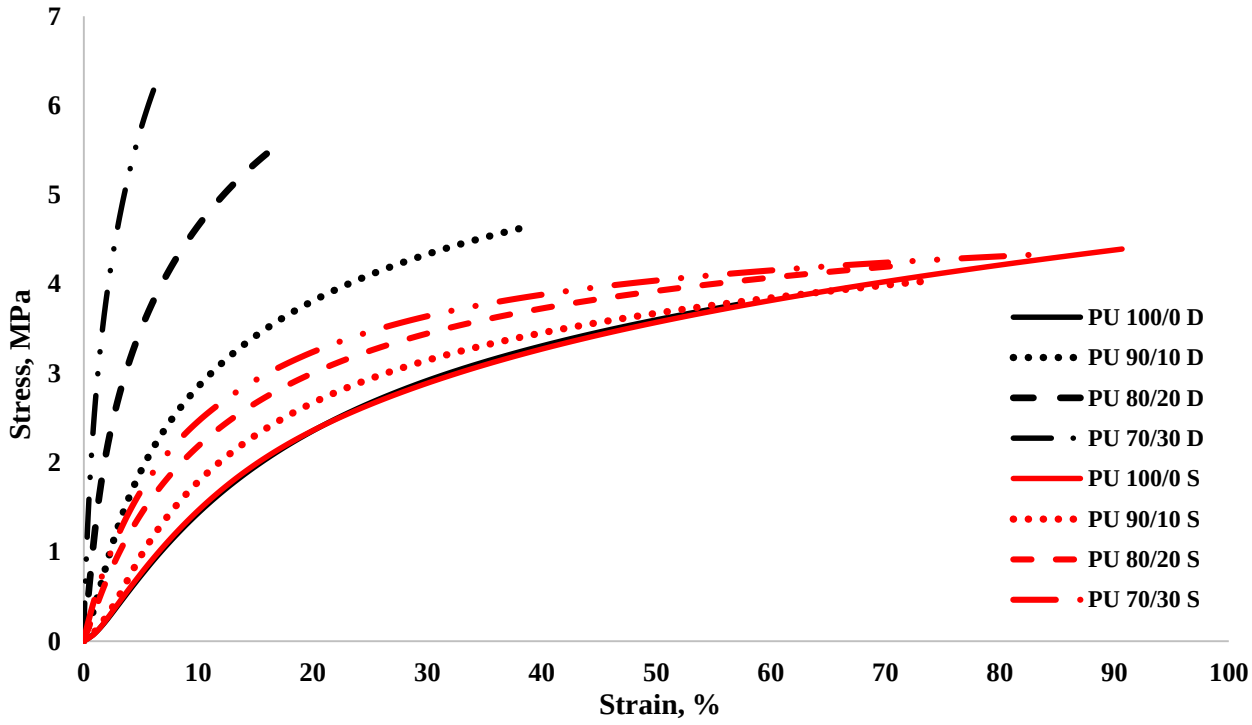

Figure 28. Tension tests of dry and swelled PU 85 samples using DMTA, denoted (Ex: PU 100/0 D for dry and PU 100/0 S for swelled).

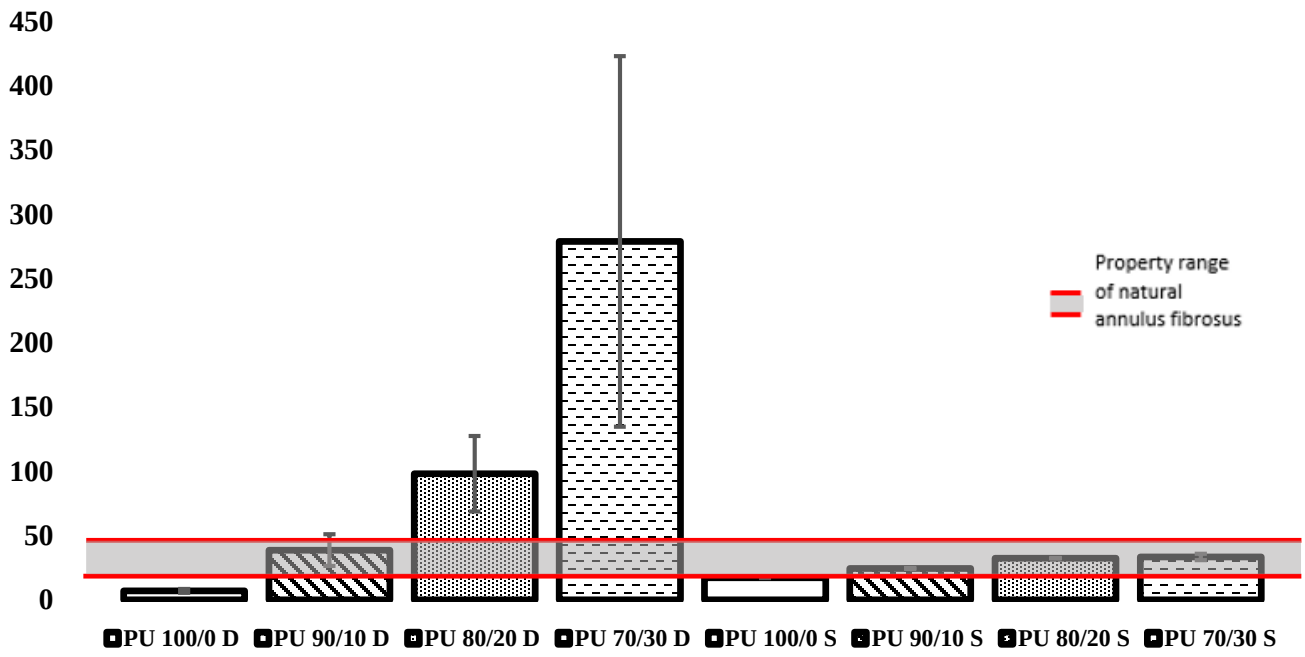

Figure 29. Tensile modulus of dry and swelled PU 85 samples, using same denotation as specified above, **Figure 28**. Lines indicate property range of natural lumbar discs [126].

Table 10. Tensile moduli, yield strength, and yield strain of samples from tension tests, which can be compared to natural annulus fibrosus **(Table S1).**

	PU 100/0	**PU 90/10**	**PU 80/20**	**PU 70/30**
Dry Modulus (E'), MPa	16.0 ± 0.3	38.7 ± 12.4	98.1 ± 29.4	278.9 ± 144.1
Swelled Modulus (E'), MPa	17.1 ± 0.2	24.4 ± 0.2	32.3 ± 0.3	33.4 ± 2.4
Dry Yield Strength, MPa	2.2 ± 0.0	2.5 ± 0.2	3.2 ± 0.5	3.5 ± 0.6
Swelled Yield Strength, MPa	2.4 ± 0.0	2.3 ± 0.1	2.2 ± 0.1	2.3 ± 0.1
Dry Elongation at Yield, %	18.2 ± 0.9	8.4 ± 1.5	5.4 ± 2.5	2.3 ± 1.0
Swelled Elongation at Yield, %	19.31 ± 0.9	13.6 ± 1.6	9.7 ± 0.6	7.6 ± 0.4

The PU 85 samples demonstrated tensile moduli very similar to those of the natural annulus fibrosus, however PU 70 samples **(SI Figure S1 and S2)**, demonstrated properties below ideal, and fractured when a composition of 30 wt% CNCs was used. Therefore, this polyurethane was disregarded in any further testing. As well as the PU 70 samples being disregarded, the 70/30 wt% PU/CNC composition for the PU 85 was too brittle to form into the ringed samples for compression testing, fracturing when wound, therefore was not used in further testing either.

Since the same material was being used for compression testing as was for tension testing, the DMTA was used for initial testing of the ringed samples. However, the compression tests on the ringed samples as well as the samples with the nucleus and endplates proved too strong for the DMTA, reaching the maximum 18 N allowed with very little strain **(Figures 30 and 31)**.

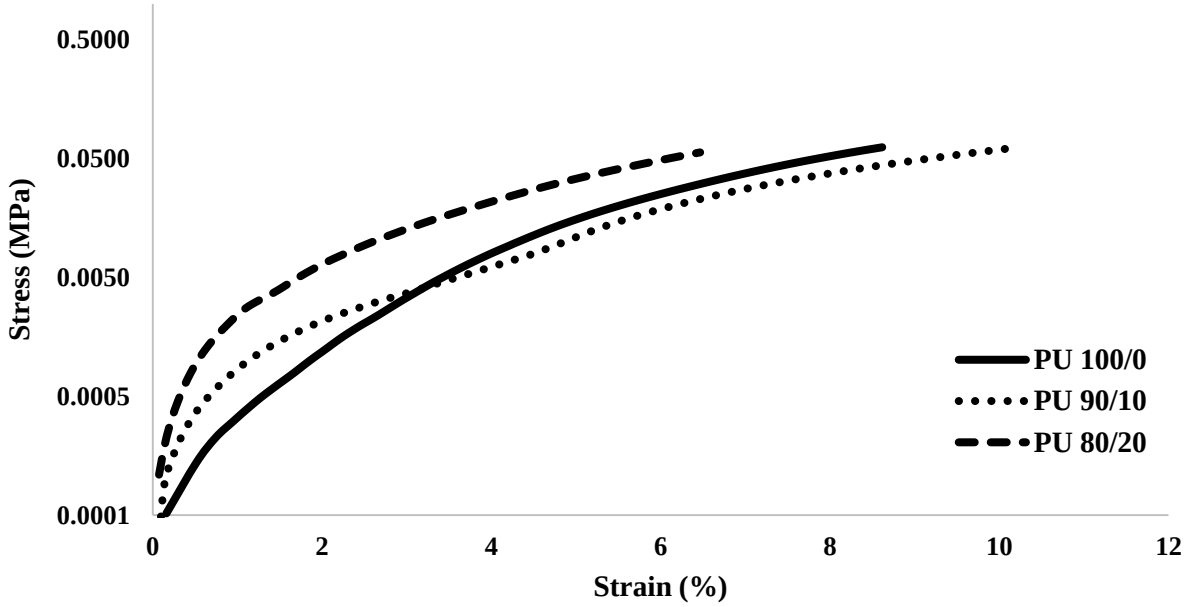

Figure 30. Compression tests of swelled, ringed samples (650 mm in length) using DMTA.

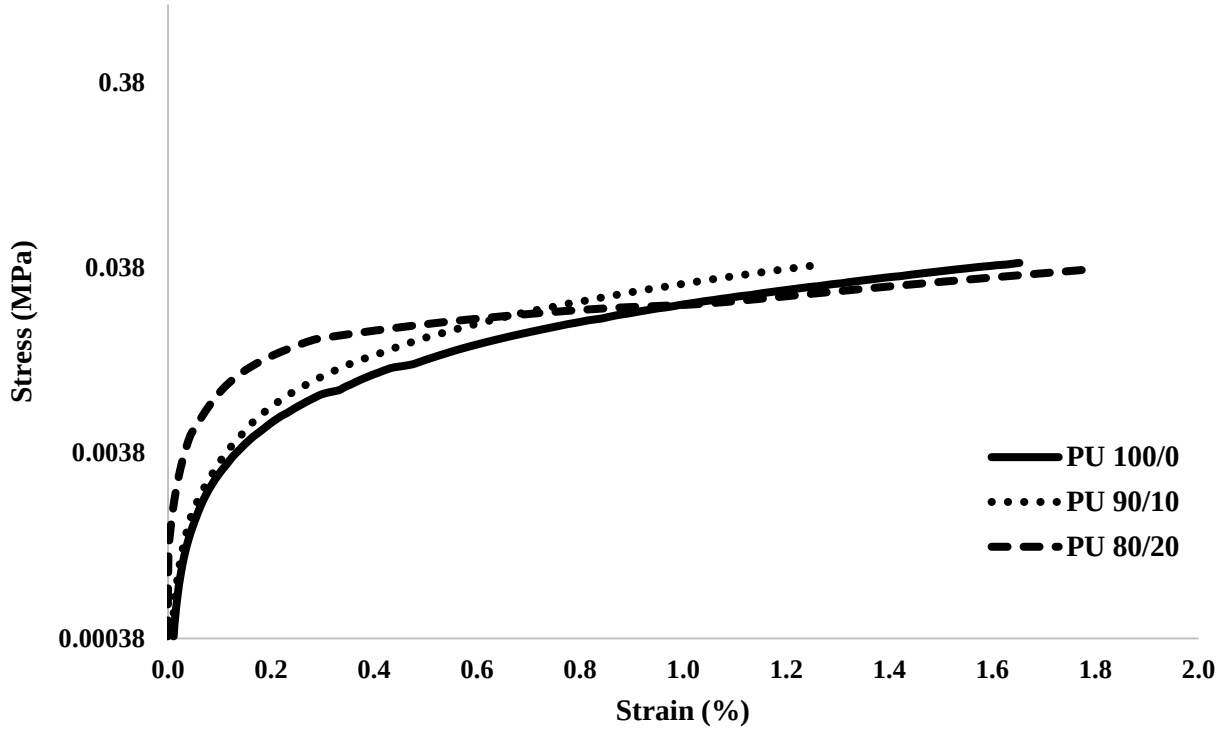

Figure 31. Compression tests of swelled, nucleus with endplate samples (650 mm in length) using DMTA.

4.3 Instron Compression Testing

Therefore, an Instron compression/tension machine was used to determine the compressive modulus, yield stress, and yield strain of both the ringed samples and samples with a nucleus and endplates **(Table 11 and 12)**. The 500 mm and 650 mm ringed samples (500 R, 600 R), and 500 mm and 650 mm nucleus with endplates samples (500 NE, 650 NE) tested, all showed much greater compressive moduli and yield stress than that of the natural disc, however fell closer to the correct range for yield strain **(Table S2)**. Each sample also showed a toe region in the beginning of the compression tests followed by a linear region and then yielding. This corresponds to the natural activity seen in tendons and tissues containing collagen fibrils with a proteoglycan matrix, such as those of the annulus fibrosus and nucleus pulposus components of the spinal disc [126, 136]. Ultimate compressive stress and strain could not be determined since each sample reached the 1 kN maximum for the load cell before showing complete compressibility.

The 500 R sample showed a toe region for the modulus until around 9-10% strain, in which the slope became more linear. The linear portion of the stress-strain curve was used to evaluate the compressive modulus, and yield strain and yield stress was determined from the hump in the beginning of the graphs, in which the samples started to fail and buckle in on themselves **(Figure 32)**. The difference between samples were as predicted increasing significantly in compressive modulus and strength as the composition of CNCs increased, however the samples all failed with only a slight increase strain, no matter the CNC content **(Table 11)**.

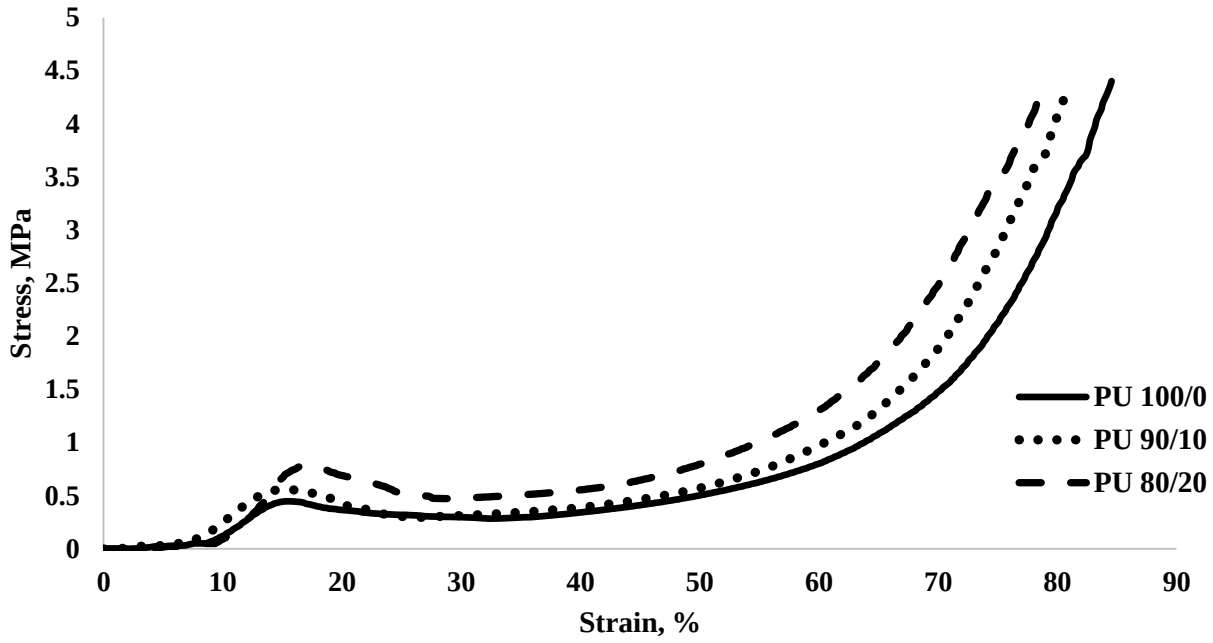

Figure 32. Compression test of swelled 500 R samples using Instron machine until 1 kN load was reached.

The 650 R sample showed a toe region for the modulus until around 8-10% strain before becoming linear, with much similarity to the 500 R sample. As well as the linearity of the slope beginning around the same strain, the 650 R samples had yield strains almost equivalent to those of the 500 R samples. The 650 R samples however, had a significantly greater magnitude of compressive modulus and yield stress than that of the 500 R samples, showing greater stiffness, resilience to deformation, and strength against loads, with the addition of more rings. The yield stresses and strains were determined from the humps observed

in the beginning of the graphs, failing in a similar manner to the 500 R samples **(Figure 33)**. Also, similar to the 500 R samples, the 650 R samples showed a significant increase in compressive modulus and yield stress as CNC content increased, however showed very little variation in yield strain, hovering around the same values **(Table 11)**.

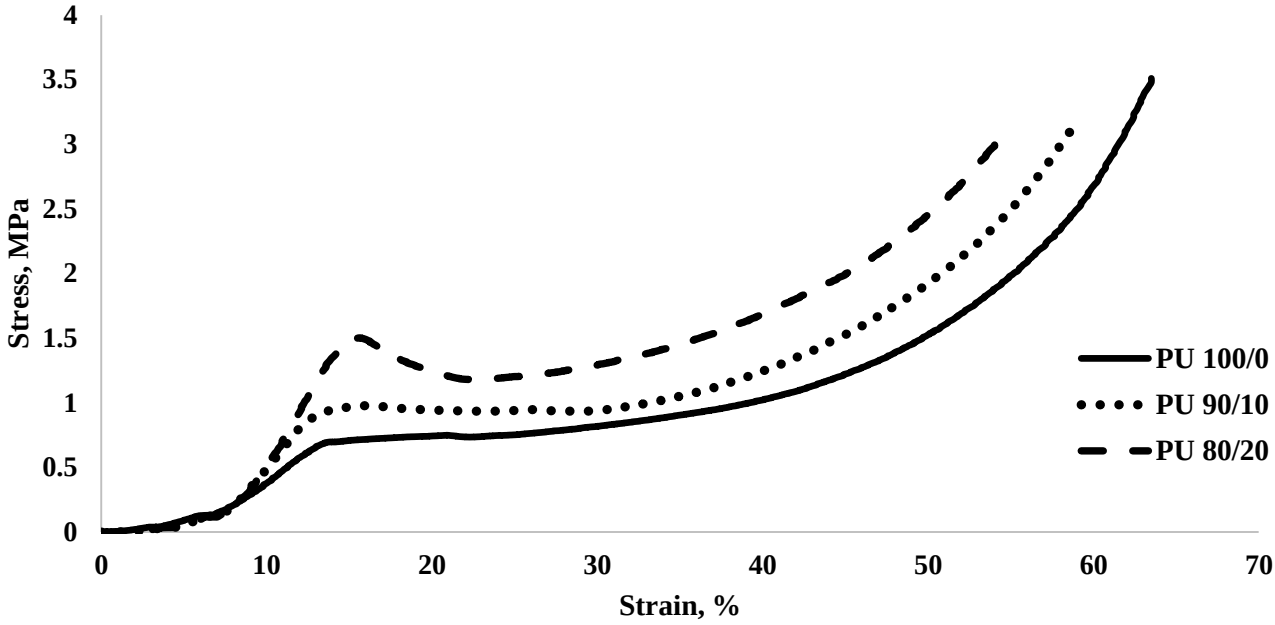

Figure 33. Compression test of swelled 650 R samples using Instron machine until 1 kN load was reached.

For all of the ringed samples, the area used for stress calculations included both the inner and outer diameter, causing the compressive modulus and yield strength to be greater than that of the nucleus with endplate samples. Therefore, the results could be misleading, directly comparing the strength and modulus of just the ringed samples to those of the nucleus with endplate samples, since the cross-sectional area used was so much smaller.

Table 11. Compressive mechanical properties of swelled ringed samples from Instron compression tests, which can be compared to natural annulus fibrosus **(Table S2)**.

500 R Sample	**PU 100/0**	**PU 90/10**	**PU 80/20**
Modulus (E'), MPa	5.9 ± 1.4	9.1 ± 1.3	14.1 ± 2.2
Yield Strength (YS), MPa	0.4 ± 0.0	0.6 ± 0.0	0.9 ± 0.1
Yield Strain (%)	14.7 ± 0.9	15.6 ± 1.5	16.8 ± 1.5
Strain at 950 N (%)	83.3 ± 0.9	78.9 ± 2.6	77.9 ± 1.0
650 R Sample	**PU 100/0**	**PU 90/10**	**PU 80/20**
Modulus (E'), MPa	10.5 ± 1.0	13.8 ± 1.5	18.8 ± 1.7
Yield Strength (YS), MPa	0.7 ± 0.0	0.9 ± 0.1	1.3 ± 0.1
Yield Strain (%)	13.9 ± 0.4	16.2 ± 1.4	14.8 ± 0.5
Strain at 950 N (%)	63.7 ± 0.5	58.4 ± 1.1	52.5 ± 3.1

The 500 NE samples showed a much smaller toe region for the modulus when compared to either of the ringed samples, becoming linear closer to 5-8% strain. The compressive modulus was evaluated using the linear portion of the stress-strain curve, and yield stress and yield strain determined from the hump in the beginning of the graphs, in which the samples failed by leaking of the nucleus through the connection of the endplate to the annulus **(Figure 34)**. The hump in the beginning of these stress-strain curves were not as prominent as the ringed samples because of the way in which the nucleus with endplate samples failed, discussed further in a later section **(Figure 36)**. With an increase in CNC content, the compressive modulus and strength of the samples tended to significantly increase, like that of the ringed samples. The yield strain showed interesting results, remaining very close in value to not only each other, but also to those of the ringed samples **(Table 12)**.

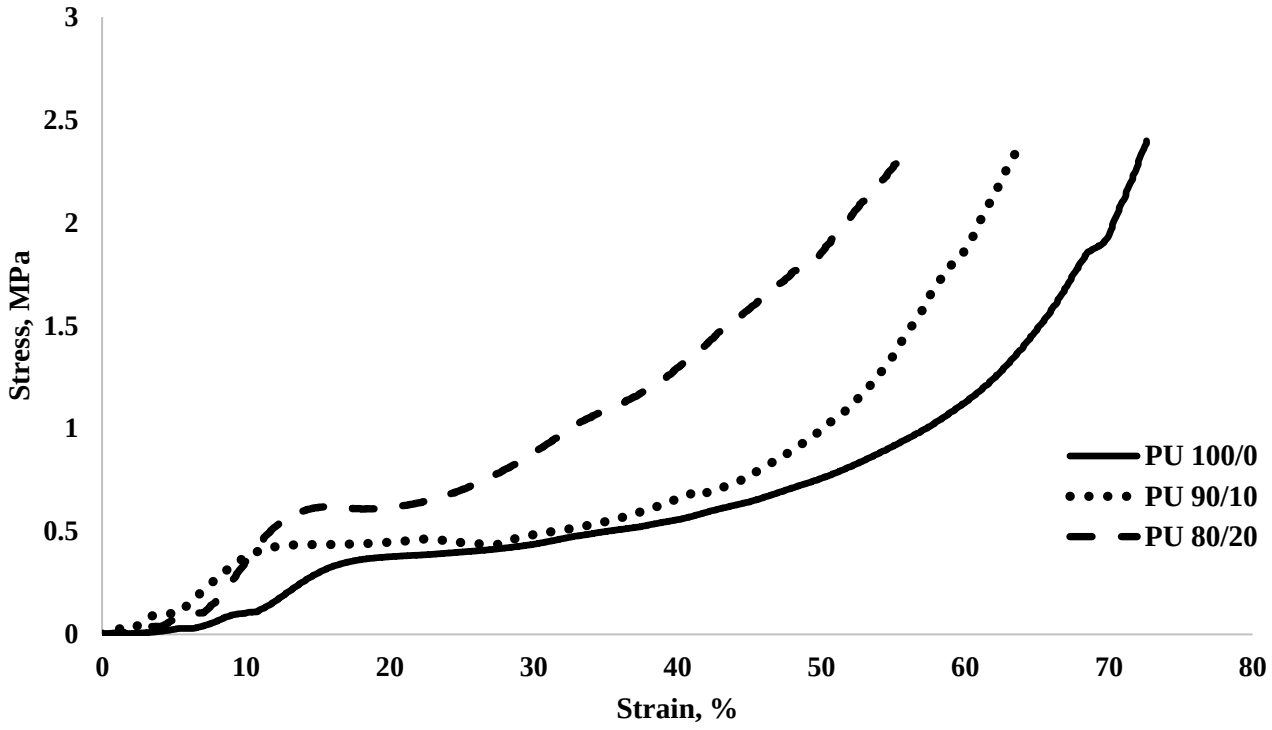

Figure 34. Compression test of swelled 500 NE samples using Instron machine until 1 kN load was reached.

The 650 NE samples showed the smallest toe region for the modulus, consistently for all compositions, when compared to any of the other samples, becoming linear closer to the 4-6% strain. Like the 500 NE samples, the compressive modulus was evaluated using the linear portion of the stress-strain curve, and yield stress and yield strain determined from the hump in the beginning of the graphs. The 650 NE samples failed in the same manner as the 500 NE samples, however the PU 90/10 and PU 80/20 samples had much less of a dramatic decrease at the yielding point, showing the most promising results and similarity to the stress-strain curves of the natural disc **(Figure 35 and S5)**. Like all of the other tested samples, an increase in modulus and strength was seen with increase in CNC content, however different from the other samples, the yield strain significantly decreased with increasing CNCs **(Table 12)**. Also, the extreme similarity between the PU 90/10 and PU 80/20 was not seen in any other previous samples, the only slight difference being an increase in the modulus of PU 80/20.

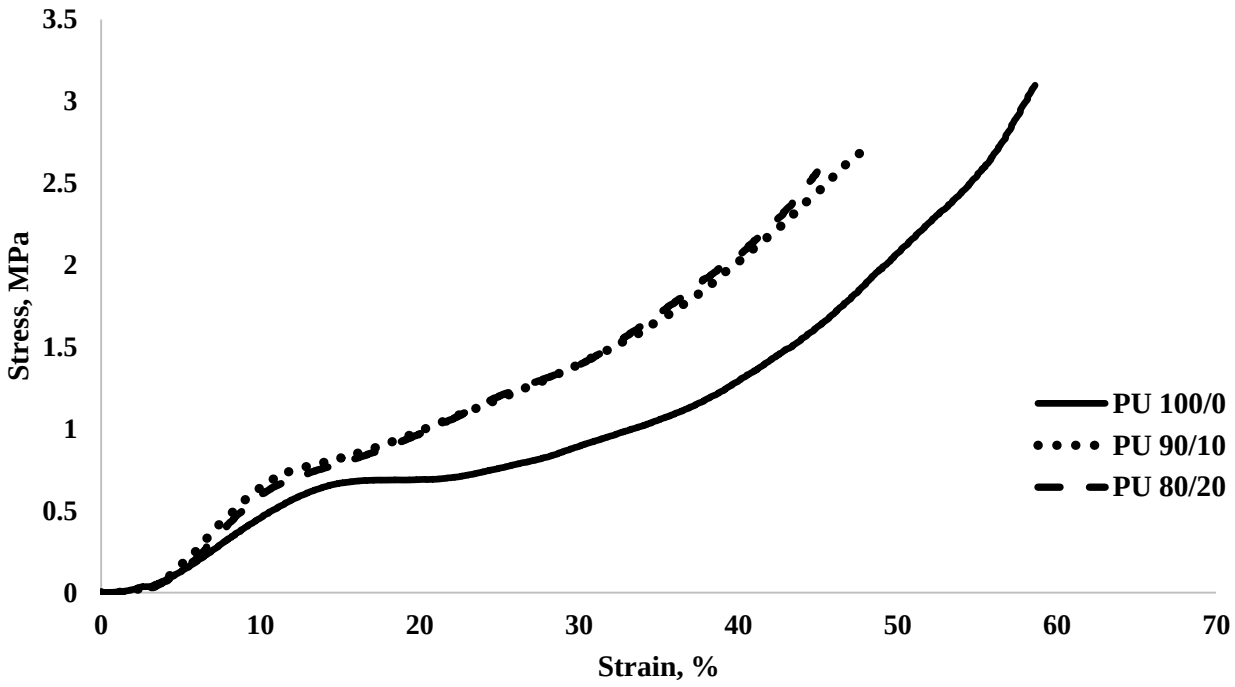

Figure 35. Compression test of swelled 650 NE samples using Instron machine until 1 kN load was reached.

For the nucleus with endplate samples, the area used for stress calculations included only the outer diameter creating a lesser modulus and stress than the above ringed samples, from the increase in cross-sectional area. However, when observing strain results between ringed and nucleus samples at highest tested load, the strains decreased with the addition of the nucleus, showing greater strength during applied loads, given the failure mechanisms of the different samples.

Table 12. Compressive mechanical properties of swelled nucleus with endplate samples from Instron compression tests, which can be compared to natural lumbar disc **(Table S2).**

500 NE Sample	**PU 100/0**	**PU 90/10**	**PU 80/20**
Modulus (E'), MPa	3.8 ± 0.7	6.1 ± 0.7	9.2 ± 0.4
Yield Strength (YS), MPa	0.3 ± 0.0	0.4 ± 0.0	0.6 ± 0.0
Yield Strain (%)	15.4 ± 1.7	13.9 ± 2.1	15.3 ± 0.4
Strain at 950 N (%)	71.3 ± 2.6	63.4 ± 0.7	56.8 ± 3.4
650 NE Sample	**PU 100/0**	**PU 90/10**	**PU 80/20**
Modulus (E'), MPa	8.8 ± 1.4	9.6 ± 1.0	10.7 ± 0.6
Yield Strength (YS), MPa	1.0 ± 0.3	0.6 ± 0.1	0.6 ± 0.0

Yield Strain (%)	18.7 ± 1.4	10.9 ± 0.6	10.8 ± 0.5
Strain at 950 N (%)	58.2 ± 7.6	47.6 ± 6.8	44.6 ± 5.6

Statistical analysis, using a two-way ANOVA, showed that there was a statistically significant interaction between the total length of sample used and the concentration of CNCs within the samples on the mechanical properties of the samples. Simple main effects analysis determined that higher CNC concentrations as well as longer length samples showed significantly greater mechanical properties of the samples.

4.4 Failure Mechanics

The ringed samples failed from deformation by buckling, and plastically deformed once a certain stress and strain was reached. This can be explained by the lack of internal pressure within the system, keeping the samples from deforming in on itself. The nucleus samples however did not fail by deformation, but instead failed from leaking of the nucleus, and had negligible plastic deformation when pressure was released. The nucleus samples did still deform, but by barreling, not buckling, showing stabilization of the structure with the addition of the endplates **(Figure 36)**. When the samples were compressed, the nucleus, being an incompressible liquid, pushed out causing internal pressure onto the rings of the samples, resembling the normal deformation mechanics of a natural intervertebral disc. The failures shown correspond to the yield stresses and strains previously discussed **(Table 11 and 12)**.

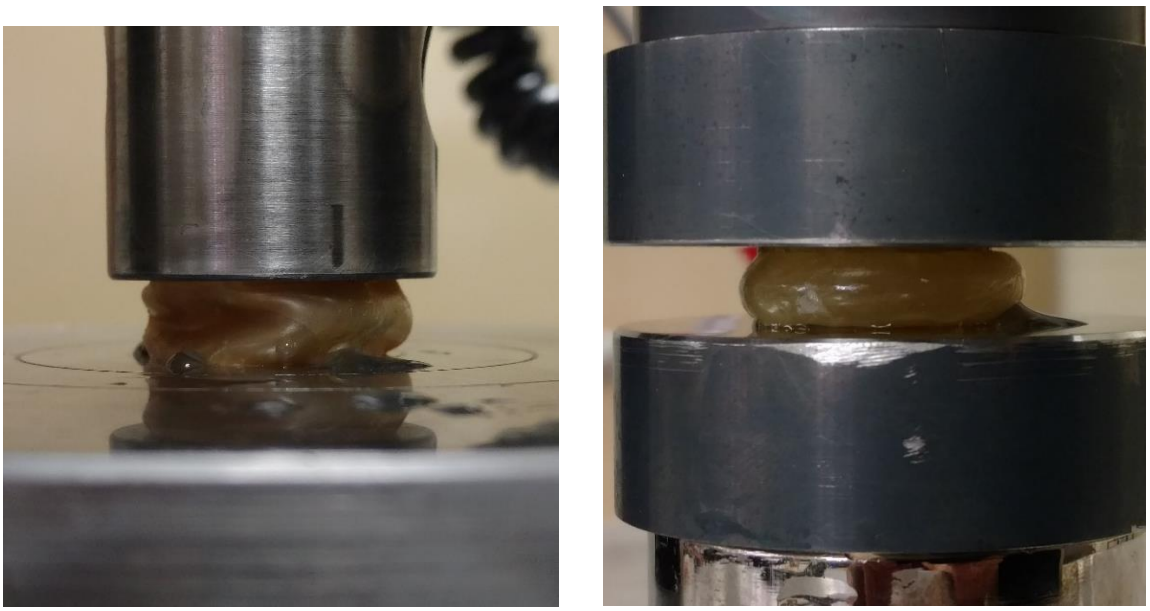

Figure 36. Deformation of the ringed samples (left) and nucleus with endplates samples (right).

4.5 p-CNC Characteristics

The TEM results showed that the optimized phosphoric acid hydrolysis produced p-CNCs with correct dimensions and aspect ratio (length:width), having an average length of 236.36 ± 25.71 nm, average width of 37.25 ± 7.34 nm, and an aspect ratio of 6.34:1. Images of the TEM are shown below with the scale bar for reference **(Figure 37)**.

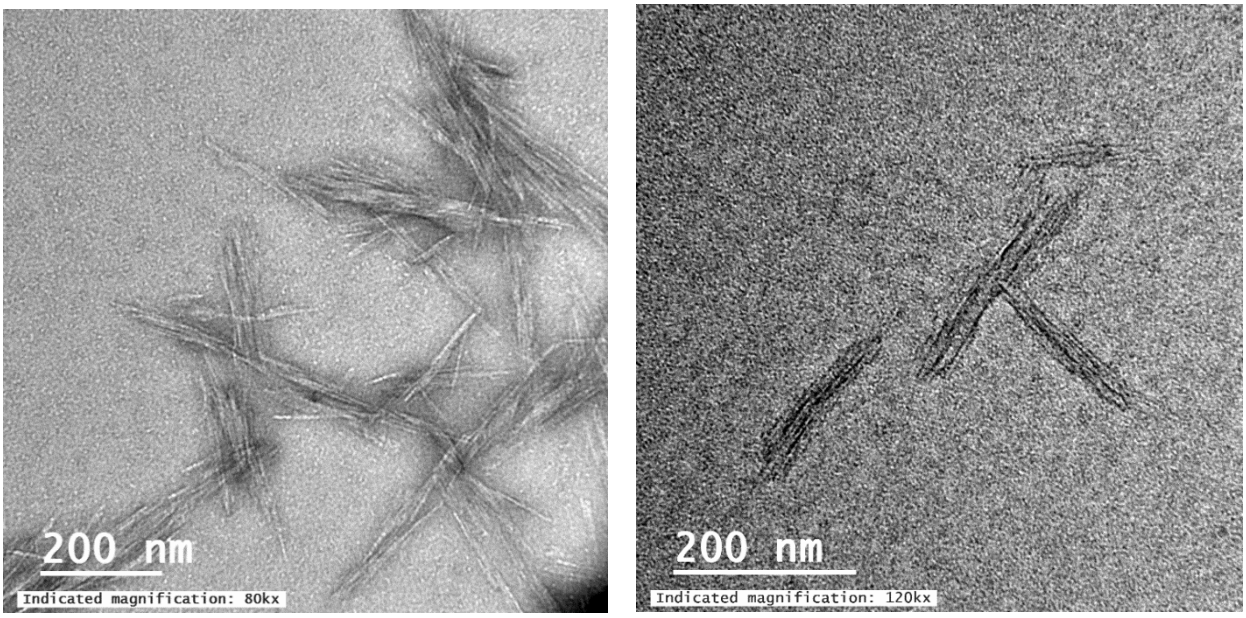

Figure 37. TEM images of p-CNCs created through phosphoric acid hydrolysis.

Conductometric titration on the p-CNCs in a HCl solution show that they have a surface charge density of 9.72 ± 4.45 mmol PO_4^{-2}/kg cellulose. Based on resulting p-CNCs, they show comparable qualities to the referenced p-CNCs [129], and should therefore have qualifying conditions for hydroxyapatite growth. With the integration of these p-CNCs into the vertebral endplates of the samples, bone integration can become feasible from the hydroxyapatites grown onto the surface of the material. However due to time constraints, these p-CNCs were not able to be integrated into the endplates.

4.6 Comparison to Current Tests

Previous studies have been conducted on the natural tissues of the human and bovine intervertebral disc, mainly those of the annulus fibrosus due it having the greatest potential to be the cause of failure. Tensile properties of the intervertebral disc are solely based on the lamella of the annulus fibrosus, therefore only ribbons of the material were tested in this study as opposed to the entire disc as a whole. These tests include tension testing of singular and multi-lamella samples in parallel and perpendicular orientation to the collagen fibrils, as well as natural flexion/extension of the spine **(Table S1)** [126, 130, 132, 140]. When comparing the tension tests of this study, only singular ribbon samples were tested during DMTA tensile

testing, and therefore multi-lamella properties could not be compared. However, since the material being used in this study is isotropic, the multi-ribbon properties of the material should act very similar to the singular ribbon tested with only the addition of shear stress and slippage. Since the CNCs disperse in the composite of this study are not oriented fibers, but more along the isotropic nature, a direct comparison between the parallel and perpendicular tension tests could not be achieved, however a direct comparison between the natural flexion/extension could be achieved showing properties in the correct range when swelled **(Figure 29)**.

Testing has been done to determine the failure load and stiffness of the vertebral endplates in the lumbar section of the spine **(Table S2)**, as well as showing that with the addition of vertebral endplates the overall strength and stiffness of the intervertebral disc increases [144]. Because the composite endplates in this study were made out of the same flexible material as the annulus ribbons, they were not able to demonstrate the needed strength and stiffness required of the hyaline cartilage endplates in the body. This shows that the wrong material was used for mimicking the strength and stiffness of the endplates. Therefore, the connection of the endplates was mainly used for proof of concept that with the addition of the endplates and nucleus, the strength of the samples increased while strain decreased, as well as determining preliminary connection strength between the endplates and the annulus.

Previous compression tests have been conducted on sections of the annulus fibrosus and nucleus pulposus, as well as the intervertebral disc as a whole, however no previous tests have been recorded for testing the annulus fibrosus as its ring structure. During certain compression testing, sections of the both the nucleus and annulus were removed and confined to determine the compressive properties of these components **(Table S2)** [126, 127]. The compression tests ran in this study were not able to determine the specific properties of the nucleus, however were able to create a comparison between the samples tested in ring form and samples tested as a complete intervertebral disc. These results are still not able to be compared to the confined compression tests however, due to the fact that this study did not confined the samples in any way, other than on the top and bottom like that of a natural disc. For the case of testing the annulus as

its whole ring structure, 3D nonlinear finite element analysis was used to determine the compressive properties. During the finite element analysis, it was also determined that the compression properties of the entire disc are based on the nucleus pressure against the inside of the annulus, and how much force the annulus can withstand [141]. Although only a computer model has been used, the testing performed in this study can be most closely compared to the testing done by the 3D nonlinear finite element analysis, since every part tested was as a whole, and was only in contact from the top and bottom as it is in the spine.

4.7 Comparison to Current Treatments

When compared to spinal fusion surgery, the composite samples in this study show a few crucial differences. The composite samples will maintain separation of the two vertebrae, of which are fused in spinal fusion surgery, allowing for the natural range of motion required of the spine. Along with this, they show incredible elastic properties, with negligible, if any, plastic deformation under high stresses, which will allow for load distribution throughout the samples instead of transferring the load to the adjacent intervertebral discs like that of fusion surgery. When longevity of the two techniques are compared, both should last for life, although the materials being used in this study have yet to be tested for extreme lengths of time inside the harsh environment of the body. Spinal fusion surgery however, has been proven to be a life-long solution, even though it comes with its own problems.

When compared to total disc replacement (TDR), the composite samples in this study show greater similarity than it did to spinal fusion. TDR for cervical discs have had great success due to the lack of heavy loads and strenuous moments put onto the cervical spine. Therefore, the main goal has been to preserve rotation, flexion/extension, and overall mobility. This is different than what is needed for the lumbar spine. The TDR, especially in the lumbar spine, needs to resist excess motion as well as reduce stress concentrations in the adjacent level tissues. The bearing designs created tend to be axially rigid and are not designed to resist bending or rotational moments, often times allowing for excess motion compared to the natural disc. Along with these problems, the ability of these lumbar TDR to absorb elastic shock and disperse loads is little to none, due to the stiffness of the metal-on-metal (MoM) or metal-on-polymer (MoP,

UHMWPE) [118]. Through DMTA tension testing and Instron compression testing, the composite samples show resistance to excess strain with applied stresses, which can potentially be correlated with the lack of excess motion when moments are applied. As well as resisting excess motion, the incredible elasticity shown in the compression tests, with little to no plastic deformation at high stresses and strains, shows that they will have much greater shock absorption and load dispersion than any other TDR out there. The composite samples can be most similarly related to the one-piece TDR in which there is a single core held together by two endplates, instead of a ball and socket configuration. These one piece TDRs allow for some shock absorption, however degrade pretty readily in the body causing fatigue failure due to the cyclic loading endured. The composite samples were not tested with cyclic loading because of the lack of a hydraulic press with a small enough load cell to test the samples, therefore they cannot be directly compared. When comparing device degradation in the body due to wear and corrosion from the articulating bearings being in a harsh environment, the composite samples show better properties. All of the TDR, whether MoM, MoP, or PEEK-on-PEEK (PoP), show degradation within the body, either from wear or corrosion, causing significant toxic and biological reactions such as metallosis, osteolysis, inflammation, and even migration of the implant to surrounding tissue or complete rejection of the implant [118]. All of the materials used in the composite samples are biocompatible and non-biodegradable, the RxT85A polyurethane being a medical grade PU currently being used in many medical devices inside the body. Another key difference is the lack of metal in the composite samples created, therefore getting rid of the potential chance for metal wear particles to enter into the body. The main flaw with the composite samples when compared to both the spinal fusion surgery and TDR though, is that they deform too much under a much lower stress than desired in the body. These mechanical properties however, can always be fine-tuned in order to achieve the desired strength and stiffness.

4.8 Potential Problems/Alternative Methods

With all experimental methods regarding the human body, some potential problems can occur, such as unforeseen failures, the body's rejection of the foreign material, and changes in the material's mechanical properties after implantation. When tested in compression, all of the samples showed a great deal of deformation under much less stress than that of the natural disc, reaching anywhere from 45% to 83% strain around 3 MPa of stress as opposed to reaching around 95% strain at 18 MPa of stress. This could cause the spinal column to undergo a much greater amount of total deformation under heavy loads, drastically shortening the spine and causing unforeseen problems to the surrounding tissue, most importantly the spinal cord. One reason for these results could have been that the samples sizes tested were much smaller than the natural disc, therefore decreasing the amount of rings used, ultimately decreasing strength and resistance to deformation. The nucleus used could also play a role in the results obtained, since the natural nucleus pulposus is a proteoglycan and collagen fibril hydrogel-like material and the nucleus synthesized was water. The change in viscosity from water to the hydrogel-like material could increase the compressive strength of the samples while limiting exceedingly high deformation, due to the added of friction between parts of the fluid.

Another potential problem could be the lack of porosity throughout the samples resulting in a lack of nutrient absorption/transport through the spine, which could be vital for surrounding tissues and bony vertebrae. This would also cause the problem of eliminating the reabsorption of water into the disc during resting periods, such as sleeping. However, if there is no water loss through the annulus of the samples during active periods, then there would be no need for the reabsorption of water.

The vertebral endplates, created out of the same material as the annulus fibrosus, proved to be problematic due to the severe lack of strength and stiffness, when compared to the hyaline cartilage of the natural endplates. Although they are able to resist fracture, if the endplates are too weak or flexible, they will undergo too much deformation causing potential damage to the synthetic disc as a whole or even to tear away from the vertebrae completely. For this reason, a different material such as UHMWPE or PEEK

should be researched for the role of the endplates both being durable, stiff, and resistant to fracture. Along with the weakness of the endplates, there is a possibility for the connection between the vertebrae and endplates to be less than ideal. If there is insufficient bone growth into the endplates, the mechanical interlocking holding the disc to the vertebrae would be too weak causing the potential problem of slippage between the disc and the vertebrae or detachment as a whole. On the opposite side of the spectrum, if the bone growth in too great through the sample then it would cause fusion between the top and bottom vertebrae, making the sample no more useful than spinal fusion surgery. To correct this potential problem, p-CNCs can be used within just the vertebral endplates to grow hydroxyapatites, and therefore bone growth promotion only through the vertebral endplates instead of throughout the entire samples.

One of the last but probably most problematic, is the possibility for herniation of the nucleus either through rupture of the annulus or poor connection between the vertebral endplates and the annulus causing leakage through the seal. During testing of the NE samples, the failure mechanism was due to the poor connection between the endplates and the annulus, instead of pressure put onto the annulus, therefore this would be the most likely cause for herniation. If these samples were to be 3D printed, injection molded or roll milled (like car tires), the connection between the endplates and annulus could be much stronger, making it less likely to herniate.

5. Conclusion and Outlook

In summary, the elastic modulus, tensile and compressive strength, and max tensile elongation of the polymer composite were found for a variety of conditions using multiple composition ratios of PU 85 to CNCs. When swelled as opposed to dry, the samples showed much closer mechanical properties to that of a natural disc than did the dry samples, showing the benefits of using this material composition in the body where fluid will be absorbed. The composition that behaved the most similar to that of the annulus fibrosus was the PU 80/20 composition, with PU 90/10 still reaching the range of acceptable values, but not as accurately as the aforementioned composition. These results prove the viability of this research project for moving spinal disc implant research in the right direction. This solution has the potential to replace discs without using metal in the body, while preserving full mobility of the spine and reducing/eliminating pain in the lower back. Not only does it show promising results for spinal disc replacements, but it also uses a novel processing and fabrication technique that has not been used previously in the body. Using a ringed sample as opposed to using a solid block of the same material has proven to resemble the natural disc's mechanical properties needed, with the solid block of material being much too strong and stiff. The goals of this study were achieved, successfully creating synthetic lamellae to mimic the annulus tensile properties as well as compressive properties when wound together into a synthetic annulus. The preliminary attachment of vertebral endplates was slightly less than successful, since the failure mechanism of the samples was strictly due to the lack of adhesion. The preliminary nucleus showed good internal pressure within the system in order to cause barreling like that of the natural disc, and added additional strength and stiffness to the composite samples. All mechanical properties were not able to be fine-tuned, however with additional time, this three-part polymer composite system shows great potential in the field on total disc replacements.

If continued, this project should look into alternate fabrications methods in order to create a better connection between the annulus and vertebral endplates. Such methods could include 3D printing, roll milling (as done in tire manufacturing), and injection molding. These would help the samples withstand the

leaking of the nucleus through the poor connection. As well as fabrication methods for vertebral endplate connection, alternate fabrication processes for a hydrogel-like nucleus should be further researched. With the increase in viscosity of a hydrogel as compared to water, the leaking of the nucleus should be decreased as well as the strength/modulus of the samples increased. Once fabrication methods have been determined, compression/relaxation tests should be run in order to determine the fatigue life and wear resistance of these samples. After mechanical properties are fine-tuned to meet the intervertebral disc needs, p-CNCs should be incorporated into vertebral endplates for hydroxyapatite growth and eventually proliferation of osteoblasts and bone growth into the surface of the vertebral endplates to show their ability to connect to the bony vertebrae. Cell viability, biocompatible properties of samples, and immune response should be determined using cell proliferation and culturing on the surface of all materials used. These will be used to determine the body's reaction to the foreign material. Finally, actual implantation techniques could be researched to determine most suitable approach during implantation stage of the replacement discs.

References

[1] The Editors of Encyclopaedia Britannica. “Vertebral Column.” Encyclopaedia Britannica, Inc. January, 2014. https://www.britannica.com/science/vertebral-column

[2] Agur AMR, Dalley II AF. “Grant’s Atlas of Anatomy: Twelfth Edition.” Lipincott Williams & Wilkins. 2009

[3] Raj PP. “Intervertebral Disc: Anatomy-Physiology-Pathophysiology-Treatment.” Pain Practice. 2008. 8(1): 18-44.

[4] http://coewww.rutgers.edu/classes/mae/mae473/LectureSpine.pdf

[5] Bogduk N, Mercer S. “Biomechanics of the cervical spine. I: Normal kinematics.” Clinical Biomechanics. 2000. 15(9): 633-48.

[6] Swartz EE, Floyd RT, Cendoma M. “Cervical Spine Functional Anatomy and the Biomechanics of Injury Due to Compressive Loading.” Journal of Athletic Training. 2005. 40(3): 155-61.

[7] Panjabi MM, Crisco JJ, Vasavada A, Oda T, Cholewicki J, Nibu K, Shin E. “Mechanical Properties of the Human Cervical Spine as Shown by Three-Dimensional Load-Displacement Curves.” Spine. December, 2001. 26(24): 2962-2700.

[8] Caridi JM, Pumberger M, Hughes AP. “Cervical Radiculopathy: A Review.” HSS Journal. 2011. 7(3): 265-72.

[9] Yeung JT, Johnson JI, Karim AS. “Cervical disc herniation presenting with neck pain and contralateral symptoms: a case report.” Journal of Medical Case Reports. 2012. 6: 166.

[10] Edmondston SJ, Singer KP. “Thoracic spine: anatomical and biomechanical considerations for manual therapy.” Manual Therapy. 1997. 2(3): 132-43.

[11] https://www.kenhub.com/en/library/anatomy/thoracic-vertebrae

[12] Son E-S, Lee S-H, Park S-Y, Kim K-T, Kang C-H, Cho S-W. “Surgical Treatment of T1-2 Disc Herniation with T1 Radiculopathy: A Case Report with Review of the Literature.” Asian Spine Journal. 2012. 6(3): 199-202.

[13] Goh S, Tan C, Price RI, Edmondston SJ, Song S, Davis S, et al. “Influence of age and gender on thoracic vertebral body shape and disc degeneration: an MR investigation of 169 cases.” Journal of Anatomy. 2000. 197(Pt 4): 647-57.

[14] Cervero F, Tattersall JEH. “Chapter 12 Somatic and visceral sensory integration in the thoracic spinal cord.” Progress in Brain Research. 1986. 67: 189-205.

[15] Boszczyk BM, Boszczyk AA, Putz R. “Comparative and functional anatomy of the mammalian lumbar spine.” The Anatomical Record. 2001. 264(2): 157-68.

[16] BenEliyahu DJ. “Magnetic resonance imaging and clinical follow-up: study of 27 patients receiving chiropractic care for cervical and lumbar disc herniations.” J Manipulative Physiol Ther. December, 1996. 19(9): 597-606.

[17] Troup JDG, Hood CA, Chapman AE. “MEASUREMENTS OF THE SAGITTAL MOBILITY OF THE LUMBAR SPINE AND HIPS.” Rheumatology. 1968. 9(8): 308-21.

[18] Haughton VM, Rogers B, Meyerand ME, Resnick DK. “Measuring the Axial Rotation of Lumbar Vertebrae in Vivo with MR Imaging.” American Journal of Neuroradiology. 2002. 23(7): 1110-6.

[19] Granhed H, Jonson R, Hansson T. “The Loads on the Lumbar Spine During Extreme Weight Lifting.” March, 1987. PDF

[20] Tan SH, Teo EC, Chua HC. “Quantitative three-dimensional anatomy of cervical, thoracic and lumbar vertebrae of Chinese Singaporeans.” European Spine Journal. 2004. 13(2): 137-46.

[21] Crawford RP, Cann CE, Keaveny TM. “Finite element models predict in vitro vertebral body compressive strength better than quantitative computed tomography.” Bone. 2003. 33(4): 744-50.

[22] Shah JS, Hampson WG, Jayson MI. “The distribution of the surface strain in the cadaveric lumbar spine.” The Bone and Joint Journal. May, 1978. 60(2): 246-251.

[23] Bogduk N. “The Innervation of the Lumbar Spine.” Spine. April, 1983.

[24] Luoma K, Riihimaki H, Luukkonen R, Raininko R, Viikari-Juntura E, Lamminen A. “Low Back Pain in Relation to Lumbar Disc Degeneration.” Spine. February, 2000. 25(4): 487-492.

[25] Nygaard O, Mellgren SI. “The Function of Sensory Nerve Fibers in Lumbar Radiculopathy: Use of Quantitative Sensory Testing in the Exploration of Different Populations of Nerve Fibers and Dermatomes.” February, 1998. 23(3): 348-352.

[26] Takahashi I, Kikuchi SI, Sato K, Sato N. “Mechanical Load of the Lumbar Spine During Forward Bending Motion of the Trunk-A Biomechanical Study.” January, 2006. 31(1): 18-23.

[27] Bogduk N. “Clinical Anatomy of the Lumbar Spine and Sacrum.” Textbook. Elsevier Health Sciences. 2005. 250 pages.
[28] Koes BW, van Tulder MW, Peul WC. “Diagnosis and treatment of sciatica.” BMJ : British Medical Journal. 2007. 334(7607): 1313-7.
[29] Grob KR, Neuhuber WL, Kissling RO. “Innervation of the sacroiliac joint of the human”. Z Rheumatol. 1995. 54(2): 117-22.
[30] Lirette LS, Chaiban G, Tolba R, Eissa H. “Coccydynia: An Overview of the Anatomy, Etiology, and Treatment of Coccyx Pain.” The Ochsner Journal. 2014. 14(1): 84-7.
[31] Humzah MD, Soames RW. “Human intervertebral disc: Structure and function.” The Anatomical Record. 1988. 220(4): 337-56.
[32] Poni JS, Hukins DWL, Harris PF, Hilton RC, Davies KE. “Comparison of the structure of human intervertebral discs in the cervical, thoracic and lumbar regions of the spine.” Surgical and Radiologic Anatomy. September, 1986. 8(3): 175-182.
[33] Mahendra KA, Rajani JA, Shailendra JS, Narsinh HG. “Morphometric Study of Cervical Intervertebral Disc.” International Journal of Anatomy Physiology and Biochemistry. May, 2015. 2(5).
[35] Davis H. “Increasing Rates of Cervical and Lumbar Spine Surgery in the United States, 1979-1990.” Spine. May, 1994. PDF
[36] Fletcher JGR, Stringer MD, Briggs CA, Davies TM, Woodley SJ. “CT morphometry of adult thoracic intervertebral discs.” European Spine Journal. October, 2015. 24(10): 2321-2329.
[37] Shao Z, Rompe G, Schiltenwolf M. “Radiographic Changes in the Lumbar Intervertebral Discs and Lumbar Vertebrae with Age.” Spine. 2002. 27(3): 263-268.
[38] Williams MP, Cherryman GR, Husband JE. “Significance of Thoracic Disc Herniation Demonstrated by MR Imaging.” JCAT. April, 1989. PDF
[39] Twomey L, Taylor J. “Age changes in lumbar intervertebral discs.” Acta Orthopaedica Scandinavica. 1985. 56(6): 496-499.
[40] http://www.medscape.com/viewarticle/543611
[41] Raj PP. “Intervertebral Disc: Anatomy-Physiology-Pathophysiology-Treatment.” Pain Practice. 2008. 8(1): 18-44.
[42] Humzah MD, Soames RW. “Human intervertebral disc: Structure and function.” The Anatomical Record. 1988. 220(4): 337-56.
[43] Galante JO. “Tensile Properties of the Human Lumbar Annuls Fibrosus.” Acta Orthopaedica Scandinavica. 1967. 38(100): 1-91.
[44] Guerin HL, Elliott DM. “Quantifying the contributions of structure to annulus fibrosus mechanical function using a nonlinear, anisotropic, hyperelastic model.” Journal of Orthopaedic Research. 2007. 25(4): 508-16.
[45] Ricard-Blum S. “The Collagen Family.” Cold Spring Harbor Perspectives in Biology. 2011. 3(1): a004978.
[46] Eyre DR, Muir H. “Types I and II Collagens in Intervertebral Disc.” Biochem J. 1976. 157: 267-270.
[47] Mouw JK, Ou G, Weaver VM. “Extracellular matrix assembly: a multiscale deconstruction.” Nature reviews Molecular cell biology. 2014. 15(12): 771-85.
[48] Yanagishita M. “Function of proteoglycans in the extracellular matrix.” Acta Pathol Jpn. June, 1993. 43(6): 283-93.
[49] Marchand F, Ahmed AM. “Investigation of the laminate structure of lumbar disc annulus fibrosus.” Spine. May, 1990. 15(5): 402-410.
[50] Adams MA. “Intervertebral Disc Tissues: Chapter 2.” Mechanical Properties of Aging Soft Tissues. 2015.
[51] Hickey SD, Hukins DWL. “Relation Between the Structure of the Annulus Fibrosus and the Function and Failure of the Intervertebral Disc.” Spine. April, 1980. PDF
[52] Smith LJ, Fazzalari NL. “The elastic fibre network of the human lumbar anulus fibrosus: architecture, mechanical function and potential role in the progression of intervertebral disc degeneration.” European Spine Journal. 2009. 18(4): 439-48.
[53] O’Connell GD, Sen S, Elliott DM. “Human Annulus Fibrosus Material Properties from Biaxial Testing and Constitutive Modeling are Altered with Degeneration.” Biomechanics and modeling in mechanobiology. 2012. 11(3-4): 493-503.
[54-55] Green TP, Adams MA, Dolan P. “Tensile properties of the annulus fibrosus II. Ultimate tensile strength and fatigue life.” Eur Spine J. December, 1993. 2(4): 209-14.
[56] Nerurkar NL, Elliott DM, Mauck RL. “Mechanical design criteria for intervertebral disc tissue engineering.” Journal of Biomechanics. 2010. 43(6): 1017-30.

[57] Ambard D, Cherblanc F. “Mechanical behavior of annulus fibrosus: a microstructural model of fibers reorientation.” Annals of Biomedical Engineering, Springer Verlag. 2009. 37(11): 2256-2265.
[58] Best B, Guilak F, Setton LA, Mow VC. “Compressive Mechanical Properties of the Human Annulus Fibrosus and Their Relationship to Biochemical Composition.” ResearchGate. January, 1994.
[59] Perie DS, Maclean JJ, Owen JP, Iatridis JC. “Correlating Material Properties with Tissue Composition in Enzymatically Digested Bovine Annulus Fibrosus and Nucleus Pulposus Tissue.” Annals of biomedical engineering. 2006. 34(5): 769-77.
[60] Iatridis JC, Setton LA, Weidenbaum M, Mow VC. “Alterations in the mechanical behavior of the human lumbar nucleus pulposus with degeneration and aging.” Journal of Orthopaedic Research. 1997. 15(2): 318-22.
[61] Trout JJ, Buckwalter JA, Moore KC. “Ultrastructure of the human intervertebral disc: II. Cells of the nucleus pulposus.” The Anatomical Record. 1982. 204(4): 307-14.
[62] Yu J, Tirlapur U, Fairbank J, Handford P, Roberts S, Winlove CP, et al. “Microfibrils, elastin fibres and collagen fibres in the human intervertebral disc and bovine tail disc.” Journal of Anatomy. 2007. 210(4): 460-71.
[63] Bonetti M. “Microfibrils: a cornerstone of extracellular matrix and a key to understand Marfan syndrome.” Ital J Anat Embryol. December, 2009. 114(4): 201-24.
[64] Akkiraju H, Nohe A. “Role of Chondrocytes in Cartilage Formation, Progression of Osteoarthritis and Cartilage Regeneration.” J. Dev. Biol. 2015. 3: 177-192.
[65] Muir H. “The chondrocyte, architect of cartilage. Biomechanics, structure, function and molecular biology of cartilage matrix macromolecules.” Bioessays. December, 1995. 17(12): 1039-48.
[66] Calve J, Galland M. “The Intervertebral Nucleus Pulposus Its Anatomy, Its Physiology, Its Pathology.” The Journal of Bone and Joint Surgery. July, 1930. 12(3): 555-578.
[67] Keyes D, Compere EL. “The Normal and Pathological Physiology of the Nucleus Pulposus of the Intervertebral Disc.” The Journal of Bone and Joint Surgery. October, 1932. PDF
[68] Lotz JC, Fields AJ, Liebenberg EC. “The Role of the Vertebral End Plate in Low Back Pain.” Global Spine Journal. 2013. 3(3): 153-64.
[69] Moore RJ. “The vertebral endplate: disc degeneration, disc regeneration.” European Spine Journal. 2006. 15(3): 333-7.
[70] Mwale F, Roughley P, Antoniou J. “DISTINCTION BETWEEN THE EXTRACELLULAR MATRIX OF THE NUCLEUS PULPOSUS AND HYALINE CARTILAGE: A REQUISITE FOR TISSUE ENGINEERING OF INTERVERTEBRAL DISC.” European Cells and Materials. 2004. 8: 58-64.
[71] Sophia Fox AJ, Bedi A, Rodeo SA. “The Basic Science of Articular Cartilage: Structure, Composition, and Function.” Sports Health. 2009. 1(6): 461-8.
[72] Miller EJ, Kent Rhodes R. “[2] Preparation and characterization of the different types of collagen.” Methods in Enzymology. 1982. 82: 33-64.
[73] Maynes R. “Structure and function of Collagen types.” Elsevier Textbook. December, 2012. 328 pages.
[74] Royce PM, Steinmann B. “Connective Tissue and Its Heritable Disorders: Molecular, Genetic, and Medical Aspects, Second Edition: Chapter 2.” Wiley-Liss Textbook. April, 2003.
[75] Grant PJ, Oxland TR, Dvorak MF. “Mapping the Structural Properties of the Lumbrosacral Vertebral Endplates.” Spine. April, 2001. 26(8): 889-896.
[76] Herkowitz HN. “The Lumbar Spine.” Lippincott Williams and Wilkins Textbook. 2004. 943 pages.
[77] Nekkanty S, Yerramshetty J, Kim D-G, Zauel R, Johnson E, Cody DD, et al. “Stiffness of the endplate boundary layer and endplate surface topography are associated with brittleness of human whole vertebral bodies.” Bone. 2010 .47(4): 783-9.
[78] Rodriguez AG, Rodriguez-Soto AE, Burghardt AJ, Berven S, Majumdar S, Lotz JC. “Morphology of the human vertebral endplate.” Journal of orthopaedic research : official publication of the Orthopaedic Research Society. 2012. 30(2): 280-7.
[79] Rudert M, Tillman B. “Lymph and blood supply of the human intervertebral disc. Cadaver study of correlations to discitis.” Acta Orthop Scand. February, 1993. 64(1): 37-40.
[80] Nerlich AG, Schaaf R, Wälchli B, Boos N. “Temporo-spatial distribution of blood vessels in human lumbar intervertebral discs.” European Spine Journal. 2007. 16(4): 547-55.
[81] Bogduk N, Tynan W, Wilson AS. “The nerve supply to the human lumbar intervertebral discs.” Journal of Anatomy. 1981. 132(Pt 1): 39-56.
[82] Edgar MA. “The nerve supply of the lumbar intervertebral disc.” Journal of Bone & Joint Surgery, British Volume. 2007. 89-B(9): 1135-9.

[83] Freemont AJ, Peacock TE, Goupille P, Hoyland JA, O'Brien J, Jayson MIV. "Nerve ingrowth into diseased intervertebral disc in chronic back pain." The Lancet. 1997. 350(9072): 178-81.
[84] Urban JPG, Roberts S. "Degeneration of the intervertebral disc." Arthritis Research & Therapy. 2003. 5(3): 120-30.
[85] Gaskin DJ, Richard P. The Economic Costs of Pain in the United States. In: Institute of Medicine (US) Committee on Advancing Pain Research, Care, and Education. "Relieving Pain in America: A Blueprint for Transforming Prevention, Care, Education, and Research." Washington (DC): National Academies Press (US); 2011. Appendix C.
[86] Crow WT, Willis DR. "Estimating Cost of Care for Patients With Acute Low Back Pain: A Retrospective Review of Patient Records." The Journal of the American Osteopathic Association. 2009. 109(4): 229-33.
[87] Roberts S, Evans H, Trivedi J, Menage J. "Histology and Pthology of the Human Intervertebral Disc." Journal of Bone and Joint Surgery. April, 2006. 88(Suppl-2): 10-14.
[88] Battie M, Videman T, Levalahti E, Gill K, Kaprio J. Genetic and Environmental Effects on Disc Degeneration by Phenotype and Spinal Level: A Multivariate Twin Study." Spine. December, 2008. 33(25): 2801-2808.
[89] Buckwater JA. "Aging and Degeneration of the Human Intervertebral Disc." Spine. June, 1995. PDF
[90] Inoue N, Espinoza Orías AA. "Biomechanics of Intervertebral Disc Degeneration." The Orthopedic clinics of North America. 2011. 42(4): 487-99.
[91] Suzuki A, Daubs MD, Hayashi T, Ruangchainikom M, Xiong C, Phan K, Scott T, Wang J. "Magnetic Resonance Classification System of Cervical Intervertebral Disc Degeneration: Its Validity and Meaning." Clinical Spine Surgery. June, 2017. 30(5): E547-E553.
[92] Sinusas K. "Osteoarthritis: diagnosis and treatment." Am Fam Physician. January, 2012. 85(1): 49-56.
[93] Goode AP, Carey TS, Jordan JM. "Low Back Pain and Lumbar Spine Osteoarthritis: How Are They Related?" Current rheumatology reports. 2013. 15(2): 305.
[94] Dunlop RB, Adams MA, Hutton WC. "Disc Space Narrowing and the Lumbar Facet Joints." British Editorial Society of Bone and Joint Surgery. November, 1984. 66(5).
[95] Fujiwara A, Tamai K, Yamato M, An HS, Yoshida H, Saotome K, et al. "The relationship between facet joint osteoarthritis and disc degeneration of the lumbar spine: an MRI study." European Spine Journal. 1999. 8(5): 396-401.
[96] Fujiwara A, Lim TH, An H, Tanaka N, Jeon CH, Andersson GB, Haughton VM. "The Effect of Disc Degeneration and Facet Joint Osteoarthritis on the Segmental Flexibility of the Lumbar Spine." Spine Journal. December, 2000. 25(23): 3036-3044.
[97] Horkoff M, Maloon S. "Dysphagia secondary to esophageal compression by cervical osteophytes: A case report." BCMJ. November, 2014. 56(9): 442-444.
[98] Milette P, Fontaine S, Lepanto L, Cardinal E, Breton G. "Differentiating Lumbar Disc Protrusions, Disc Bulges, and Discs with Normal Contour but Abnormal Signal Intensity: Magnetic Resonance Imaging with Discographic Correlations." Spine. January, 1999. 24(1): 44-53.
[99] Adams MA, Hutton WC. "Gradual Disc Prolapse." Spine. August, 1985. PDF
[100] Hong J, Ball PA. "Resolution of Lumbar Disc Herniation without Surgery." N Engl J Med. 2016. 374: 1564.
[101] Kortelainen P, Puranen J, Koivisto E, Lahde S. "Symptoms and Signs of Sciatica and Their Relation to the Localization of the Lumbar Disc Herniation." Spine. February, 1985. PDF
[102] http://search.proquest.com/docview/1882127135?accountid=14826
[103] Taher F, Essig D, Lebl DR, Hughes AP, Sama AA, Cammisa FP, Girardi FP. "Lumbar Degenerative Disc Disease: Current and Future Concepts of Diagnosis and Management." Advances in Orthopedics. April, 2012: 2012: 970752.
[104] American Physical Therapy Association. "Physical Therapist's Guide to Degenerative Disc Disease." June, 2011. http://www.moveforwardpt.com/symptomsconditionsdetail.aspx?cid=514086b4-1272-4584-8742-ec6d2aa8f8cb
[105] Adams MA, Stefanakis M, Dolan P. "Healing of a painful intervertebral disc should not be confused with reversing disc degeneration: Implications for physical therapies for discogenic back pain." Clinical Biomechanics. 2010. 25(10): 961-71.
[106] http://www.arksurgicalhospital.com/will-steroid-injections-help-my-degenerative-disc-disease/
[107] Buttermann GR. "The effect of the spinal steroid injections for degenerative disc disease." Spine J. September, 2004. 4(5): 495-505.
[108] Chou R, Huffman L. "Medications for acute and chronic low back pain: A review of the evidence for an american pain society/american college of physicians clinical practice guideline." Annals of Internal Medicine. 2007. 147(7): 505-14.

[109] Highsmith JM. “Drugs, Medications, and Spinal Injections for Degenerative Disc Disease.” SpineUniverse. June, 2016.
[110] Sluijter ME, Cosman ER. “Method and apparatus for heating an intervertebral disc for relief of back pain.” Google Patents; 1995.
[111] Sluijter ME, Cosman ER. “Thermal denervation of an intervertebral disc for relief of back pain.” Google Patents; 1996.
[112] Sulaiman SB, Keong TK, Cheng CH, Saim AB, Idrus RBH. “Tricalcium phosphate/hydroxyapatite (TCP-HA) bone scaffold as potential candidate for the formation of tissue engineered bone.” The Indian Journal of Medical Research. 2013. 137(6): 1093-101.
[113] Nouh MR. “Spinal fusion-hardware construct: Basic concepts and imaging review.” World J Radiol. May, 2012. 4(5): 193-207.
[114] Spivak JM. “Multilevel Spinal Fusion for Low Back Pain.” Spine-health. August, 2007.
[115] Quirno, M., Goldstein, J. A., Bendo, J. A., Kim, Y., & Spivak, J. M. “The Incidence of Potential Candidates for Total Disc Replacement among Lumbar and Cervical Fusion Patient Populations.” Asian Spine Journal. 2011. 5(4): 213–219.
[116] https://search.proquest.com/docview/223949531?pq-origsite=gscholar
[117] Kim CW. “Confusion About Spinal Fusion.” SpineUniverse. February, 2017.
[118] Reeks J, Liang H. “Materials and Their Failure Mechanisms in Total Disc Replacements.” Lubricants. 2015. 3: 346-364.
[119] Serhan H, Mhatre D, Defossez H, Bono CM. “Motion-preserving technologies for degenerative lumbar spine: The past, present, and future horizons.” SAS Journal. 2011. 5: 75-89.
[120] Guterl CC, See EY, Blanquer SBG, Pandit A, Ferguson SJ, Benneker LM, et al. “CHALLENGES AND STRATEGIES IN THE REPAIR OF RUPTURED ANNULUS FIBROSUS.” European cells & materials. 2013. 25: 1-21.
[121] Bron JL, Helder MN, Meisel HJ, Van Royen BJ, Smit TH. “Repair, regenerative and supportive therapies of the annulus fibrosus: achievements and challenges.” Eur Spine J. 2009. 18: 301-313.
[122] Vadalà G, Mozetic P, Rainer A, Centola M, Loppini M, Trombetta M, et al. “Bioactive electrospun scaffold for annulus fibrosus repair and regeneration.” European Spine Journal. 2012. 21(Suppl 1): 20-6.
[123] Alini M, Roughley PJ, Antoniou J, Stoll T, Aebi M. “A biological approach to treating disc degeneration: not for today, but maybe for tomorrow.” In: Gunzburg R, Mayer HM, Szpalski M, Aebi M, editors. Arthroplasty of the Spine. Berlin, Heidelberg: Springer Berlin Heidelberg; 2004. p. 159-64.
[124] Sakai D, Mochida J, Iwashina T, Hiyama A, Omi H, Imai M, et al. “Regenerative effects of transplanting mesenchymal stem cells embedded in atelocollagen to the degenerated intervertebral disc.” Biomaterials. 2006. 27(3): 335-45.
[125] Bron JL, Helder MN, Meisel H-J, Van Royen BJ, Smit TH. “Repair, regenerative and supportive therapies of the annulus fibrosus: achievements and challenges.” European Spine Journal. 2009. 18(3): 301-13.
[126] Nerurkar NL, Elliot DM, Mauck RL. “Mechanical Design Criteria for Intervertebral Disc Tissue Engineering.” J Biomech. April, 2010. 43(6): 1017-1030.
[127] Best BA, Guilak F, Setton LA, Zhu W, Saed-Nejad F, Ratcliffe A, Weidenbaum M, Mow VC. “Compressive Mechanical Properties of the Human Annulus Fibrosus and Their Relationship to Biochemical Composition.” SPINE. 1994. 19(2): 212-221.
[128] “Product Center Thermoplastic Polyurethanes.” Covestro. September, 2015.
[129] Espinosa SC, Kuhnt T, Foster EJ, Weder C. “Isolation of thermally stable cellulose nanocrystals by phosphoric acid hydrolysis.” Biomacromolecules. 2013. 14(4): 1223-1230.
[130] Green TP, Adams MA, Dolan P. “Tensile properties of the annulus fibrosus.” Eur Spine J. 1993. 2: 209.
[131] Adams MA. Derby B, Akhtar R. “Mechanical Properties of Aging Soft Tissues: *Intervertebral Disc Tissues.*” Engineering Materials and Processes. 2015. Chapter 2.
[132] Keller TS, Spengler DM, Hansson TH. “Mechanical Behavior of the Human Lumbar Spine. I. Creep Analysis During Static Compressive Loading.” Jour of Ortho Res. 1987. 5: 467-478.
[133] Iatridis JC, Setton LA, Weidenbaum M, Mow VC. “Alterations in the mechanical behavior of the human lumbar nucleus pulposus with degeneration and aging.” J Orthop Res. Mar, 1995. 15(2): 318-322.
[134] Moore RJ. “The vertebral endplate: disc degeneration, disc regeneration.” Eur Spine J. August, 2006. 15(3): 333-337.
[135] Lotz JC, Fields AJ, Liebenberg EC. “The Role of the Vertebral Endplate in Low Back Pain.” Global Spine J. June, 2013. 3(3): 153-164.

[136] Inoue N, Espinoza Orias AA. “Biomechanics of Intervertebral Disc Degeneration.” Orthop Clin North Am. October, 2011. 42(4): 487-499.
[137] O’Connell GD, Vresilovic EJ, Elliott DM. “Comparative Intervertebral Disc Anatomy Across Several Animal Species.” Transactions of the Orthopaedic Research Society, 52nd Annual Meeting.
[138] Twomey L, Taylor J. “Age changes in lumbar intervertebral discs.” Acta Orthopaedica Scandinavica. 1985. 56(6): 496-499.
[139] Pooni JS, Hukins DWL, Harris PF, Hilton RC, Davies KE. “Comparison of the structure of human intervertebral discs in the cervical, thoracic and lumbar regions of the spine.” Surg Radiol Anat. September, 1986. 8(3): 175-182.
[140] Schechtman H, Robertson PA, Broom ND. “Quasi-static and cyclic compressive loading studies of the intervertebral disc with combined flexion and torsion.” Rev. Bras. Eng. Biomed. December, 2012. 28(4): 311-318.
[141] Shirazi-Adl SA, Shrivastava SC, Ahmed AM. “Stress Analysis of the Lumbar Disc-Body Unit in Compression: A Three-Dimensional Nonlinear Finite Element Study.” Spine. 1984. 9(2): 120-134.
[142] Jordon J, Konstantinou K, O’Dowd J. “Herniated lumbar disc.” BMJ Clin Evid. March, 2009. (2009): 1118.
[143] Kortelainen P, Puranen J, Koivisto E, Lahde S. “Symptoms and Signs of Sciatica and Their Relation to the Localization of the Lumbar Disc Herniation.” Spine. 1985. 10(1): 88-92.
[144] Grant JP. “Mapping the Structural Properties of the Lumbosacral Vertebral Endplates.” B.Eng. Sci. The University of Western Ontario. 1997.
[145] Holzapfel GA, Schulze-Bauer CAJ, Feigl G, Regitnig P. “Singular lamellar mechanics of the human lumbar annulus fibrosus.” Model Mechanobiol. March, 2005. 3(3): 215-140.

Supplemental Information

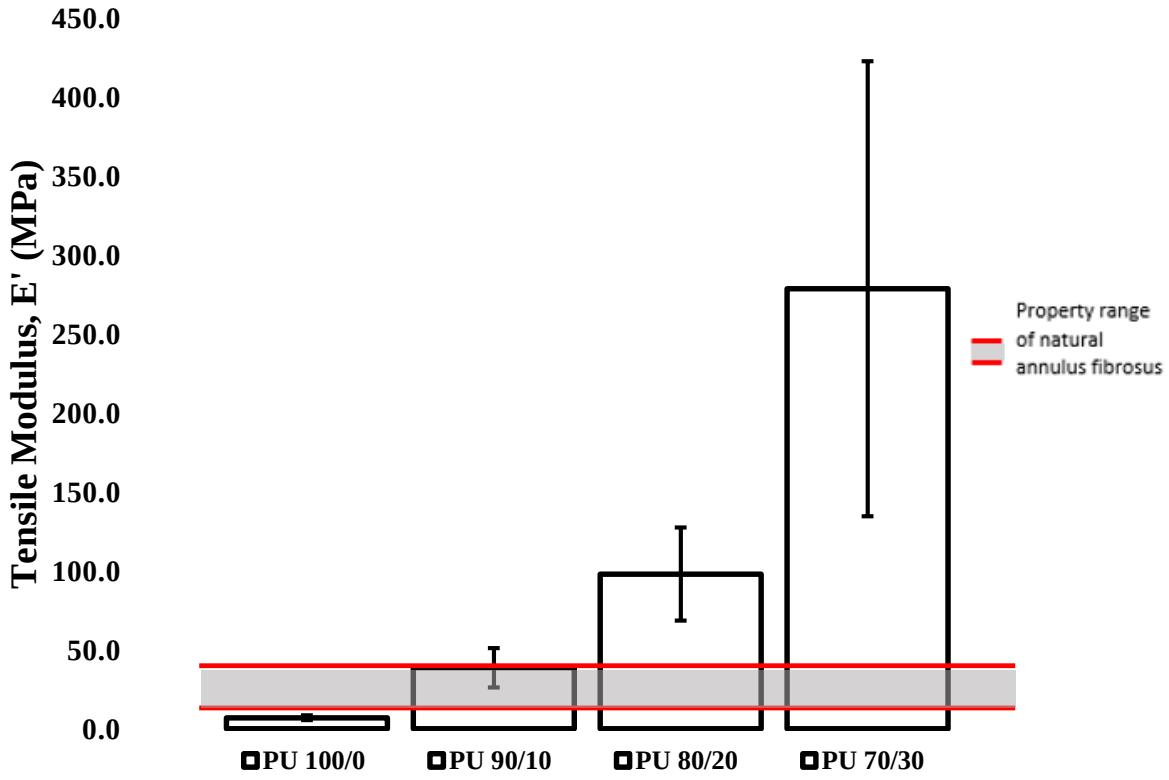

Figure S1. Tensile modulus of dry PU 70 samples using DMTA. Lines indicate property range of natural lumbar discs [126].

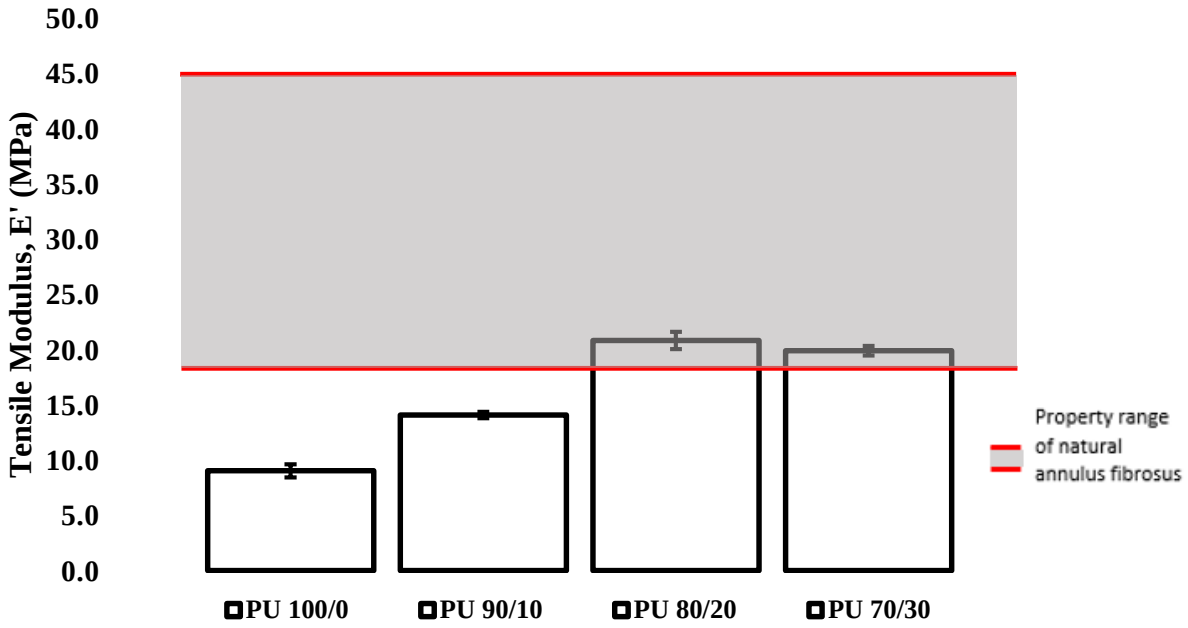

Figure S2. Tensile modulus of swelled PU 70 samples using DMTA. Lines indicate property range of natural lumbar discs [126].

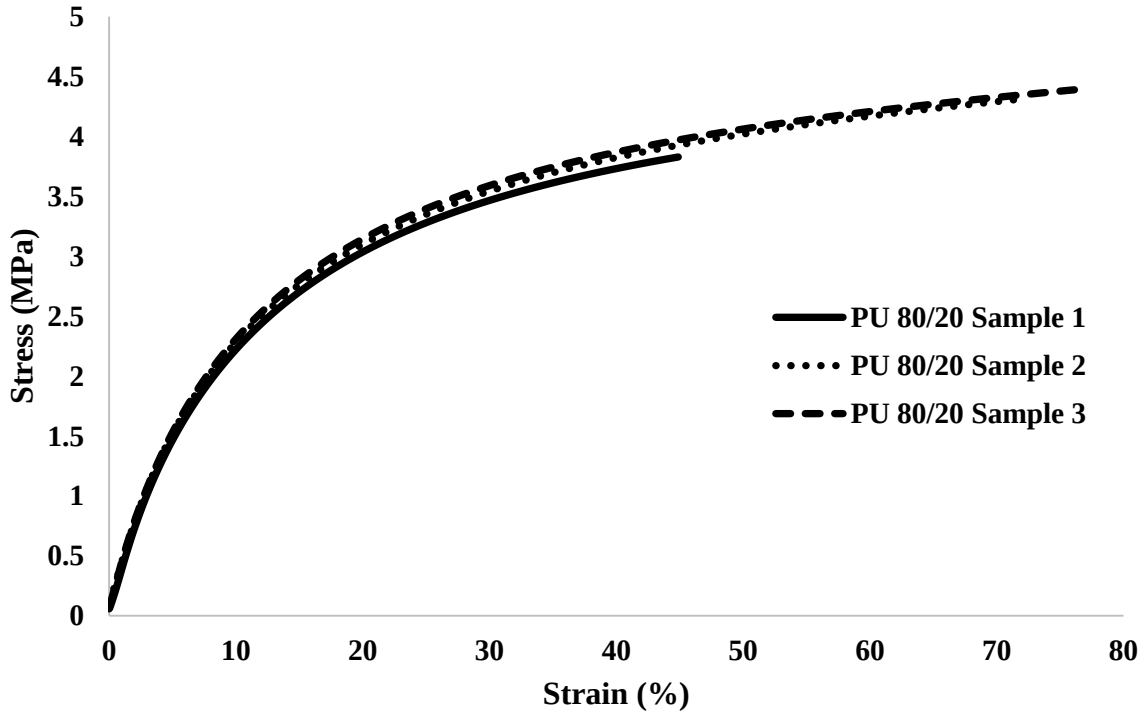

Figure S3. Tension tests of three different swelled (80/20 wt%) PU 85 samples to show repeatability between samples. Representation of why the error bars and standard deviations are so small in **Figure 29 and Table 13**.

Table S1. Tensile properties to mimic for annulus fibrosus based on natural disc properties [126, 130, 132, 140, 145].

Sample	Sample Specification	Yield Stress, MPa	Ultimate Stress, MPa	Elastic Modulus, MPa	Yield Strain, %	Ultimate Strain, %	Stiffness, N/m
Bulk Annulus	**Outer, A**	--	3.9 ± 1.8	16.4 ± 7.0	20 – 30*	65 ± 16	5.7 ± 3.4
	Outer, P	--	8.6 ± 4.3	61.8 ± 23.2	20 – 30*	34 ± 11	5.7 ± 3.4
	Inner	--	2.0 ± 1.5	--	20 – 30*	64 ± 36	1.2 ± 1.1
Single Lamella	**Parallel**	--	--	28 – 78	--	--	--
	Perpendicular	--	--	0.22	--	--	--

* Strains were recorded for the annulus fibrosus as a whole.

Table S2. Compression properties to mimic from natural intervertebral disc properties [126, 127, 141, 144].

Section of Annulus Fibrosus	Swell Pressure, (P_{sw}), MPa	Modulus, (H_A), MPa	Permeability, (k), ($x10^{-15}$ m^4/N-s)
Anterior	0.11 ± 0.05	0.36 ± 0.15	0.26 ± 0.12
Posterior	0.14 ± 0.06	0.40 ± 0.18	0.23 ± 0.09
Outer	0.11 ± 0.07	0.44 ± 0.21	0.25 ± 0.11
Middle	0.14 ± 0.04	0.42 ± 0.10	0.22 ± 0.06
Inner	0.12 ± 0.04	0.27 ± 0.11	0.27 ± 0.13
Bulk Material	--	4.2	--
Nucleus Pulposus	0.138	1.0	0.9

Section of Vertebral Endplates	Stiffness, N/mm	Failure Load, N
Superior	121.3	93.0
Inferior	156.7	137.7

	Yield Stress, MPa	Ultimate Stress, MPa	Yield Strain (%)	Ultimate Strain (%)
Intervertebral Disc	--	18.0 ± 7.1	--	95.4 ± 4.4

Table S3. Dimensions of ringed samples used for Instron compression testing.

500 mm Sample	PU 100/0	PU 90/10	PU 80/20	Natural Disc* [137, 138, 139]
Thickness, mm	9.5 ± 0.1	9.2 ± 0.0	9.3 ± 0.0	11.3 ± 1.3
Inner Diameter, mm	15.2 ± 0.1	15.3 ± 0.0	15.4 ± 0.0	31.6**
Outer Diameter, mm	22.5 ± 0.2	22.6 ± 0.1	22.9 ± 0.1	38.8 ± 1.8
Area, mm^2	217.4 ± 6.2	219.5 ± 3.3	226.1 ± 2.1	398.1

650 mm Sample	PU 100/0	PU 90/10	PU 80/20	Natural Disc* [137, 138, 139]
Thickness, mm	9.4 ± 0.0	9.4 ± 0.1	9.4 ± 0.1	11.3 ± 1.3
Inner Diameter, mm	12.2 ± 0.1	12.2 ± 0.0	12.2 ± 0.1	31.6**
Outer Diameter, mm	22.7 ± 0.2	23.3 ± 0.1	23.8 ± 0.1	38.8 ± 1.8
Area, mm^2	288.1 ± 5.5	310.5 ± 3.7	329.8 ± 1.3	398.1

* Dimensions taken from the L4/L5 lumbar intervertebral disc segment of a male.
** Inner diameter calculated from nucleus pulposus diameter, given from ratio of nucleus pulposus to disc area.

Table S4. Dimensions of nucleus with endplates samples used for Instron compression testing. Only difference in thickness and area is shown, since endplates only add to the thickness of the samples and take away the inner diameter.

500 mm Sample	PU 100/0	PU 90/10	PU 80/20	Natural Disc** [138, 139]
Thickness, mm	10.7 ± 0.1	10.4 ± 0.0	10.5 ± 0.0	11.3 ± 1.3
Area, mm^2	398.8 ± 6.5	402.6 ± 3.0	411.6 ± 2.0	1182.4 ± 2.5
650 mm Sample	**PU 100/0**	**PU 90/10**	**PU 80/20**	**Natural Disc** [138, 139]**
Thickness, mm	10.8 ± 0.0	10.7 ± 0.2	10.8 ± 0.1	11.3 ± 1.3
Outer Diameter, mm	20.9 ± 0.3	21.7 ± 0.2	20.4 ± 0.5	38.8 ± 1.8
***Area, mm^2**	325.8 ± 16.9	344.2 ± 9.1	370.1 ± 5.6	1182.4 ± 2.5

* A different outer diameter was used since extra samples had to be fabricated.
** Dimensions taken from the L4/L5 lumbar intervertebral disc segment of a male.

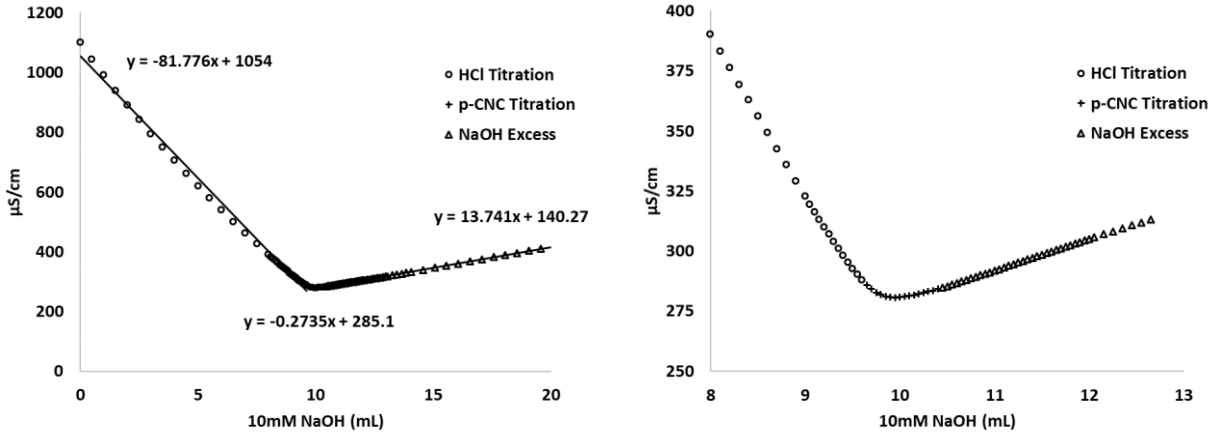

Figure S4. Example titration curve of the phosphorylated CNCs [129]. (Used under fair use, 2017).

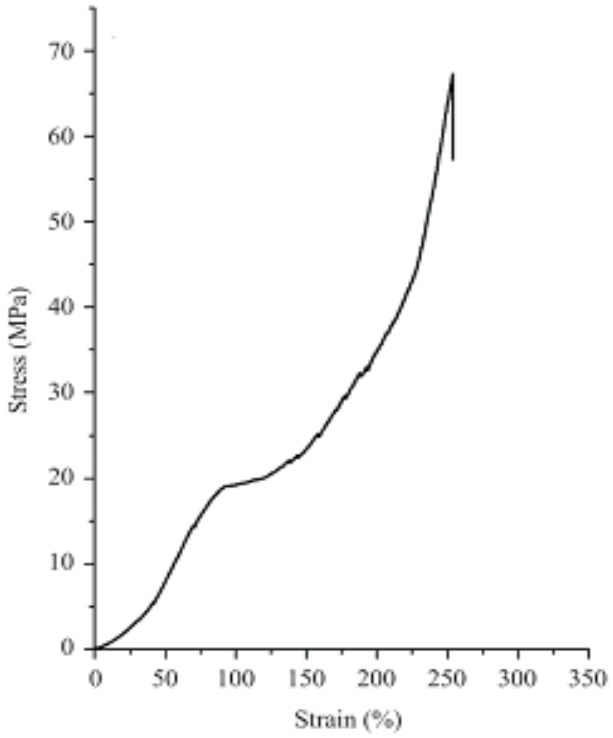

Figure S5. Typical stress-strain response of the natural intervertebral disc during a quasi-static compression test of the spine [140]. (Used under fair use, 2017).